Number 37 Year 2021

Journal of New Theory

ISSN: 2149-1402

www.dergipark.org.tr/en/pub/jnt

Journal of New Theory (abbreviated as J. New Theory or JNT) is a mathematical journal focusing on new mathematical theories or a mathematical theory's applications to science.

J. New Theory is an open-access journal.

Language: JNT accepts contributions in English only.

JNT was founded on 18 November 2014, and its first issue was published on 27 January 2015.

Editor-in-Chief: Naim Çağman

E-mail: journalofnewtheory@gmail.com

APC: JNT incurs no article processing charges.

Review Process: Blind Peer Review

Policy of Screening for Plagiarism: JNT accepts submissions for pre-review only if their reference-excluded similarity rate is a **maximum of 30%**.

Publication Ethics: The governance structure of Journal New Theory and its acceptance procedures are transparent and designed to ensure the highest quality of published material. JNT adheres to the international standards developed by the Committee on Publication Ethics (COPE).

Aim & Scope

Journal of New Theory aims to share new ideas in pure or applied mathematics with the world of science.

Journal of New Theory is an international, online, open access, and peer-reviewed journal.

Journal of New Theory publishes original research articles and reviews from all science branches that use mathematics theories.

Journal of New Theory is concerned with the studies in the areas of AMS2020, but not limited to:

· Fuzzy Sets
· Soft Sets
· Neutrosophic Sets
· Decision-Making
· Algebra
· Number Theory
· Analysis
· Theory of Functions
· Geometry
· Applied Mathematics
· Topology
· Fundamental of Mathematics
· Mathematical Logic
· Mathematical Physics
· Mathematical Statistics

Journal Boards

Pabitra Kumar Maji

Department of Mathematics, Bidhan Chandra College, Asansol 713301, Burdwan (W), West Bengal, India.

pabitra_maji@yahoo.com

Harish Garg

School of Mathematics, Thapar Institute of Engineering & Technology, Deemed University, Patiala-147004, Punjab, India

harish.garg@thapar.edu

Jianming Zhan

Department of Mathematics, Hubei University for Nationalities, Hubei Province, 445000, P. R. China

zhanjianming@hotmail.com

Surapati Pramanik

Department of Mathematics, Nandalal Ghosh B.T. College, Narayanpur, Dist- North 24 Parganas, West Bengal 743126, India

sura_pati@yaho.co.in

Muhammad Irfan Ali

Department of Mathematics, COMSATS Institute of Information Technology Attock, Attock 43600, Pakistan

mirfanali13@yahoo.com

Said Broumi

Department of Mathematics, Hassan II Mohammedia-Casablanca University, Kasablanka 20000, Morocco

broumisaid78@gmail.com

Mumtaz Ali

The University of Southern Queensland, Darling Heights QLD 4350, Australia

Mumtaz.Ali@usq.edu.au

Oktay Muhtaroğlu

Department of Mathematics, Gaziosmanpaşa University, 60250 Tokat, Turkey

oktay.muhtaroglu@gop.edu.tr

Ahmed A. Ramadan

Mathematics Department, Faculty of Science, Beni-Suef University, Beni-Suef, Egypt

aramadan58@gmail.com

Sunil Jacob John

Department of Mathematics, National Institute of Technology Calicut, Calicut 673 601 Kerala, India

sunil@nitc.ac.in

Aslıhan Sezgin

Department of Statistics, Amasya University, Amasya, Turkey

aslihan.sezgin@amasya.edu.tr

Alaa Mohamed Abd El-latif

Department of Mathematics, Faculty of Arts and Science, Northern Border University, Rafha, Saudi Arabia

alaa_8560@yahoo.com

Kalyan Mondal

Department of Mathematics, Jadavpur University, Kolkata, West Bengal 700032, India

kalyanmathematic@gmail.com

Jun Ye

Department of Electrical and Information Engineering, Shaoxing University, Shaoxing, Zhejiang, P.R. China

yehjun@aliyun.com

Ayman Shehata

Department of Mathematics, Faculty of Science, Assiut University, 71516-Assiut, Egypt

drshehata2009@gmail.com

İdris Zorlutuna

Department of Mathematics, Cumhuriyet University, Sivas, Turkey

izorlu@cumhuriyet.edu.tr

Murat Sarı

Department of Mathematics, Yildiz Technical University, İstanbul, Turkey

sarim@yildiz.edu.tr

Daud Mohamad

Faculty of Computer and Mathematical Sciences, University Teknologi Mara, 40450 Shah Alam, Malaysia

daud@tmsk.uitm.edu.my

Content

Journal of New Theory
ISSN: 2149-1402

37 (2021) 1-7
Journal of New Theory
https://dergipark.org.tr/en/pub/jnt
Open Access

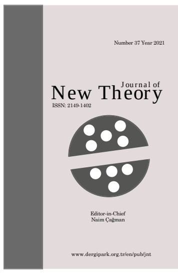

Some Results of Common Fixed Point for Compatible Mappings in Ƒ-Metric Spaces

Demet Binbaşıoğlu[1]

Article History
Received: 14 Oct 2021
Accepted: 29 Dec 2021
Published: 31 Dec 2021
10.53570/jnt.1009413
Research Article

Abstract − Recently, Ƒ-metric space has been started, and a natural topology has been described in these spaces by Jleli and Samet. Furthermore, a new form of the Banach contraction principle has been given in the new spaces. In this work, we present some common fixed-point theorems for two weakly compatible mappings in the Ƒ-metric spaces. We also mention examples that confirm our results.

Keywords *– Common fixed point, Ƒ-metric space, weakly compatible*

Mathematics Subject Classification (2020) − 47H10, 54A20

1. Introduction

Metric space is the general theory underlying various branches of mathematics. These days, generalizations of the metric space have emerged. Lately, some authors have given various generalizations of metric spaces. This situation allows authors to find new work areas. Czerwik described the concept of b–metric [1]. Khamsi and Hussain redefined the b–metric concept, and they called it metric-type [2]. Fagin et al. gave s–relaxed$_p$ metric concept [3]. Here, b–metric is more general than the s–relaxed$_p$ metric [4]. Gahler began the concept of a 2–metric [5]. This metric function is identified on the product set $X \times X \times X$. The notion of 2–metric is a generalization of the usual metric. Mustafa and Sims defined the $\mathcal{G}$–metric space concept [6]. The notion is more general than the usual metric. Branciari proposed a new extension of the notion of metric, modified the triangle inequality (iii) with a more general inequality confusing four points. Matthews defined the partial metric [7]. Jleli and Samet defined the JS–metric [8]. Currently, Jleli and Samet have given the Ƒ-metric space [9]. They compare their concepts with existing generalizations in the literature. Then, they define a natural topology $\tau_{Ƒ}$ on these spaces and examine their topological properties. Also, a new version of the Banach contraction principle is created in the tuning of Ƒ-metric spaces. They proved that their new concept is more general than the standard metric concept by showing that any metric space is an Ƒ-metric space, but the reverse is generally false. They also compared their concept with previous generalizations of metric spaces. After that, Alnaser et al. gave relation theoretic contraction and proved some generalization of fixed-point theorems in these spaces [10]. Moreover, in these generalized spaces, the coincidence points and common fixed-point

[1]demet.binbasioglu@gop.edu.tr (Corresponding Author)
[1]Department of Mathematics, Faculty of Arts and Sciences, Tokat Gaziosmanpaşa University, Tokat, Turkey

theorems are also frequently studied [11]. In this paper, we give some common fixed-point theorems and results in Ƒ-metric spaces. Moreover, some examples that provide the theorems are presented.

2. Preliminaries

Definition 2.1. [9] Let Ƒ-be the set of function $g: (0,\infty) \to \mathbb{R}$. This function provides the below terms.

Ƒ1. g be a non-decreasing function

Ƒ2. $\lim_{n\to\infty} a_n = 0 \Leftrightarrow \lim_{n\to\infty} g(a_n) = -\infty$, for every sequence $\{a_n\} \subseteq (0 +\infty)$.

Definition 2.2. [9] Let $X \neq \emptyset$, $D: X \times X \to [0,\infty)$ is a mapping, and there exist $g \in$ Ƒ and $\gamma \in [0,\infty)$. If the following terms are satisfied, D be defined as an Ƒ-metric on X. In this case, (X, D) is defined as an Ƒ-metric space.

D_1. $(a,b) \in X \times X,\ a = b \Leftrightarrow D(a,b) = 0$,

D_2. $D(a,b) = D(b,a)$ for all $a, b \in X$,

D_3. $\forall a, b \in X, n \in \mathbb{N}, n \geq 2$ and $(t_i)_{i=1}^{n} \subset X$ with $(t_1, t_{n_0}) = (a,b)$ we have

$$D(a,b) > 0 \Rightarrow g(D(a,b)) \leq g(\Sigma_{i=1}^{n-1} D(t_i, t_{i+1})) + \gamma$$

Remark 2.3. [9] The metric space is an Ƒ-metric space. But the contrary of this proposition is false.

Example 2.4. [9] Let $\mathbb{N}$ be positive real numbers set. $D: \mathbb{N} \times \mathbb{N} \to [0,\infty)$ be the mapping and for all

$a, b \in \mathbb{N}$,

$$D(a,b) = \begin{cases} (a-b)^2, & a, b \in [0,3] \\ |a-b|, & a, b \notin [0,3] \end{cases}$$

Therefore, D is an Ƒ-metric with $g(a) = \ln a$, $a > 0$ and $\gamma = \ln 3$.

Example 2.5. [9] Let $\mathbb{N}$ be the natural numbers set, $D: \mathbb{N} \times \mathbb{N} \to [0,\infty)$ and for all $a, b \in \mathbb{N}$,

$$D(a,b) = \begin{cases} \exp(|a-b|), & a \neq b \\ 0, & a = b \end{cases}$$

Therefore, D is an Ƒ-metric with $g(a) = -1 / a$, $a > 0$ and $\gamma = 1$.

Definition 2.6. [9] Suppose that D be an Ƒ-metric on X, $\{a_n\} \subset X$ is a sequence.

i. If $\{a_n\}$ be convergent to an element according to Ƒ-metric D, $\{a_n\}$ is Ƒ –convergent to element a.

ii. If $\lim_{m,n\to\infty} D(a_n, a_m) = 0$ then the sequence $\{a_n\}$ is Ƒ-Cauchy.

iii. If any Ƒ-Cauchy sequence be convergent, (X, D) is Ƒ-complete.

Definition 2.7. [11] Let T and S be self-maps on a set X. If $Tx = Sx = y$ for some $x \in X$, then x, y are defined as a coincident point and a coincidence point, respectively. If $x = Tx = Sx$ for some $x \in X$, x defined as a common fixed point.

Remark 2.8. [11] If T and S are weakly compatible, then the coincidence point y is the unique common fixed point.

Theorem 2.9. [9] Let (X, D) be an Ƒ-metric space, $f: X \to X$. Assume that the Ƒ-metric space (X, D) is Ƒ-complete and there exists $\alpha \in (0,1)$ such that $D(f(a), f(b)) \leq \alpha D(a,b)$ for $a, b \in X$. Then f has a unique fixed point $a^* \in X$. Furthermore, the sequence $\{a_n\} \subset X$ given by $a_{n+1} = f(a_n)$, $n \in \mathbb{N}$ is Ƒ-convergent to a^*, for any $a_0 \in X$.

Remark 2.10. In the theorems and results we have given throughout the article; we will think that the map $g \in Ƒ$ is surjective and $\gamma = 0$ for the proof to proceed smoothly.

3. Main Results

In this part, we give generalizations of some known fixed-point theorems in the Ƒ-metric spaces. These are coincidence points and common fixed-point theorems. Moreover, we denote some examples of the presented results.

Theorem 3.1. Let (X, D) be an Ƒ-metric. Assume that S, T: $X \to X$ provides the below conditions

i. For $\forall a, b \in X$,

$$D(T(a), T(b)) \leq kD(S(a), T(a)) + lD(S(b), T(b)) + mD(S(a), T(b)) + pD(S(b), T(a)) + tD(S(a), S(b))$$

where k, l, m, p, and t are non-negative and $k + l + m + p + t < 1$,

ii. $T(X) \subset S(X)$,

iii. $T(X)$ or $S(X)$ be an Ƒ-complete subspace.

Therefore, T and S have a unique coincidence point.

Furthermore, if T and S are weakly compatible, they have a unique common fixed point.

Proof.

Let $g \in Ƒ$, $\gamma = 0$ be such that for every $a, b \in X$ for $\forall n \in \mathbb{N}$, $n \geq 2$ and for $\forall (t_i)_{i=1}^{n} \subset X$ with $(t_1, t_{n_0}) = (a, b)$, we have

$$D(a, b) > 0 \Rightarrow g(D(a, b)) \leq g(\Sigma_{i=1}^{n-1} D((t_i, t_{i+1})) + \gamma$$

From $Ƒ_2$, for every sequence $\{a_n\} \subseteq (0, +\infty)$, there exists a $\varepsilon > 0$ such that

$$\lim_{n\to\infty} a_n = 0 \Leftrightarrow \lim_{n\to\infty} g(a_n) = -\infty \text{ and } 0 < a < \varepsilon \Rightarrow g(a) < g(\varepsilon) - \gamma$$

Let a_0, $a_1 \in X$ be arbitrary and $\{a_n\} \subset X$ be the sequence defined by $Sa_{n+1} = Ta_n = b_n$ for $n \in \mathbb{N}$. We have that

$$D(b_n, b_{n+1}) \leq (k + t)D(b_{n-1}, b_n) + lD(b_n, b_{n+1}) + mD(b_{n-1}, b_{n+1})$$

and

$$D(b_{n+1}, b_n) \leq kD(b_n, b_{n+1}) + (l + m)D(b_{n-1}, b_n) + pD(b_{n-1}, b_{n+1})$$

for all n. Hence, from the above remark,

$$D(b_n, b_{n+1}) \leq \frac{k + l + t + p + 2m}{2 - (k + l + m + p)} D(b_{n-1}, b_n)$$

If we choose $c = \frac{k+l+t+p+2m}{2-(k+l+m+p)}$, then $c \in [0,1)$ and $D(b_n, b_{n+1}) \leq c\, D(b_{n-1}, b_n)$ is hold. We have

$$D(b_n, b_{n+1}) \leq c^n D(b_0, b_1)$$

Thus, for all n and z,

$$\begin{aligned} D(b_n, b_{n+z}) &\leq D(b_n, b_{n+1}) + D(b_{n+1}, b_{n+2}) + \cdots + D(b_{n+z-1}, b_{n+z}) \\ &\leq (c^n + c^{n+1} + \cdots + c^{n+z-1}) D(b_0, b_1) \\ &\leq \frac{c^n}{1 - c} D(b_0, b_1) \end{aligned}$$

holds.

Since $\lim_{n\to\infty}\frac{c^n}{1-c}D(b_0,b_1)=0$, there exists a $n_0\in\mathbb{N}$ such that $0<\frac{c^n}{1-c}D(b_0,b_1)<\varepsilon,\ n\geq n_0$. From conditions $0<b<\varepsilon\Rightarrow g(b)<g(\varepsilon)-\gamma$ and since g is non-decreasing.

$$g(\Sigma_{i=n}^{n+z-1}D(b_i,b_{i+1}))\leq g(\frac{c^n}{1-c}D(b_0,b_1))<g(\varepsilon)-\gamma, n\geq n_0 \text{ ....*}$$

Using conditions (D_3) and (*),

$$D(b_n,b_{n+z})>0, n\geq n_0\Rightarrow g(D(b_n,b_{n+z}))\leq g(\Sigma_{i=n}^{n+z-1}D(b_i,b_{i+1}))+\gamma<g(\varepsilon)$$

Thus, we obtain that $D(b_n,b_{n+z})<\varepsilon, n\geq n_0$ by $(Ƒ_1)$. It is seen that this sequence $\{b_n\}$ is an Ƒ −Cauchy.

Because of the range of S contains the range of T and the range of at least one is Ƒ-complete, there exists a $d\in S(X)$ such that $\lim_{n\to\infty}D(Sa_n,d)=0$. Therefore there exists a sequence (x_n) in $[0,+\infty)$ and $x_n\to 0$, $D(Sa_n,d)\leq x_n$. Moreover, an $e\in X$ can be found, $Se=d$.

Now, show that $Te=d$. Suppose that $D(Te,d)>0$. From the condition (D_3),

$$g(D(Te,d))\leq g(D(Te,Tb_n))+D(Tb_n,d)+\gamma, n\in\mathbb{N}$$

Using condition of theorem and g is non-decreasing,

$$g(D(Te,d))\leq g[c(D(Te,d)+2D(Tb_n,b_n)+D(b_n,d))]+\gamma, n\in\mathbb{N}$$

Otherwise, using $\lim_{n\to\infty}b_n=0\Leftrightarrow\lim_{n\to\infty}g(b_n)=-\infty$ and $\lim_{n\to\infty}[D(Te,d)+2D(Tb_n,b_n)+D(b_n,d)]=0$, we obtain that

$$\lim_{n\to\infty}g(c[D(Te,d)+2D(Tb_n,b_n)+D(b_n,d)])+\gamma=-\infty$$

This is a contradiction. Consequently, $D(Te,d)=0$, i.e., $Te=d$ and so d is a coincidence point of T and S.

If d_1 is another coincidence point, there is $e_1\in X$ with $Te_1=Se_1=d_1$. Therefore,

$$D(d,d_1)=D(Te,\mathrm{T}e_1)\leq cD(d,d_1)$$

Hence, $D(d,d_1)=0$ that is $d=d_1$. If T and S are weakly compatible, *d* is a unique common fixed point. □

Corollary 3.2. Let (X,D) be an Ƒ-metric space. Assume S, T: $X\to X$ provides the below conditions

i. For $\forall a,b\in X$, $D(T(a),T(b))\leq cD(S(a),S(b))$ where $c<1$,

ii. $T(X)\subset$ S(X),

iii. $T(X)$ or S(X) be Ƒ-complete subspace.

Therefore, T and S have a unique coincidence point.

Besides, if T and S are weakly compatible, they have a unique common fixed point in X.

Example 3.3. Let $X=\mathbb{N}$ be the set of positive real numbers. $D:\mathbb{N}\times\mathbb{N}\to[0,\infty)$ be the mapping and for all $a,b\in\mathbb{N}$,

$$D(a,b)=\begin{cases}(a-b)^2, & a,b\in[0,10]\\ |a-b|, & a,b\notin[0,10]\end{cases}$$

If take $g(a)=\ln a$, we can show that D be an Ƒ-metric by a routine calculation. Next, define $T(a)=a^2+1$ and $S(a)=2a^2$. Then, for all $a,b\in\mathbb{N}$ we have

$$D(T(a),T(b))=\tfrac{1}{2}D(S(a),S(b))\leq cD(S(a),S(b)) \text{ for } c<1$$

$T(X)=[1,\infty)\subset[0,\infty)=S(X)$. Moreover, $T(X)$ is an Ƒ-complete subspace. That is, all conditions of corollary are satisfied. T and S have a unique coincidence point.

If $c = 2$ be a unique coincident point, $a = 1$ and $b = -1$ be coincidence points of S and T. But since $T(S(1)) \neq S(T(1))$, S and T are not weakly compatible, so S and T have no common fixed points.

Theorem 3.4. Let (X, D) be an Ƒ-metric, S, T: $X \to X$, S^2 be a continuous, and T commute with S. Assume the below conditions is satisfied,

i. For all $a, b \in X$, $D\big(T(a), T(b)\big) \leq \alpha u(a, b)$ where $\alpha \in \left(0, \frac{1}{2}\right)$ is a constant and

$$u(a,b) \in \{D\big(S(a), S(b)\big), D\big(S(a), T(a)\big), D\big(S(b), T(b)\big), D\big(S(a), T(b)\big), D\big(S(b), T(a)\big)\}$$

ii. $TS(X) \subset S^2(X)$,

iii. $T(X)$ or S(X) be Ƒ-complete subspace.

Therefore, T and S have a unique common fixed point.

Proof.

Let $g \in$ Ƒ, $\gamma \in [0, \infty)$ be such that for $\forall a, b \in X$ for every $n \in \mathbb{N}, n \geq 2$ and for every $(t_i)_{i=1}^{n} \subset X, (t_1, t_{n_0}) = (a, b)$, we have

$$D(a, b) > 0 \Rightarrow g(D(a, b)) \leq g(\Sigma_{i=1}^{n-1} D((t_i, t_{i+1})) + \gamma$$

From Ƒ$_2$, for every sequence $\{a_n\} \subseteq (0, +\infty)$, there exists a $\varepsilon > 0$ such that

$$n \to \infty \lim_{n\to\infty} a_n = 0 \Leftrightarrow \lim_{n\to\infty} g(a_n) = -\infty \text{ and } 0 < a < \varepsilon \Rightarrow g(a) < g(\varepsilon) - \gamma$$

Let $a_0 \in S(X)$ be arbitrary and $\{b_n\} \subset S(X)$ be the sequence defined by $Sa_{n+1} = Ta_n = b_n$ for $n \in \mathbb{N}$. Now $Sb_{n+1} = STa_{n+1} = TSa_{n+1} = Tb_n = c_n, n \geq 1$. We show that $\{c_n\}$ is an Ƒ-Cauchy sequence, so convergent to some c$\in X$. We denote that $S^2c = TSc$.

Since $\lim_{n\to\infty} Sb_n = \lim_{n\to\infty} STa_n = \lim_{n\to\infty} TSa_n = \lim_{n\to\infty} Tb_n = \lim_{n\to\infty} c_n = c$, it follows that $\lim_{n\to\infty} S^4a_n = \lim_{n\to\infty} S^3Ta_n = \lim_{n\to\infty} TS^3a_n = S^2c$, since S^2 is continuous. Thus, we get

$$D(S^2c, TSc) \leq D(S^2c, S^3Ta_n) + D(S^3Ta_n, TSc) \leq D(S^2c, S^3Ta_n) + \alpha u_n$$

where $u_n \in \{D(S^4a_n, S^2c), D(S^4a_n, TS^3a_n), D(S^2c, TSc), D(S^4a_n, TSc), D(S^2c, TS^3a_n)\}$.

Choose any $n_0 \in \mathbb{N}$, for all $n \geq n_0$, since $S^3Ta_n \to S^2c$ and $S^4a_n \to S^2c$, then we have $D(S^2c, S^3Ta_n) \leq x_n$ and $D(S^4a_n, S^2c) \leq y_n$, as $x_n \to 0$ and $y_n \to 0$. We have the five cases:

Case 1: $D(S^2c, TSc) \leq D(S^2c, S^3Ta_n) + \alpha D(S^4a_n, S^2c) \leq x_n + \alpha y_n$

Case 2:

$$\begin{aligned} D(S^2c, TSc) &\leq D(S^2c, S^3Ta_n) + \alpha D(S^4a_n, TS^3c) \\ &\leq D(S^2c, S^3Ta_n) + \alpha\big(D(S^4a_n, S^2c) + \alpha D(TS^3a_n, S^2c)\big) \\ &\leq x_n + \alpha(y_n + x_n) \\ &= (1+\alpha)x_n + \alpha y_n \end{aligned}$$

Case 3: $D(S^2c, TSc) \leq D(S^2c, S^3Ta_n) + \alpha D(S^2c, TSc) \leq \frac{x_n}{1-\alpha}$

Case 4:

$$\begin{aligned} D(S^2c, TSc) &\le D(S^2c, S^3Ta_n) + \alpha D(S^4a_n, TS^3c) \\ &\le D(S^2c, S^3Ta_n) + \alpha\big(D(S^4a_n, S^2c) + D(TSc, S^2c)\big) \\ &\le \frac{x_n + \alpha y_n}{(1-\alpha)} \end{aligned}$$

Case 5:

$$\begin{aligned} D(S^2c, TSc) &\le D(S^2c, S^3Ta_n) + \alpha D(S^2c, TS^3a_n) \\ &\le x_n + \alpha x_n \\ &\le (1+\alpha)x_n \end{aligned}$$

Therefore, $D(S^2c, TSc) = 0$ that is $S^2c = TSc$. TSc is a common fixed point for T and S. Put in the inequality $D(Ta, Tb) \le \alpha u(a, b), a = TSc,\ b = Sc$ we get $T(TSc) = TSc$. Since $S^2c = TSc$, i.e. $S(Sc) = T(Sc)$, we have $S(TSc) = TS^2c = T(TSc) = TSc$.

4. Conclusion

In this work, we present some new common fixed-point theorems in Ƒ-metric spaces. Moreover, we give some examples that support our results. Our results extend and generalize the fixed-point theory. We hope that our research results offer a mathematical foundation. In future studies, we will explore the concrete applications of the obtained results.

Author Contributions

The author read and approved the last version of the manuscript.

Conflicts of Interest

The author declares no conflict of interest.

References

[1] S. Czerwik, *Contraction Mappings in b-Metric Spaces*, Acta Mathematica et Informatica Universitatis Ostraviensis 1(1) (1993) 5–11.

[2] M. A. Khamsi, N. Hussain, *KKM Mapping in Metric Type Spaces*, Nonlinear Analysis 7(9) (2010) 3123–3129.

[3] R. Fagin, R. Kumar, D. Sivakumar, *Comparing Top k Lists*, SIAM Journal on Discrete Mathematics 17(1) (2003) 134–160.

[4] W. Kirk, N. Shahzad, *Fixed Point Theory in Distance Spaces*, Springer: Cham, 2014.

[5] V. S. Gahler, *2-Metrische Raume und ihre Topologishe Strüktür,* Mathematische Nachrichten 26 (1963/1964) 115–118.

[6] Z. Mustafa, B. Sims, *A New Approach to Generalized Metric Spaces,* Journal of Nonlinear and Convex Analysis 7(2) (2006) 289–297.

[7] S. G. Matthews, *Partial Metric Topology*. In: Proceedings of the 8th Summer Conference on General Topology and Applications. Annals of the New York Academy of Sciences 728 (1994) 183–197.

[8] M. Jleli, B. Samet, *A Generalized Metric Space and Related Fixed-Point Theorems*, Fixed Point Theory and Its Applications Article Number 61 (2015) 1–14.

[9] M. Jleli, B. Samet, *On a New Generalization of Metric Spaces*, Journal of Fixed-Point Theory and Applications Article Number 128 20 (2018) 1–20.

[10] A. L. Alnaser, D. Lateef, A. H. Fouad, J. Ahmad, *Relation Theoretic Contraction Results in $\mathcal{F}$-Metric Spaces*, Journal of Nonlinear Sciences and Applications 12 (2019) 337–344.

[11] M. Abbas, G. Jungck, *Common Fixed-Point Results for Non-Commuting Mappings without Continuity in Cone Metric Spaces*, Journal of Mathematical Analysis and Applications 341 (2008) 416–420.

Journal of New Theory
ISSN: 2149-1402

37 (2021) 8-25
Journal of New Theory
https://dergipark.org.tr/en/pub/jnt
Open Access

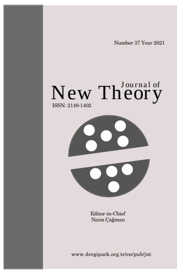

New Exact Solutions of Conformable Time-Fractional Bad and Good Modified Boussinesq Equations

Zafer Öztürk[1], Sezer Sorgun[2], Halis Bilgil[3], Ümmügülsüm Erdinç[4]

Article History
Received: 03 Nov 2021
Accepted: 22 Dec 2021
Published: 31 Dec 2021
10.53570/jnt.1018383
Research Article

Abstract − The new exact solutions of the conformable time-fractional Bad and Good modified Boussinesq equations are obtained using the Exp-function method, which is different from previous literature works. These equations play a significant role in mathematical physics, engineering sciences and applied mathematics. Plentiful exact solutions with arbitrary parameters are effectively obtained by the method. The obtained solutions are shown graphically. It is shown that the Exp-function method provides a simpler but more effective mathematical tool for constructing exact solutions of non-linear evolution equations.

Keywords − *Conformable time fractional Bad and Good modified Boussinesq equations, conformable fractional derivative, exact solution, Exp-function method*

Mathematics Subject Classification (2020) – 35R11, 34A08

1. Introduction

Many phenomena in the real world are governed by nonlinear evolution equations (NLEEs). Hence, it is essential to obtain exact solutions to these equations, and many methods have been proposed to get exact solutions. The most known methods are the Exp-function method [1], the tanh-method [2], the homogeneous balance method [3], the trial function method [4], the $\left(\frac{G'}{G}\right)$ expansion methods [5], the Kudryashov method [6]. The Exp-function method was used by many researchers to solutions of various NLEEs [7-10]. Also, new exact solutions of the nonlinear evolution equations may be obtained using different methods.

Travelling waves arise naturally in many physical systems, usually described by partial differential equations. Solitary waves, also known as 'solitons', are a particular travelling wave class with some special properties. Solitons can usually propagate over large distances without dispersion due to certain nonlinear effects cancelling out dispersive effects. They also have the additional property that they can interact with other solitons such that they emerge following a collision without changing shape, apart from a small phase change.

[1]zaferozturk@aksaray.edu.tr (Corresponding Author); [2]ssorgun@nevsehir.edu.tr; [3]halis@aksaray.edu.tr; [4]ummugulsumerdinc@aksaray.edu.tr
[1,2] Department of Mathematics, Nevşehir HacıBektaş Veli University, Nevşehir, Turkey
[3,4] Department of Mathematics, Aksaray University, Aksaray, Turkey

Traditional real problems are defined with integer-order nonlinear evolution equations, characterized by theirs. However, the nonlinear evolution equations with integer-order derivatives are ideal classic events, which are not suitable for describing irregular phenomena. On the other hand, Fractional differential equations have become preferable, despite the difficulty in calculations, since they give more real results than standard integer order nonlinear evolution equations. Difficulties in fractional calculus have begun to be overcome thanks to new fractional derivative definitions and theorems made in recent years. The most popular definitions of the fractional derivative can be listed as the conformable derivative [11], the Caputo derivative [12], Riemann-Liouville derivative [12], Atangana-Baleanu derivative [13]. The new trends in exact solution research are to find new exact solutions and to develop new solution mechanisms.

Lately, Khalil et al. defined a limit-based fractional derivative in 2014 [11], named the conformable fractional derivative. The structure of this new definition of fractional derivative is simpler than that of other popular fractional derivatives.

The definition of conformable fractional derivative is given as follow.

Let f: $[0,\infty]\rightarrow\mathbb{R}$. Then, the conformable fractional derivative of order α is defined by

$$T_\alpha\big(f(t)\big) = \lim_{\varepsilon\to 0}\frac{f(t+\varepsilon t^{1-\alpha}) - f(t)}{\varepsilon} \tag{1}$$

for all $t > 0$ and $\alpha \in (0,1]$. If f is α-differentiable in some $(0,\alpha)$, $\alpha > 0$ and $\lim_{t\to 0^+} T_\alpha\big(f(t)\big)$ exists, then

$$(T_\alpha f)(0) = \lim_{t\to 0^+} T_\alpha\big(f(t)\big) \tag{2}$$

In addition to this definition, it is known that $T_\alpha\big(f(t)\big) = \lim_{\varepsilon\to 0}\frac{f^{\lceil\alpha-1\rceil}(t+\varepsilon t^{\lceil\alpha\rceil-\alpha}) - f^{\lceil\alpha-1\rceil}(t)}{\varepsilon}$ such that $\alpha \in (n, n+1]$ and function f is n-th order differentiable at a point for $t > 0$, where $\lceil . \rceil$ ceil function, $\lceil\alpha\rceil$ is the smallest integer no larger than α [11].

This paper applies the Exp-function method to new exact solutions of fractional Bad and Good modified Boussinesq equations with conformable derivative. The rest of this paper is organized as follows: Some useful properties of the conformable fractional derivative and mechanism of the Exp-function method are given in Section 2. Exact solutions of the fractional Bad and Good modified Boussinesq equations are obtained in Section 3. Finally, the conclusions of this paper are given in Section 4.

2. Preliminary and The Exp-Function Method

It is well known that most of the events that develop in mathematical, physics and engineering fields can be described by partial differential equations (PDEs). So, partial differential equations are useful tools for mathematical modelling. First, the Exp-function method is defined by He and Wu (2006) and applied to various applications by many scientists [14-20]. The exact solution of non-linear partial differential equations is obtained by the Exp-function method. First, the partial differential equation is reduced to the ordinary differential equation and referred to the exact solution using the exponential function method. The Exp-function method is an effective method for solutions of the non-linear evolution equations that emerges in mathematical physics, applied mathematics and engineering applications. The Exp-function method also gives generalized single and periodic solutions of the nonlinear evolution equation. Some solutions of fractional Bad and Good modified Boussinesq equations with the aid of auxiliary equation method are obtained by Durur et al. [21].

We consider a general nonlinear PDE in the form

$$P = (x, y, u, u_x, u_y, u_{xx}, u_{xy}, u_{yy}, \dots) = 0 \tag{3}$$

Let us introduce a complex variable $\xi = kx + wt$ where k and w are constants. We rewrite Equation (3) in the subsequent nonlinear ODE:

$$Q(u,u',u'',u''',\dots)=0 \tag{4}$$

where the prime denotes the derivation concerning ξ [4]. According to the Exp-function method, we assume that the solution can be expressed in the form

$$u\,(\xi)=\frac{\sum_{n=-c}^{d} a_n e^{(n\xi)}}{\sum_{m=-p}^{q} b_m\, e^{(m\xi)}} \tag{5}$$

where c,d,p and q are positive integers, a_n and b_m are unknown constants to be observed. Without loss of generality, if we take $d=q=c=p=1$ then Equation (5) can be written as follow,

$$u\,(\xi)=\frac{a_{-1}\xi+\ a_0+\ a_1 e^{\xi}}{b_{-1}e^{-\xi}+\ b_0+\ e^{\xi}} \tag{6}$$

Here, the constant b_1 is taken as 1 for simplicity. It will arrive us to a set of algebraic equations for the unknowns a_0, a_1 , a_{-1}; b_0, b_{-1}; k, w. Some useful theorems are given by Ebaid [22] for this subject.

Theorem 2.1. Suppose that $u^{(r)}$ and $u^{(\gamma)}$ are respectively the highest order linear term and the highest order nonlinear term of a nonlinear ODE, where r and γ are both positive integers. Then the balancing procedure using the Exp-function ansatz; $u\,(\xi)=\frac{\sum_{n=-c}^{d} a_n e^{(n\xi)}}{\sum_{m=-p}^{q} b_m e^{(m\xi)}}$ leads to $c=d$ and $p=q$, $\forall\, r\geq 1$, $\forall\gamma\geq 1$ [14].

i) Suppose that $u^{(r)}$ and $u^{(s)}u^{(k)}$ are respectively the highest order linear term and the highest order nonlinear term of a nonlinear ODE, where r,s and k are all positive integers. Then the balancing procedure using the Exp-function ansatz leads to $c=d$ and $p=q, \forall r,s,k\geq 1$

ii) Let $u^{(r)}$ and $(u^{(s)})^{\gamma}$ be respectively the highest order linear term and the highest order nonlinear term of a nonlinear ODE, where r,s and γ are all positive integers. Then the balancing procedure using the Exp-function ansatz leads to $c=d$ and $p=q$, $\forall r,s\geq 1$, $\forall\gamma\geq 2$

iii) Suppose that $u^{(r)}$ and $(u^{(s)})^{\gamma}u^{(\lambda)}$ are respectively the highest order linear term and the highest order nonlinear term of a nonlinear ODE, where r,s,γ and λ are all positive integers. Then the balancing procedure using the Exp-function ansatz leads to $c=d$ and $p=q$, $\forall r,s,\gamma,\lambda\geq 1$

Theorem 2.2. [11] If f and g functions are α -differentiable at a point $t>0$ for $\alpha\in(0,1]$, then

a) $T_\alpha\big(\lambda f(t)+\delta g(t)\big)=\lambda T_\alpha\big(f(t)\big)+\delta T_\alpha\big(g(t)\big)$, for all $\delta,\lambda\in\mathbb{R}$

b) $T_\alpha(t^p)=pt^{p-\alpha}$, for all $p\in\mathbb{R}$

c) $T_\alpha(c)=0$ for all constant c.

d) $T_\alpha\big(f(t)g(t)\big)=f(t)T_\alpha\big(g(t)\big)+g(t)T_\alpha\big(f(t)\big)$

e) $T_\alpha\left(\frac{f(t)}{g(t)}\right)=\frac{g(t)T_\alpha(f(t))-f(t)T_\alpha(g(t))}{(g(t))^2}$

f) If the function f is differentiable, $T_\alpha\big(f(t)\big)=t^{1-\alpha}\frac{df}{dt}$.

In addition, α-th order conformable fractional derivatives of some functions are given as,

i) $T_\alpha(e^{at})=at^{1-\alpha}e^{at}$, $\forall a\ \in\mathbb{R}$

ii) $T_\alpha(\sin\,(bt))=bt^{1-\alpha}\cos\,(bt)$, $\forall b\in\mathbb{R}$

iii) $T_\alpha(\cos\,(ct))=-ct^{1-\alpha}\sin(ct)$, $\forall c\ \in\mathbb{R}$

iv) $T_\alpha\left(\frac{t^\alpha}{\alpha}\right)=1$

v) $T_\alpha\left(\sin\left(\frac{t^\alpha}{\alpha}\right)\right) = \cos\left(\frac{t^\alpha}{\alpha}\right)$

vi) $T_\alpha\left(\cos\left(\frac{t^\alpha}{\alpha}\right)\right) = -\sin\left(\frac{t^\alpha}{\alpha}\right)$

vii) $T_\alpha\left(e^{\frac{t^\alpha}{\alpha}}\right) = e^{\frac{t^\alpha}{\alpha}}$

3. Fractional Bad and Good Modified Boussinesq Equations

The Boussinesq equation is first discovered by Joseph Boussinesq in 1870 [23]. This equation is one of the non-linear partial differential equations in plasma that have applications in many areas, such as ion sound waves, shallow water waves modelling, longitudinal propagation waves in elastic bars, suppressed waves in liquid-gas foam mixtures and the propagation model of these waves. Then, the Boussinesq equation is modified to adapt to deeper water problems and hence there are many new forms of this equation in the literature [21,23].

Time-Fractional Bad Modified Boussinesq Equation is denoted by

$$D_t^{(2\alpha)}u - D_x^2u - D_x^4u - 3D_x^2(u^2) + 3D_x(u^2D_xu) = 0 \tag{7}$$

Time-Fractional Good Modified Boussinesq Equation is denoted by

$$D_t^{(2\alpha)}u - D_x^2u + D_x^4u - 3D_x^2(u^2) + 3D_x(u^2D_xu) = 0 \tag{8}$$

We are now ready for solutions of Time-Fractional Bad Modified Boussinesq Equation using the Exp-function method to produce a solution set. In view of the Exp-function method, we assume that the solutions of Equation (7) can be expressed in the form,

$$u\,(\xi) = \frac{\sum_{n=-c}^{d} a_n e^{(n\xi)}}{\sum_{m=-p}^{q} b_m\, e^{(m\xi)}}$$

By using Theorem 2. 2. (f) and the travelling wave transformation as follow,

$$u(x,t) = u(\xi)\,, \xi = x - w\frac{t^\alpha}{\alpha} \tag{9}$$

and therefore, the Equation (7) convert to an ordinary differential equation. Here a_n and b_m are unknown constants, w denotes the velocity of the wave, and prime denotes the derivative of the functions concerning ξ.

By applying the wave transform in (9), the equation in (7) is obtained to the following ordinary differential equation.

$$(-\mathrm{w}^2 - 1)u'' - u^{iv} - 6u'^2 - 6uu'' + 6uu'^2 + 3u^2u'' = 0 \tag{10}$$

By applying the wave transform in (9), the equation in (8) is obtained to the following ordinary differential equation.

$$(-\mathrm{w}^2 - 1)u'' + u^{iv} - 6u'^2 - 6uu'' + 6uu'^2 + 3u^2u'' = 0 \tag{11}$$

Firstly, substitute Equation (6) into Equation (10) and Equation (11), then the unknown parameters are obtained by using Maple Software.

Hence, we obtain all the solutions related to Bad and Good Modified Boussinesq Equations cases. We balance the linear term of the highest order of Equation (10) u^{iv} with the highest order nonlinear term u^2u'',we set $p = c = 1$ and $q = d = 1$; then the trial solution of Equation (10), reduces to

$$\frac{-1}{A}\left[C_4e^{4\xi} + C_3e^{3\xi} + C_2e^{2\xi} + C_1e^{\xi} + C_0 + C_{-1}e^{-\xi} + C_{-2}e^{-2\xi} + C_{-3}e^{-3\xi} + C_{-4}e^{-4\xi}\right] = 0 \tag{12}$$

and all coefficients must be zero for the solutions of Equation (12). Hence, we get

$A \;= b_{-1}(e^{-\xi} + \; b_0 + \; e^{\xi})^5\;;$

$C_4 \;= -2a_0 + 3a_1^2 a_0 - 6a_0 a_1 + 6a_1^2 b_0 - 3a_1^3 b_0 + 2a_1 b_0 - w^2 a_0 + w^2 a_1 b_0;$

$C_3 = -20a_{-1} + 24a_1^2 b_{-1} + 20a_1 b_{-1} + 12a_1^2 a_{-1} + 9a_1^3 b_0^2 - 6a_1^2 b_0^2 - 12a_1^3 b_{-1} + 12a_1 a_0^2$

$-24a_1 a_{-1} - 4w^2 a_{-1} - 10a_1 b_0^2 + 10a_0 b_0 + 4w^2 a_1 b_{-1} + 18a_1 b_0 a_0 - w^2 a_0 b_0 + w^2 a_1 b_0^2$

$-21a_1^2 a_0 b_0 - 12a_0^2;$

$C_2 \;= 9a_0^3 + 4w^2 a_0 b_{-1} - 70a_1 b_{-1} b_0 - 12a_1^2 b_0 b_{-1} - w^2 a_1 b_0^3 - 12a_1 a_{-1} b_0 - 21a_1^2 a_{-1} b_0$

$-21a_1 b_0 a_0^2 + 12a_0 a_1^2 b_0^2 + +18a_1 a_0 b_0^2 + 78a_1 a_0 b_{-1} - 11w^2 a_{-1} b_0 - 66a_0 a_1^2 b_{-1} - 10a_0 b_0^2$

$+80a_0 b_{-1} - 54a_{-1} a_0 - 10a_{-1} b_0 - 12a_1^2 b_0^3 + +33a_1^3 b_0 b_{-1} + w^2 a_0 b_0^2 + 7w^2 a_1 b_0 b_{-1}$

$+10a_1 b_0^3 - 6a_0^2 b_0 + 54a_1 a_0 a_{-1};$

$C_1 \;= -w^2 a_1 b_0^4 - 84a_1 a_0^2 b_{-1} + 4w^2 a_1 b_{-1}^2 - 24a_1^2 b_{-1}^2 + 56a_1 b_0^2 b_{-1} - 6a_0 a_1 b_0^3 - 78a_{-1} a_0 b_0$

$+3a_0^2 a_1 b_0^2 + 3a_{-1} a_1^2 b_0^2 - 4w^2 a_{-1} b_{-1} + 12a_{-1} a_1 b_0^2 + 72a_{-1} a_1 b_{-1} - 54a_1^2 b_{-1} b_0^2 - 11w^2 a_{-1} b_0^2$

$+w^2 a_0 b_0^3 - 84a_1^2 a_{-1} b_{-1} \pm 34a_0 b_0 b_{-1} + 36a_0^2 b_{-1} - 48a_{-1}^2 + 2a_0 b_0^3 + 48a_{-1} a_0^2 - 2a_1 b_0^4$

$-172a_1 b_{-1}^2 - 3a_0^3 b_0 + 48a_1 a_{-1}^2 + 36a_1^3 b_{-1}^2 + +6a_0^2 b_0^2 + 172a_{-1} b_{-1} - 22a_{-1} b_0^2$

$+51a_0 a_1^2 b_0 b_{-1} + 84a_0 a_1 b_0\, b_{-1} + 13w^2 a_0 b_0 b_{-1} - 2w^2 a_1 b_{-1} b_0^2 - 18a_{-1} a_0 a_1 b_0;$

$C_0 \;= 110a_{-1} b_{-1} b_0 - 90a_1^2 b_{-1}^2 b_0 + 15a_{-1} b_0 a_0^2 + 15a_{-1} a_1^2 b_{-1} b_0 + 75a_0 a_1^2 b_{-1}^2 + 30a_0 a_1 b_{-1}^2$

$-5w^2 a_{-1} b_{-1} b_0 + 10w^2 a_0 b_{-1} b_0^2 + 15a_1 b_0 a_0^2 b_{-1} + 10w^2 a_0 b_{-1}^2 - 10a_{-1} b_0^3 - 220a_0 b_{-1}^2$

$+30a_{-1} a_0 b_{-1} - 5w^2 a_{-1} b_0^3 + 15a_{-1}^2 a_1 b_0 + 110a_1 b_{-1}^2 b_0 - 10a_1 b_{-1} b_0^3 + 20a_0 b_{-1} b_0^2 - 30a_0^3 b_{-1}$

$-30a_1 a_0 b_0^2 b_{-1} - 30a_{-1} b_0^2 a_0 - 5w^2 a_1 b_{-1}^2 b_0 + 60a_0^2 b_{-1} b_0 - 90a_{-1}^2 b_0 + 120a_{-1} a_1 b_{-1} b_0$

$-5w^2 a_1 b_{-1} b_0^3 - 180a_{-1} a_0 a_1 b_{-1} + 75a_0 a_{-1}^2;$

$C_{-1} = -172a_{-1} b_{-1}^2 + 172a_1 b_{-1}^3 - 24a_{-1}^2 b_{-1} + 36a_0^2 b_{-1}^2 - 2a_{-1} b_0^4 - 48a_1^2 b_{-1}^3 - 54a_{-1}^2 b_0^2$

$+48a_1 a_0^2 b_{-1}^2 - 22a_1 b_{-1}^2 b_0^2 + 6a_0^2 b_{-1} b_0^2 - 84a_{-1} a_0^2 b_{-1} - 6a_0 a_{-1} b_0^3 - 34a_0 b_{-1}^2 b_0$

$+48a_{-1} a_1^2 b_{-1}^2 + 3a_{-1}^2 b_0^2 a_1 + 3a_0^2 a_{-1} b_0^2 + 4w^2 a_{-1} b_{-1}^2 - 3a_0^3 b_{-1} b_0 + 72a_1 a_{-1} b_{-1}^2 - w^2 a_{-1} b_0^4$

$+51a_0 a_{-1}^2 b_0 - 4w^2 a_1 b_{-1}^3 + w^2 a_0 b_{-1} b_0^3 + 12a_{-1} b_0^2 a_1 b_{-1} + 13w^2 a_0 b_{-1}^2 b_0 - 2w^2 a_{-1} b_0^2 b_{-1}$

$-11w^2 a_1 b_0^2 b_{-1}^2 + 2a_0 b_{-1} b_0^3 - 84a_{-1}^2 a_1 b_{-1} + 84a_{-1} a_0 b_{-1} b_0 - 78a_1 b_{-1}^2 a_0 b_0$

$-18a_{-1} a_0 a_1 b_{-1} b_0 + 36a_{-1}^3 + 56a_{-1} b_{-1} b_0^2;$

$C_{-2} = 9a_0^3 b_{-1}^2 - 12a_{-1}^3 b_0^3 + 80a_0 b_{-1}^3 + 33a_{-1}^3 b_0 + 12a_0 a_{-1}^2 b_0^2 + 4w^2 a_0 b_{-1}^3 + 10a_{-1} b_{-1} b_0^3$

$-54a_0 a_1 b_{-1}^3 - 70a_{-1} b_{-1}^2 b_0 - 12a_{-1}^2 b_{-1} b_0 - 66a_{-1}^2 a_0 b_{-1} + 78a_{-1} a_0 b_{-1}^2 - 10a_1 b_{-1}^3 b_0$

$$-6a_0^2b_{-1}^2b_0 - 10a_0b_{-1}^2b_0^2 + 18a_{-1}b_0^2a_0b_{-1} + w^2a_0b_{-1}^2b_0^2 - 12a_{-1}b_0a_1b_{-1}^2 - 21a_{-1}b_0a_0^2b_{-1}$$

$$-11w^2a_1b_{-1}^3b_0 + 54a_{-1}a_1a_0b_{-1}^2 - w^2a_{-1}b_0^3b_{-1} - 21a_{-1}^2a_1b_0b_{-1} + 7w^2a_{-1}b_{-1}^2b_0;$$

$$C_{-3} = 18a_{-1}b_0a_0b_{-1}^2 - 21a_{-1}^2a_0b_0b_{-1} - 12a_{-1}^3b_{-1} + 24a_{-1}^2b_{-1}^2 - 20a_1b_{-1}^4 + 10a_0b_{-1}^3b_0$$

$$-w^2a_0b_{-1}^3b_0 + w^2a_{-1}b_{-1}^2b_0^2 - 12a_0^2b_{-1}^3 + 9a_{-1}^3b_0^2 + 20a_{-1}b_{-1}^3 - 10a_{-1}b_{-1}^2b_0^2 + 4w^2a_{-1}b_{-1}^3$$

$$+12a_{-1}^2a_1b_{-1}^2 - 4w^2a_1b_{-1}^4 - 6a_{-1}^2b_0^2b_{-1} + 12a_{-1}a_0^2b_{-1}^2 - 24a_{-1}a_1b_{-1}^3;$$

$$C_{-4} = w^2a_{-1}b_{-1}^3b_0 - 2a_0b_{-1}^4 + 6a_{-1}^2b_{-1}^2b_0 + 2a_{-1}b_{-1}^3b_0 - 3a_{-1}^3b_0b_{-1} + 3a_{-1}^2a_0b_{-1}^2 - 6a_{-1}a_0b_{-1}^3$$

$$-w^2a_0b_{-1}^4\ ;$$

All the coefficients of $e^{n\xi}$ must be zero. Hence, we produce a system of algebraic equations which the Maple can tackle to produce the subsequent cases of solutions:

Case 1:

$$a_0 = a_1b_0\,, a_{-1} = a_1b_{-1} \tag{13}$$

Replace these outcomes into Equation (6), we produce a subsequent exact solution,

$$u(\xi) = a_1 \tag{14}$$

where a_1 is a free parameter.

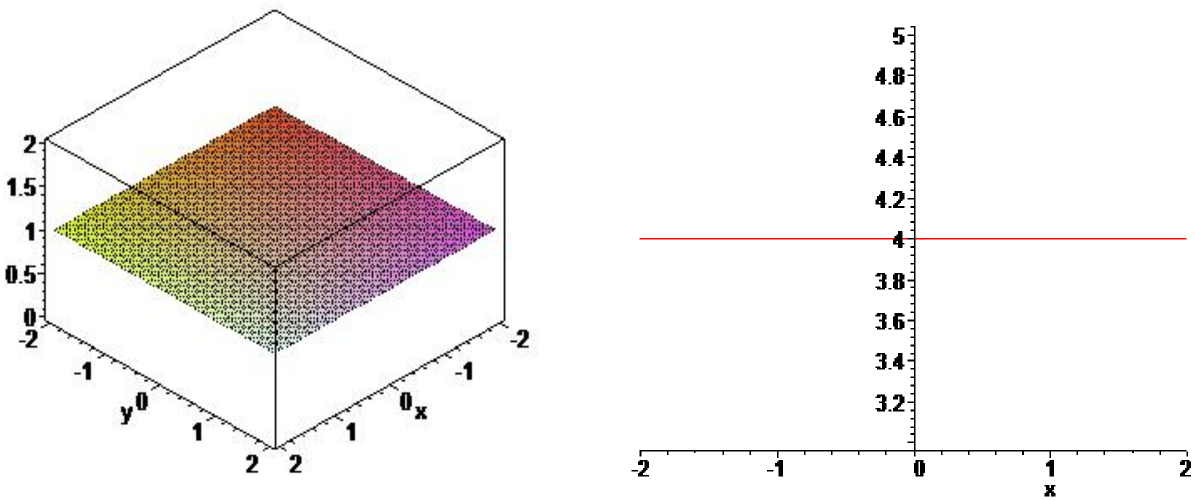

Fig. 1. 3D and 2D plots of travelling wave solutions (Case 1)

The plots indicate the wave solutions for $a_1 = 4$ in Equation (14).

Case 2:

$$a_0 = 0, \qquad b_0 = 0, a_1 = 1, w = 2\sqrt{2}I, w = -2\sqrt{2}I,\ b_{-1} = 0 \tag{15}$$

Replace these outcomes into Equation (6), we produce a subsequent exact solution,

$$u(\xi) = \frac{a_{-1}e^{-\xi} + e^{\xi}}{e^{\xi}} \tag{16}$$

where a_{-1} is a free parameter.

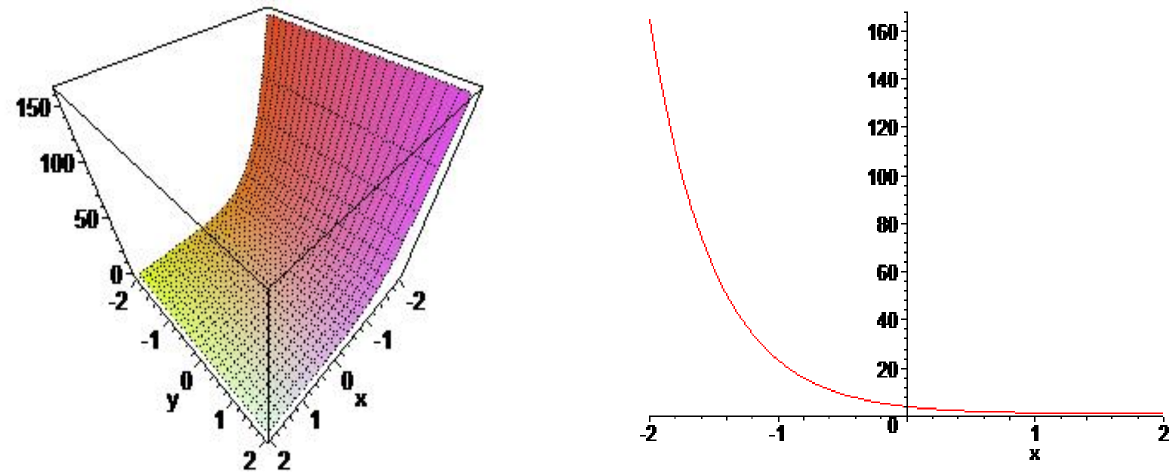

Fig. 2. 3D and 2D plots of travelling wave solutions (Case 2)

The plots indicate the wave solutions for $a_{-1}=3$ in Equation (16).

<u>Case 3:</u>

$$a_0=0, b_0=0, a_1=1+\sqrt{2},\ a_1=1-\sqrt{2}, w=I\sqrt{2}, w=-I\sqrt{2} \tag{17}$$

$$a_{-1}=-(1+\sqrt{2})\,b_{-1}+2b_{-1},\ a_{-1}=-(1-\sqrt{2})b_{-1}+2b_{-1}$$

Replace these outcomes into Equation (6), we produce a subsequent exact solution,

$$u(\xi)=\frac{\left(-(1+\sqrt{2})\,b_{-1}+2b_{-1}\right)e^{-\xi}+(1+\sqrt{2})e^{\xi}}{b_{-1}e^{-\xi}+e^{\xi}} \tag{18}$$

where b_{-1} is a free parameter.

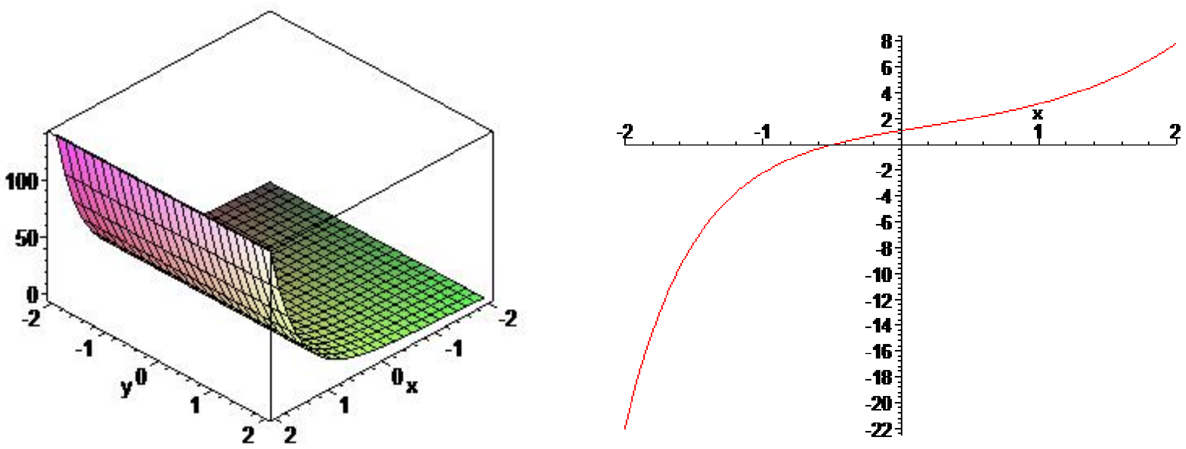

Fig. 3. 3D and 2D plots of travelling wave solutions (Case 3)

The plots indicate the wave solutions for $b_{-1}=5$ in Equation (18).

<u>Case 4:</u>

$$a_{-1}=0, b_{-1}=0, a_1=1+\frac{1}{2}\sqrt{2},\ a_1=1-\frac{1}{2}\sqrt{2}, w=\frac{1}{2}I\sqrt{14} \tag{19}$$

$$w = -\frac{1}{2}I\sqrt{14},\ a_0 = -\left(1 - \frac{1}{2}\sqrt{2}\right)b_0 + 2b_0, a_0 = -\left(1 + \frac{1}{2}\sqrt{2}\right)b_0 + 2b_0$$

Replace these outcomes into Equation (6), we produce a subsequent exact solution,

$$u(\xi) = \frac{-\left(1 - \frac{1}{2}\sqrt{2}\right)b_0 + 2b_0 + (1 - \frac{1}{2}\sqrt{2})e^{\xi}}{b_0 + e^{\xi}} \tag{20}$$

where b_0 is a free parameter.

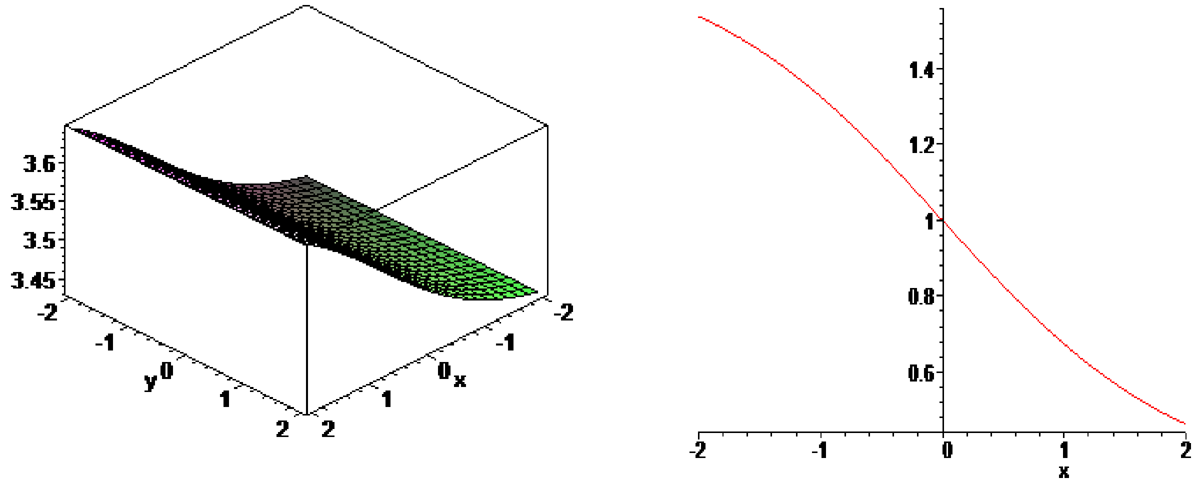

Fig. 4. 3D and 2D plots of travelling wave solutions (Case 4)

The plots indicate the wave solutions for $b_0 = 2$ in Equation (20).

<u>Case 5:</u>

$$a_{-1} = 0, b_0 = a_0, a_1 = 0, w = I\sqrt{2}, w = -I\sqrt{2},\ b_{-1} = \frac{1}{8}{a_0}^2 \tag{21}$$

Replace these outcomes into Equation (6), we produce a subsequent exact solution,

$$u(\xi) = \frac{a_0}{\frac{1}{8}{a_0}^2 e^{-\xi} + a_0 + e^{\xi}} \tag{22}$$

where a_0 is a free parameter.

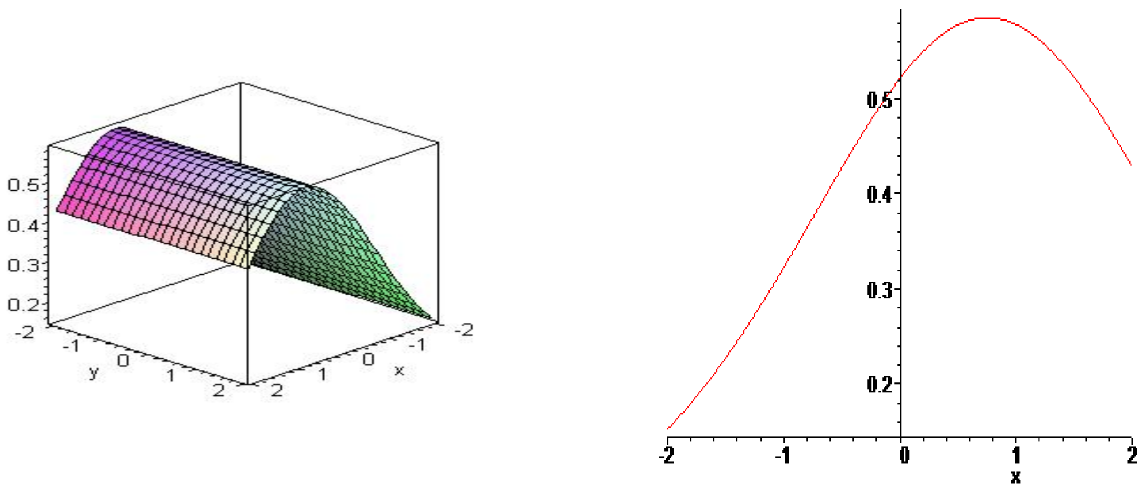

Fig. 5. 3D and 2D plots of travelling wave solutions (Case 5)

The plots indicate the wave solutions for $a_0 = 6$ in Equation (22).

<u>Case 6:</u>

$$a_{-1} = -a_0{}^2 + \frac{1}{2}\left(1 - \frac{1}{2}\sqrt{2}\right) a_0{}^2 - \left(1 - \frac{1}{2}\sqrt{2}\right) b_0 a_0 + \frac{1}{4}\left(1 - \frac{1}{2}\sqrt{2}\right) b_0{}^2 + 2b_0 a_0 - \frac{1}{2} b_0{}^2$$

$$a_{-1} = -a_0{}^2 + \frac{1}{2}\left(1 + \frac{1}{2}\sqrt{2}\right) a_0{}^2 - \left(1 + \frac{1}{2}\sqrt{2}\right) b_0 a_0 + \frac{1}{4}\left(1 + \frac{1}{2}\sqrt{2}\right) b_0{}^2 + 2b_0 a_0 - \frac{1}{2} b_0{}^2 \tag{23}$$

$$b_{-1} = b_0 a_0 - \frac{1}{2} a_0{}^2 - \frac{1}{4} b_0{}^2, w = \frac{1}{2} I\sqrt{14}, w = -\frac{1}{2} I\sqrt{14}, a_1 = 1 - \frac{1}{2}\sqrt{2}, a_1 = 1 + \frac{1}{2}\sqrt{2}$$

Replace these outcomes into Equation (6), we produce a subsequent exact solution,

$$u(\xi) = \frac{\left(-a_0{}^2 + \frac{1}{2}\left(1 - \frac{1}{2}\sqrt{2}\right) a_0{}^2 - \left(1 - \frac{1}{2}\sqrt{2}\right) b_0 a_0 + \frac{1}{4}\left(1 - \frac{1}{2}\sqrt{2}\right) b_0{}^2 + 2b_0 a_0 - \frac{1}{2} b_0{}^2\right) e^{-\xi} + a_0 + (1 - \frac{1}{2}\sqrt{2}) e^{\xi}}{\left(b_0 a_0 - \frac{1}{2} a_0{}^2 - \frac{1}{4} b_0{}^2\right) e^{-\xi} + b_0 + e^{\xi}} \tag{24}$$

where b_0 and a_0 are free parameters.

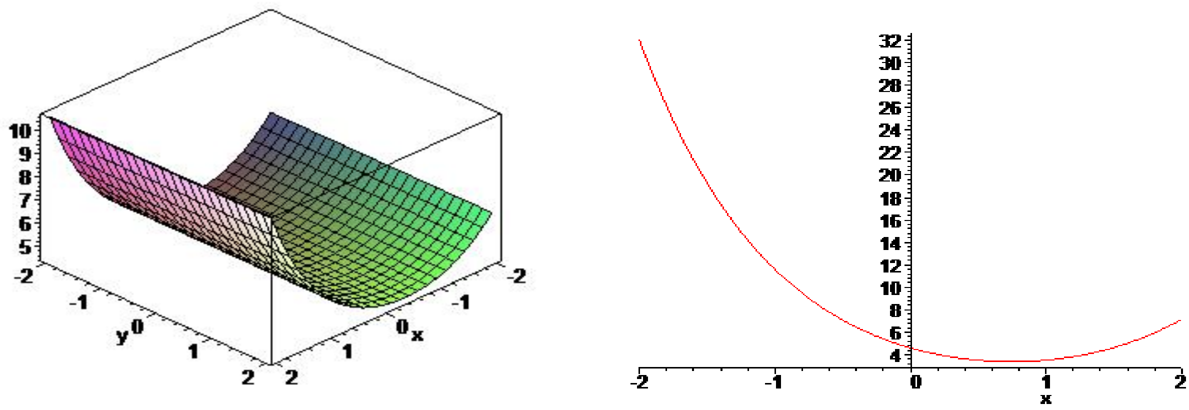

Fig. 6. 3D and 2D plots of travelling wave solutions (Case 6)

The plots indicate the wave solutions for $a_0 = 1, b_0 = 1$ in Equation (24).

<u>Case 7:</u>

$$a_0 = \frac{b_0(a_1{}^2 - a_1 - 1)}{-1 + a_1}, w = \sqrt{-6\, a_1 + 3a_1{}^2 - 2}, w = -\sqrt{-6\, a_1 + 3a_1{}^2 - 2} \tag{25}$$

$$b_{-1} = \frac{1}{8}\frac{b_0{}^2(2a_1{}^2 - 4a_1 + 1)}{(-1 + a_1)^2}, a_{-1} = \frac{1}{8}\frac{b_0{}^2(2a_1{}^2 - 4a_1 + 1)a_1}{(-1 + a_1)^2}$$

Replace these outcomes into Equation (6), we produce a subsequent exact solution,

$$u(\xi) = \frac{\left(\frac{1}{8}\frac{b_0{}^2(2a_1{}^2 - 4a_1 + 1)a_1}{(-1 + a_1)^2}\right) e^{-\xi} + \frac{b_0(a_1{}^2 - a_1 - 1)}{-1 + a_1} + a_1 e^{\xi}}{\left(\frac{1}{8}\frac{b_0{}^2(2a_1{}^2 - 4a_1 + 1)}{(-1 + a_1)^2}\right) e^{-\xi} + b_0 + e^{\xi}} \tag{26}$$

where b_0 and a_1 are free parameters.

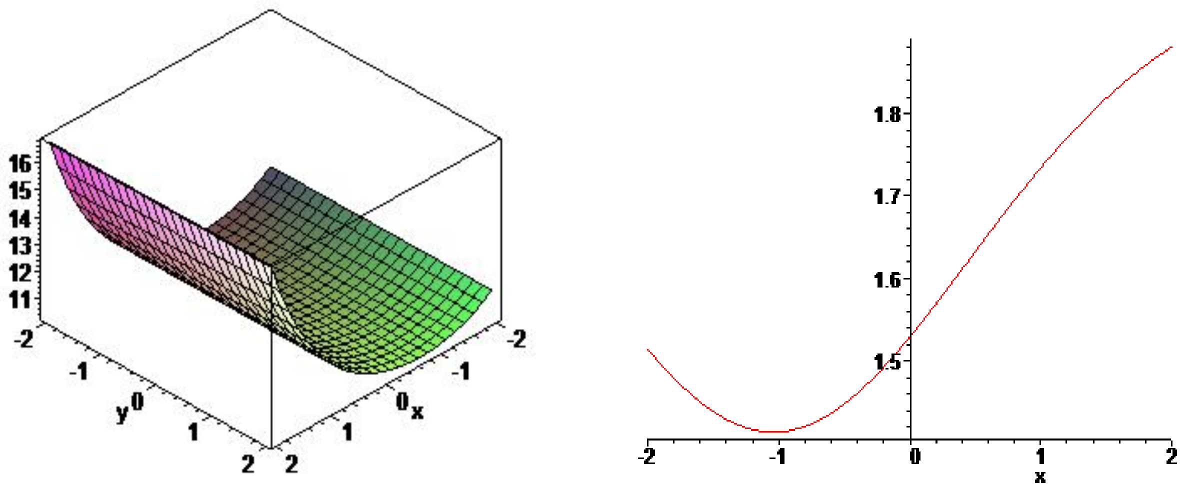

Fig. 7. 3D and 2D plots of travelling wave solutions (Case 7)

The plots indicate the wave solutions for $a_1 = 2, b_0 = 1$ in Equation (26).

Case 8:

$$a_{-1} = -\frac{1}{8}{a_0}^2, b_0 = 0, a_1 = 1, w = I\sqrt{5}, w = -I\sqrt{5}, b_{-1} = \frac{1}{8}{a_0}^2 \tag{27}$$

Replace these outcomes into Equation (6), we produce a subsequent exact solution,

$$u(\xi) = \frac{-{a_0}^2 e^{-\xi} + 8a_0 + 8e^{\xi}}{{a_0}^2 e^{-\xi} + 8e^{\xi}} \tag{28}$$

where a_0 is a free parameter.

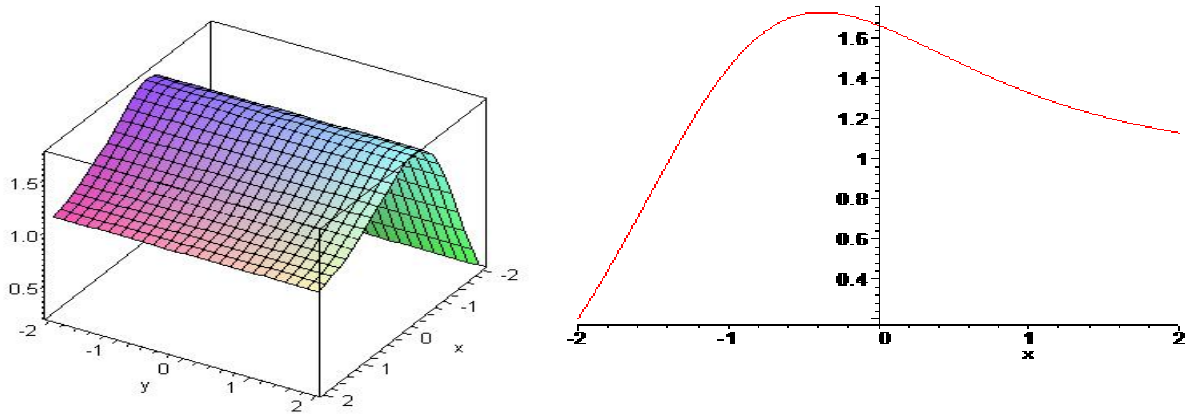

Fig. 8. 3D and 2D plots of travelling wave solutions (Case 8)

The plots indicate the wave solutions for $a_0 = 1$ in Equation (28).

Therefore, the full solutions of the Time-Fractional Bad Modified Boussinesq equation for the above conditions have been obtained. Now let's solve the Time-Fractional Good Modified Boussinesq equation using the Exp-function method.

We balance the linear term of the highest order of Equation (11) u^{iv} with the highest order nonlinear term u^2u'', we set $p = c = 1$ and $q = d = 1$; then the trial solution, Equation (11), reduces to

$$\frac{-1}{B}\left[D_4e^{4\xi}+D_3e^{3\xi}+D_2e^{2\xi}+D_1e^{\xi}+D_0+D_{-1}e^{-\xi}+D_{-2}e^{-2\xi}+D_{-3}e^{-3\xi}+D_{-4}e^{-4\xi}\right]=0 \qquad (29)$$

and for the solutions of Equation (29), all coefficients must be zero.

$B=(b_{-1}e^{-\xi}+\ b_0+\ e^{\xi})^5;$

$D_4\ =w^2a_1b_0-3a_1^3b_0-6a_1a_0+6a_1^2b_0-w^2a_0+3a_1^2a_0;$

$D_3\ =24a_1^2b_{-1}-12a_1b_{-1}-24a_1a_{-1}+12a_1^2a_{-1}+12a_1b_0^2+12a_1a_0^2-12a_1^3b_{-1}-4w^2a_1$
$+9a_1^3b_0^2-21a_0a_1^2b_0-6a_1^2b_0^2-12a_0b_0+4w^2a_1b_{-1}-w^2a_0b_0+w^2a_1b_0^2-12a_0^2+12a_{-1}$
$+18a_1b_0a_0;$

$D_2\ =-12a_1b_0^3-72a_0b_{-1}-12a_1^2b_0^3-12a_{-1}b_0-66a_1^2b_{-1}a_0+12a_0b_0^2-54a_{-1}a_0+9a_0^3$
$+18a_1b_0^2a_0-11w^2a_{-1}b_0+33a_1^3b_{-1}b_0+12a_0a_1^2b_0^2-21a_1^2b_{-1}b_0+54a_{-1}a_0a_1-12a_{-1}a_1b_0$
$+84a_1b_{-1}b_0+4w^2a_0b_{-1}+w^2a_0b_0^2-21a_1b_0a_0^2-w^2a_1b_0^3+78a_1b_{-1}a_0-12a_1^2b_{-1}b_0$
$-6a_0^2b_0+7w^2a_1b_{-1}b_0;$

$D_1\ =-3a_0^3b_0+180a_1b_{-1}^2+36a_0^2b_{-1}+48a_{-1}a_0^2-24a_1^2b_{-1}^2+6a_0^2b_0^2+48a_1a_{-1}^2+36a_1^3b_{-1}^2$
$-180a_{-1}b_{-1}+3a_{-1}a_1^2b_0^2-18a_{-1}a_0a_1b_0-2w^2a_1b_0^2b_{-1}-11w^2a_{-1}b_0^2-78a_{-1}a_0b_0$
$+13w^2a_0b_0b_{-1}+84a_1b_{-1}a_0b_0+51a_0a_1^2b_{-1}b_0+72a_{-1}a_1b_{-1}-84a_1b_{-1}a_0^2-54a_1^2b_{-1}b_0^2$
$+60a_0b_{-1}b_0+4w^2a_1b_{-1}^2-6a_0a_1b_0^3-48a_{-1}^2+w^2a_0b_0^3+12a_{-1}a_1b_0^2-84a_1^2a_{-1}b_{-1}$
$+3a_0^2a_1b_0^2-w^2a_1b_0^4-60a_1b_{-1}b_0^2-4w^2a_{-1}b_{-1};$

$D_0\ =-30a_0a_1b_{-1}^2+75a_0a_1^2b_{-1}^2+10w^2a_0b_{-1}^2+240a_0b_{-1}^2+120a_{-1}a_1b_{-1}b_0+15a_1^2a_{-1}b_{-1}b_0$
$-90a_1^2b_{-1}^2b_0-90a_{-1}^2b_0-30a_{-1}^2a_0b_0^2+15a_{-1}b_0a_0^2-120a_1b_{-1}^2b_0-120a_{-1}b_{-1}b_0$
$-30a_1b_0^2a_0b_{-1}+15a_1a_{-1}^2b_0-180a_0a_{-1}a_1b_{-1}+10w^2a_0b_0^2b_{-1}+15a_1b_0a_0^2b_{-1}+75a_0a_{-1}^2$
$-5w^2a_{-1}b_{-1}b_0-5w^2a_1b_0^3b_{-1}-5w^2a_1b_0b_{-1}^2-5w^2a_{-1}b_0^3-30a_0^3b_{-1}+60a_0^2b_{-1}b_0$
$+30a_0a_{-1}b_{-1};$

$D_{-1}=36a_{-1}^3-6a_0a_{-1}b_0^3-4w^2a_1b_{-1}^3-3a_0^3b_{-1}b_0+3a_0^2a_{-1}b_0^2+6a_0^2b_{-1}b_0^2-w^2a_{-1}b_0^4$
$-84a_{-1}^2a_1b_{-1}-84a_0^2a_{-1}b_{-1}+48a_1a_0^2b_{-1}^2+60a_0b_{-1}^2b_0-60a_{-1}b_{-1}b_0^2+3a_{-1}^2a_1b_0^2$
$+4w^2a_{-1}b_{-1}^2+51a_0a_{-1}^2b_0+48a_{-1}a_1^2b_{-1}^2+72a_{-1}a_1b_{-1}^2+180a_{-1}b_{-1}^2-180a_1b_{-1}^3-48a_1^2b_{-1}^3$
$-54a_{-1}^2b_0^2-24a_{-1}^2b_{-1}+36a_0^2b_{-1}^2+w^2a_0b_{-1}b_0^3+13w^2a_0b_{-1}^2b_0-78a_1b_{-1}^2a_0b_0$
$-11w^2a_1b_0^2b_{-1}^2-18a_0a_{-1}a_1b_0b_{-1}+12a_{-1}b_0^2a_1b_{-1}-2w^2a_{-1}b_0^2b_{-1}+84a_{-1}a_0b_0b_{-1};$

$D_{-2}=w^2a_0b_{-1}^2b_0^2+54a_{-1}a_0a_1b_{-1}^2-21a_{-1}a_0^2b_0b_{-1}-11w^2a_1b_{-1}^3b_0+18a_{-1}b_0^2a_0b_{-1}$

$$+7w^2a_{-1}b_{-1}^2b_0-12a_{-1}b_0a_1b_{-1}^2-21a_{-1}^2a_1b_0b_{-1}-w^2a_{-1}b_0^3b_{-1}+9a_0^3b_{-1}^2-72a_0b_{-1}^3$$

$$+33a_{-1}^3b_0-12a_{-1}^2b_0^3-66a_{-1}^2a_0b_{-1}+84a_{-1}b_{-1}^2b_0-12a_1b_{-1}^3b_0+78a_{-1}a_0b_{-1}^2-6a_0^2b_{-1}^2b_0$$

$$+4w^2a_0b_{-1}^3-12a_{-1}b_{-1}b_0^3+12a_0b_{-1}^2b_0^2+12a_0a_{-1}^2b_0^2-54a_1b_{-1}^3a_0-12a_{-1}^2b_0b_{-1};$$

$$D_{-3}=24a_{-1}^2b_{-1}^2+12a_1b_{-1}^4-12a_{-1}b_{-1}^3+9a_{-1}^3b_0^2-12a_0^2b_{-1}^3-12a_{-1}^3b_{-1}+12a_{-1}a_0^2b_{-1}^2$$

$$+12a_{-1}b_{-1}^2b_0^2-12a_0b_{-1}^3b_0+w^2a_{-1}b_{-1}^2b_0^2-21a_{-1}^2a_0b_{-1}b_0+18a_{-1}a_0b_{-1}^2b_0-w^2a_0b_{-1}^3b_0$$

$$+12a_{-1}^2a_1b_{-1}^2-4w^2a_1b_{-1}^4-6a_{-1}^2b_0^2b_{-1}+4w^2a_{-1}b_{-1}^3-24a_{-1}a_1b_{-1}^3;$$

$$D_{-4}=w^2a_{-1}b_{-1}^3b_0-3a_{-1}^3b_{-1}b_0-w^2a_0b_{-1}^4-6a_{-1}a_0b_{-1}^3+6a_{-1}^2b_{-1}^2b_0+3a_{-1}^2a_0b_{-1}^2;$$

All the coefficients of $e^{n\xi}$ must be zero. Hence, we produce a system of algebraic equations which the Maple can tackle to produce the subsequent cases of solutions:

<u>Case 1:</u>

$$a_0 = a_1b_0\,, a_{-1} = a_1b_{-1} \tag{30}$$

Replace these outcomes into Equation (6), we produce a subsequent exact solution,

$$u(\xi) = a_1 \tag{31}$$

where a_1 is a free parameter.

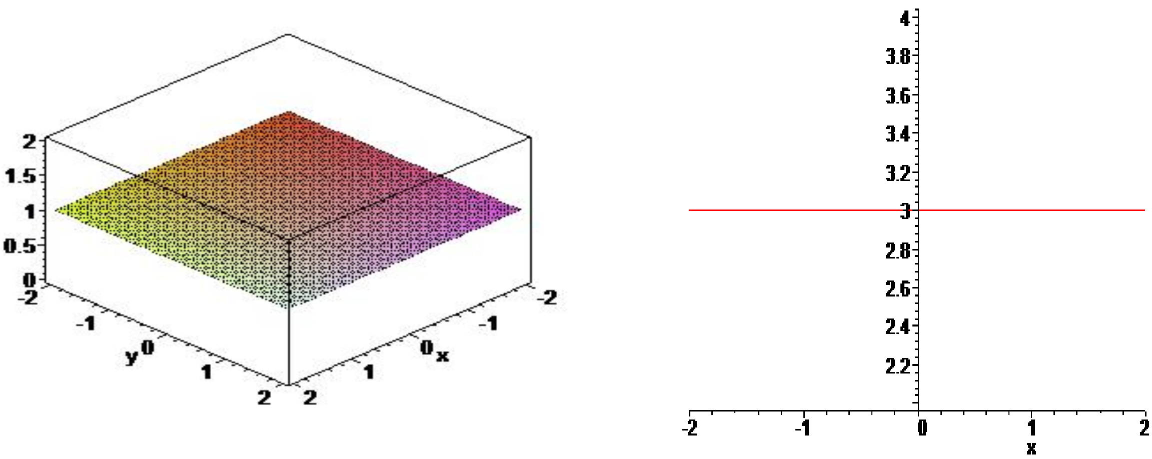

Fig. 9. 3D and 2D plots of travelling wave solutions (Case 1)

The plots indicate the wave solutions for $a_1 = 3$ in Equation (31).

<u>Case 2:</u>

$$a_0 = 0, b_0 = 0,\ a_1 = 1, w = 0,\ b_{-1} = 0 \tag{32}$$

Replace these outcomes into Equation (6), we produce a subsequent exact solution,

$$u(\xi) = \frac{a_{-1}e^{-\xi} + e^{\xi}}{e^{\xi}} \tag{33}$$

where a_{-1} is a free parameter.

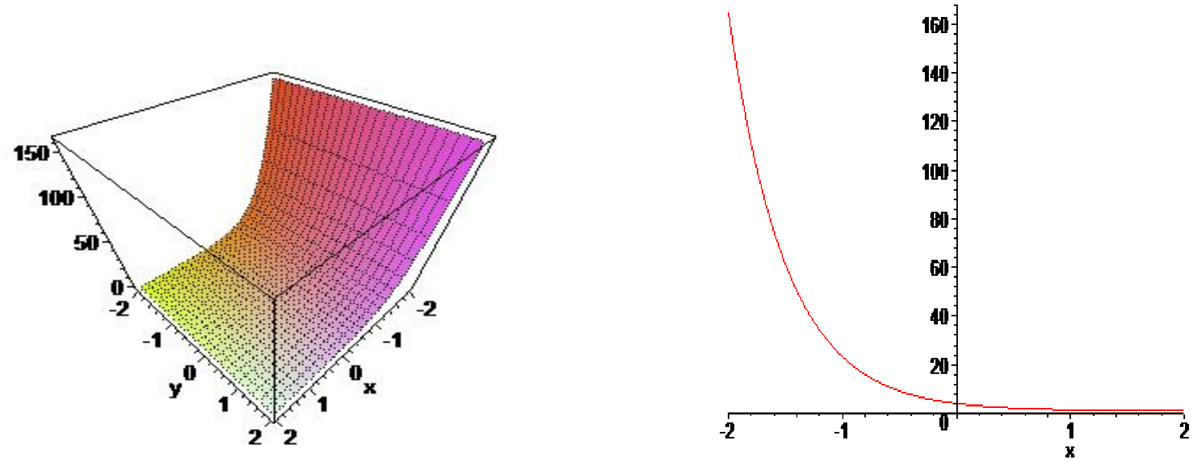

Fig. 10. 3D and 2D plots of travelling wave solutions (Case 2)

The plots indicate the wave solutions for $a_{-1} = 3$ in Equation (33).

Case 3:

$$a_0 = 0,\ b_0 = 0,\ a_1 = 1 + I\sqrt{2},\ a_1 = 1 - I\sqrt{2}\,, w = I\sqrt{6}\,, w = -I\sqrt{6} \tag{34}$$

$$a_{-1} = -(1 + I\sqrt{2})\, b_{-1} + 2b_{-1},\ a_{-1} = -(1 - I\sqrt{2})b_{-1} + 2b_{-1}$$

Replace these outcomes into Equation (6), we produce a subsequent exact solution,

$$u(\xi) = \frac{\left(-(1 + I\sqrt{2})\, b_{-1} + 2b_{-1}\right)e^{-\xi} + (1 + I\sqrt{2})e^{\xi}}{b_{-1}e^{-\xi} + e^{\xi}} \tag{35}$$

where b_{-1} is a free parameter.

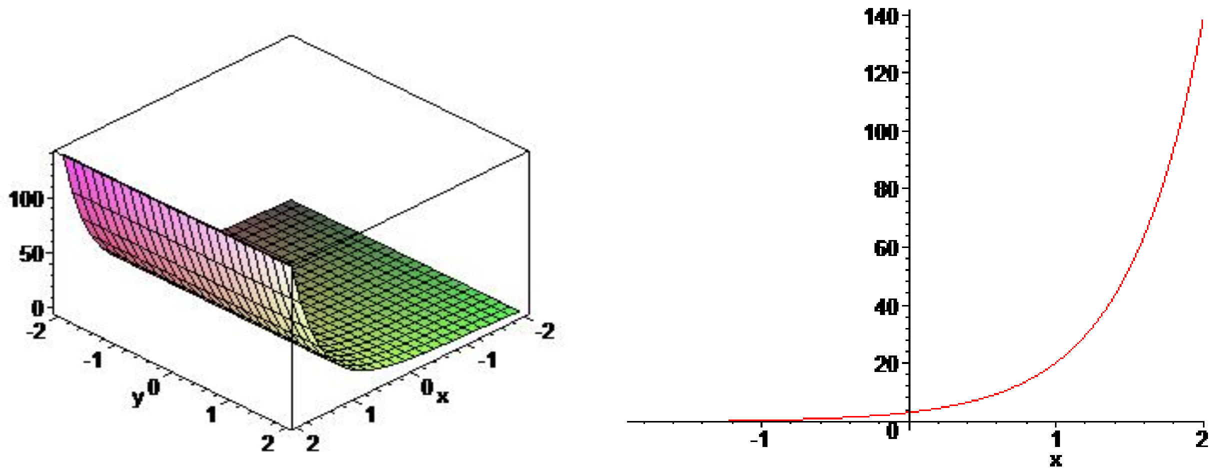

Fig. 11. 3D and 2D plots of travelling wave solutions (Case 3)

The plots indicate the wave solutions for $b_{-1} = 1$ in Equation (35).

Case 4:

$$a_{-1} = 0, b_{-1} = 0, \qquad a_1 = 1 + \frac{1}{2}I\sqrt{2},\ a_1 = 1 - \frac{1}{2}I\sqrt{2}\,, w = \frac{3}{2}I\sqrt{2} \tag{36}$$

$$w = -\frac{3}{2}I\sqrt{2},\ a_0 = -\left(1 - \frac{1}{2}I\sqrt{2}\right)b_0 + 2b_0,\ a_0 = -\left(1 + \frac{1}{2}I\sqrt{2}\right)b_0 + 2b_0$$

Replace these outcomes into Equation (6), we produce a subsequent exact solution,

$$u(\xi)=\frac{-\left(1-\frac{1}{2}\sqrt{2}\right)b_0+2b_0+(1-\frac{1}{2}\sqrt{2})e^{\xi}}{b_0+e^{\xi}} \tag{37}$$

where b_0 is a free parameter.

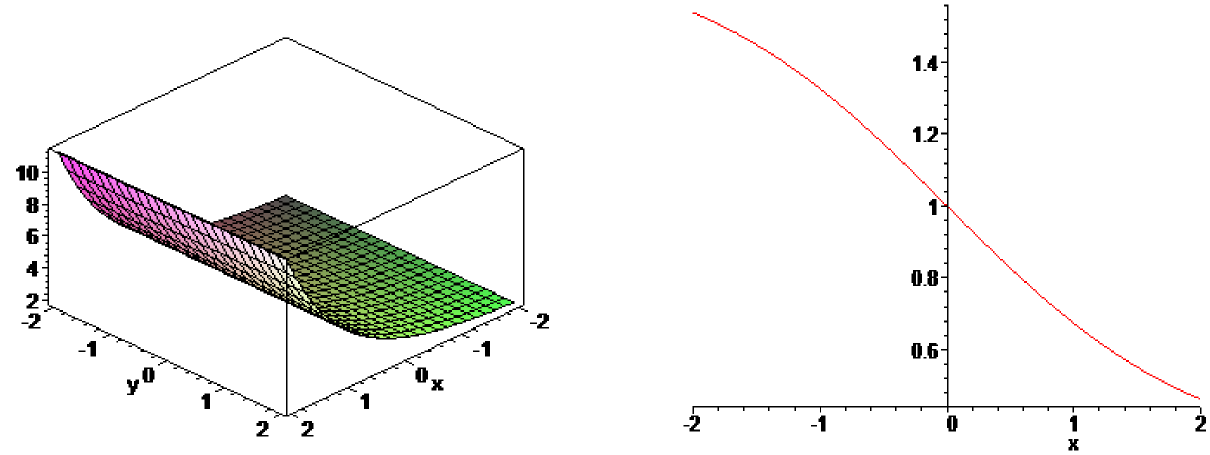

Fig. 12. 3D and 2D plots of travelling wave solutions (Case 4)

The plots indicate the wave solutions for $b_0=1$ in Equation (37).

Case 5:

$$a_{-1}=0, b_0=-a_0, a_1=0, w=0, b_{-1}=\frac{3}{8}{a_0}^2 \tag{38}$$

Replace these outcomes into Equation (6), we produce a subsequent exact solution,

$$u(\xi)=\frac{a_0}{\frac{3}{8}{a_0}^2e^{-\xi}-a_0+e^{\xi}} \tag{39}$$

where a_0 is a free parameter.

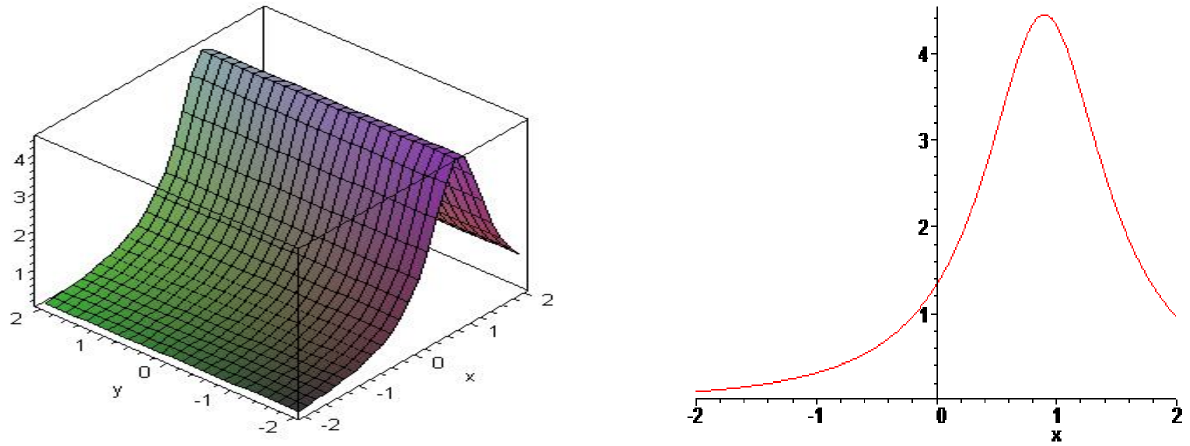

Fig. 13. 3D and 2D plots of travelling wave solutions (Case 5)

The plots indicate the wave solutions for $a_0 = 4$ in Equation (39).

Case 6:

$$a_{-1} = {a_0}^2 - \frac{1}{2}\left(1+\frac{1}{2}I\sqrt{2}\right){a_0}^2 + \left(1+\frac{1}{2}I\sqrt{2}\right)b_0a_0 - \frac{3}{4}\left(1+\frac{1}{2}I\sqrt{2}\right){b_0}^2 - 2b_0a_0 + \frac{3}{2}{b_0}^2$$

$$a_{-1} = {a_0}^2 - \frac{1}{2}\left(1-\frac{1}{2}I\sqrt{2}\right){a_0}^2 + \left(1-\frac{1}{2}I\sqrt{2}\right)b_0a_0 - \frac{3}{4}\left(1-\frac{1}{2}I\sqrt{2}\right){b_0}^2 - 2b_0a_0 + \frac{3}{2}{b_0}^2 \quad (40)$$

$$b_{-1} = -b_0a_0 + \frac{1}{2}{a_0}^2 + \frac{3}{4}{b_0}^2, w = \frac{3}{2}I\sqrt{2}, w = -\frac{3}{2}I\sqrt{2}, a_1 = 1-\frac{1}{2}I\sqrt{2}, a_1 = 1+\frac{1}{2}I\sqrt{2}$$

Replace these outcomes into Equation (6), we produce a subsequent exact solution,

$$u(\xi) = \frac{\left({a_0}^2 - \frac{1}{2}\left(1+\frac{1}{2}I\sqrt{2}\right){a_0}^2 + \left(1+\frac{1}{2}I\sqrt{2}\right)b_0a_0 - \frac{3}{4}\left(1+\frac{1}{2}I\sqrt{2}\right){b_0}^2 - 2b_0a_0 + \frac{3}{2}{b_0}^2\right)e^{-\xi} + a_0 + (1-\frac{1}{2}I\sqrt{2})e^{\xi}}{\left(-b_0a_0 + \frac{1}{2}{a_0}^2 + \frac{3}{4}{b_0}^2\right)e^{-\xi} + b_0 + e^{\xi}} \quad (41)$$

where b_0 and a_0 are free parameters.

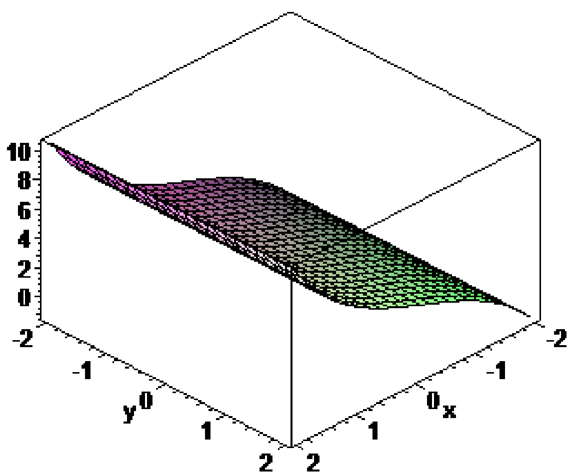

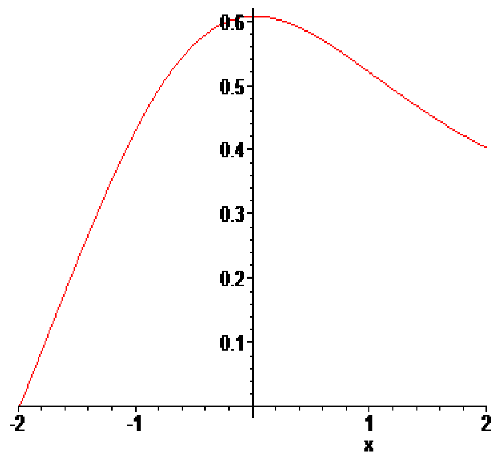

Fig. 14. 3D and 2D plots of travelling wave solutions (Case 6)

The plots indicate the wave solutions for $a_0 = 1, b_0 = 1$ in Equation (41)

Case 7:

$$a_0 = \frac{b_0({a_1}^2 - a_1 + 1)}{-1+a_1}, w = \sqrt{-6\,a_1 + 3{a_1}^2}, w = -\sqrt{-6\,a_1 + 3{a_1}^2} \quad (42)$$

$$b_{-1} = \frac{1}{8}\frac{{b_0}^2(2{a_1}^2 - 4a_1 + 3)}{(-1+a_1)^2}, a_{-1} = \frac{1}{8}\frac{{b_0}^2(2{a_1}^2 - 4a_1 + 3)a_1}{(-1+a_1)^2}$$

Replace these outcomes into Equation (6), we produce a subsequent exact solution,

$$u(\xi) = \frac{\left(\frac{1}{8}\frac{{b_0}^2(2{a_1}^2 - 4a_1 + 3)a_1}{(-1+a_1)^2}\right)e^{-\xi} + \frac{b_0({a_1}^2 - a_1 + 1)}{-1+a_1} + a_1e^{\xi}}{\left(\frac{1}{8}\frac{{b_0}^2(2{a_1}^2 - 4a_1 + 3)}{(-1+a_1)^2}\right)e^{-\xi} + b_0 + e^{\xi}} \quad (43)$$

where b_0 and a_1 are free parameters.

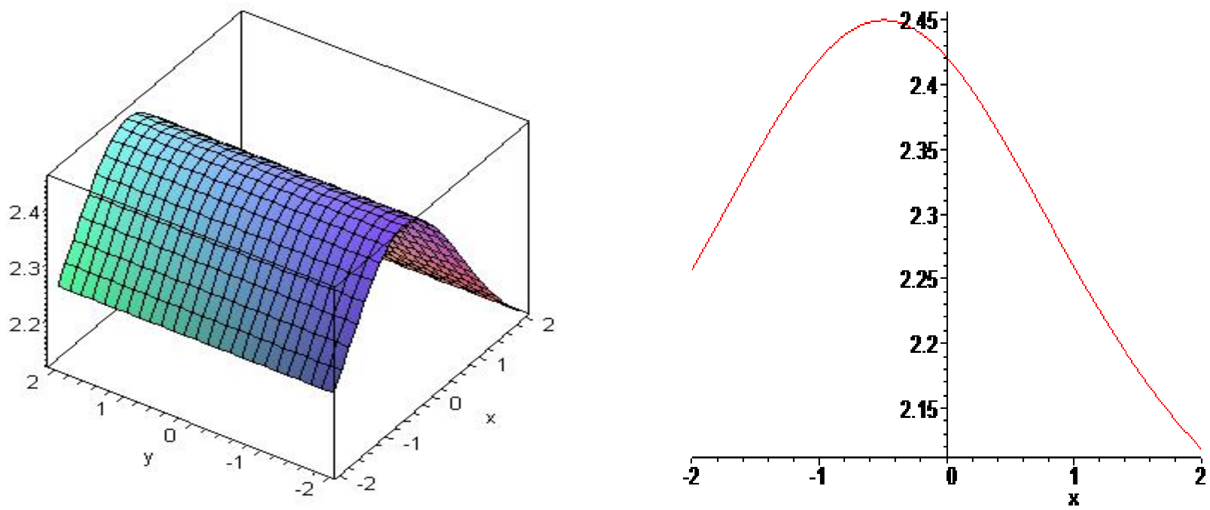

Fig.15. 3D and 2D plots of travelling wave solutions (Case 7)

The plots indicate the wave solutions for $a_1 = 2, b_0 = 1$ in Equation (43).

<u>Case 8:</u>

$$a_{-1} = \frac{1}{8}{a_0}^2, b_0 = 0, \qquad a_1 = 1, w = I\sqrt{3}\,, w = -I\sqrt{3},\ b_{-1} = \frac{1}{8}{a_0}^2 \tag{44}$$

Replace these outcomes into Equation (6), we produce a subsequent exact solution,

$$u(\xi) = \frac{-{a_0}^2 e^{-\xi} + 8a_0 + 8e^{\xi}}{{a_0}^2 e^{-\xi} + 8e^{\xi}} \tag{45}$$

where a_0 is a free parameter.

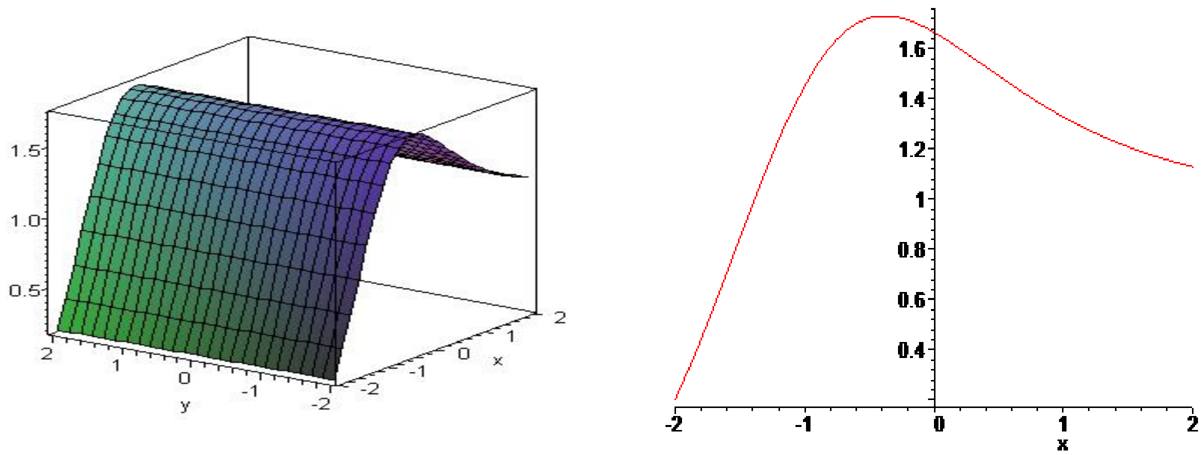

Fig. 16. 3D and 2D plots of travelling wave solutions (Case 8)

The plots indicate the wave solutions for $a_0 = 1$ in Equation (45).

Remark: With the aid of Maple, we have verified all solutions in Section 3 by putting them back into the originals Equations (10) and (11).

4. Conclusion

In this paper, we have been obtained the new exact solution of the Conformable Time Fractional Bad and Good Modified Boussinesq Equations. We converted the Conformable Time Fractional Bad and Good Modified Boussinesq Equations into an ordinary differential equation with the help of a travelling wave transformation. We obtained new exact solutions by using the Exp-function method, which is different from previous literature works. These results show that the Exp-function method is a powerful and effective method to obtain the exact solutions of nonlinear evolution equations born in mathematical physics and non-linear dynamic systems.

Author Contributions

All the authors contributed equally to this work. They all read and approved the last version of the manuscript.

Conflict of Interest

The authors declare no conflict of interest.

References

[1] J. H. He, X. H. Wu, *Exp-Function Method for Nonlinear Wave Equations*, Chaos, Soliton and Fractals 30(3) (2006) 700–708.

[2] E. M. E. Zayed, M. A. M. Abdelaziz, *The Tanh- Function Method Using a Generalized Wave Transformation for Nonlinear Equations*, International Journal of Nonlinear Sciences and Numerical Simulation 11(8) (2010) 595–601.

[3] E. Fan, H. Zhang, *A Note on the Homogeneous Balance Method*, Physics Letters A 246(5) (1998) 403–406.

[4] Y. Gurefe, A. Sönmezoğlu, E. Mrsırlı, *Application of The Trial Equation Method for Solving Some Nonlinear Evolution Equations Arising in Mathematical Physics*, Pramana 77(6) (2011) 1023–1029.

[5] N. A. Kudryashov, *A Note on the* $(\frac{G'}{G})$*-expansion Method*, Applied Mathematics and Computation 217(4) (2010) 1755–1758.

[6] P. N. Ryabov, D. I. Sinelshchikov, M. B. Kochanov, *Application of the Kudryashov Method for Finding Exact Solutions of the High Order Nonlinear Evolution Equations*, Applied Mathematics and Computation 218(7) (2011) 3965–3972.

[7] J. H. He, *Exp-function Method for Fractional Differential Equations*, International Journal of Nonlinear Sciences and Numerical Simulation 14(6) (2013) 363–366.

[8] Z. Öztürk, H. Bilgil, *Exact Solutions of Rosenzweig-Macarthur (RM) Model Equations by Using Exp Function Method*, European Journal of Science and Technology (16) (2019) 427–433.

[9] A. Ebaid, *Application of the Exp-Function Method for Solving Some Evolution Equations with Nonlinear Terms of Any Orders*, Zeitschrift fur Naturforschung A 65(12) (2010) 1039–1044.

[10] S. Zhang, *Exp-Function Method for Riccati Equation and New Exact Solutions with Two Arbitrary Functions of (2 + 1)-Dimensional Konopelchenko-Dubrovsky Equations*, Applied Mathematics and Computation 216(5) (2010) 1546–1552.

[11] R. Khalil, M. A. Horani, A. Yousef, M. Sababheh, *A New Definition of Fractional Derivative*, Journal of Computational and Applied Mathematics 264 (2014) 65–70.

[12] I. Podlubny, Fractional Differential Equations: An Introduction to Fractional Derivatives, Fractional Differential Equations, to Methods of Their Solution and Some of Their Applications, Elsevier, 1998.

[13] A. Atangana, I. Koca, *Chaos in A Simple Nonlinear System with Atangana–Baleanu Derivatives with Fractional Order*, Chaos, Solitons and Fractals 89 (2016) 447–454.

[14] N. S. Kottakkaran, O. I Ilhan, S. T. Abdulazeez, J. Manafian, S. A. Mohammed, M. S. Osman, *Novel Multiple Soliton Solutions for Some Nonlinear Pdes via Multiple Exp-Function Method*, Results in Physics 21 (2021) 103769.

[15] K. A. Gepreel, E. M. E. Zayed, *Multiple Wave Solutions for Nonlinear Burgers Equations Using the Multiple Exp-Function Method*, International Journal of Modern Physics C (2021) 2150149.

[16] H. M. Ahmed, M. M. A. El-Sheikh, A. H. Arnous, W. B. Rabiel, *Solitons and Other Solutions to (N+1)-Dimensional Modified Zakharov–Kuznetsov Equation by Exp-Function Method*, SeMA Journal 78 (2021) 1–13.

[17] A. G. Hossam, H. Abd-Allah, M. Zakarya, *Exact Solutions of Stochastic Fractional Korteweg De–Vries Equation with Conformable Derivatives*, Chinese Physics B 29(3) (2020) 30203.

[18] H. C. Yaslan, A. Girgin, *Exp-Function Method for The Conformable Space-Time Fractional STO, ZKBBM and Coupled Boussinesq Equations*, Arab Journal of Basic and Applied Sciences 26(1) (2019) 163–170.

[19] L. K. Ravi, S. S. Ray, S. Sahoo, *New Exact Solutions of Coupled Boussinesq–Burgers Equations by Exp-Function Method*, Journal of Ocean Engineering and Science 2(1) (2017) 34–46.

[20] E. M. Eskandari, N. Taghizadeh, *Exact Solutions of Two Nonlinear Space-time Fractional Differential Equations by Application of Exp-function Method*, Applications and Applied Mathematics: An International Journal 15(2) (2020) 970–977.

[21] H. Durur, O. Taşbozan, A. Kurt, *New Analytical Solutions of Conformable Time Fractional Bad and Good Modified Boussinesq Equations*, Applied Mathematics and Nonlinear Sciences 5(1) (2020) 447–454.

[22] A. Ebaid, *An Improvement on The Exp-Function Method When Balancing the Highest Order Linear and Nonlinear Terms*, Journal of Mathematical Analysis and Applications 392(1) (2012) 1–5.

[23] J. Boussinesq, *Thorie Des Ondes Et Des Remous Qui Se Propagent Le Long D'un Canal Rectangulaire Horizantal,En Communiquant Au Liquide Contenu Dans Ce Canal Des Vitesses Sensiblement Pareilles De La Surface Au Fond*, Journal de Mathmmatiques Pures at Appliques (1872) 55–108.

Journal of New Theory
ISSN: 2149-1402

37 (2021) 26-34
Journal of New Theory
https://dergipark.org.tr/en/pub/jnt
Open Access

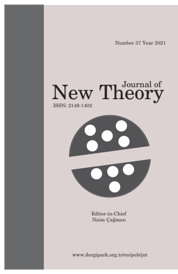

The Transmittal-Characteristic Function of Three-Interval Periodic Sturm-Liouville Problem with Transmission Conditions

Kadriye Aydemir[1], **Oktay Mukhtarov**[2]

Article History
Received: 03 Nov 2021
Accepted: 28 Dec 2021
Published: 31 Dec 2021
10.53570/jnt.1018600
Research Article

Abstract — In this paper, we study the periodic Sturm-Liouville problem, defined on three non-intersecting intervals with four supplementary conditions which are imposed at two internal points of interaction, the so-called transmission conditions. We first prove that the eigenvalues are real and the system of eigenfunctions is an orthogonal system. Secondly, some auxiliary initial-value problems are defined and transmittal-characteristic function is constructed in terms of solutions of these initial-value problems. Finally, we establish that the eigenvalues of the considered problem are the zeros of the transmittal-characteristic function.

Keywords — *Periodic transmittal Sturm-Liouville problem, characteristic function, spectrum*

Mathematics Subject Classification (2020) — 34B24, 34L15

1. Introduction

This paper is aimed at studying a discontinuous spectral problem consisting of the three-interval Sturm-Liouville equation

$$\Xi_\lambda y := -y''(x) + q(x)y = \lambda y(x) \quad x \in [\daleth_1, c_1) \cup (c_1, c_2) \cup (c_2, \daleth_2] \tag{1}$$

the periodic boundary conditions

$$\ell_1 y := y(\daleth_1) - y(\daleth_2) = 0 \tag{2}$$

$$\ell_2 y := y'(\daleth_1) - y'(\daleth_2) = 0 \tag{3}$$

and supplementary transmission conditions, which are imposed at the points of interaction c_1 and c_2, given by

$$\ell_3 y := y(c_1^-) - y(c_1^+) = 0 \tag{4}$$

$$\ell_4 y := y'(c_1^-) - y'(c_1^+) = 0 \tag{5}$$

and

$$\ell_5 y := y(c_2^-) - \beta y(c_2^+) = 0 \tag{6}$$

$$\ell_6 y := y'(c_2^-) - \frac{1}{\beta} y'(c_2^+) = 0 \tag{7}$$

respectively, where $q(x)$ is a real-valued function, $\lambda \in C$ is a complex spectral parameter and the coefficient $\beta \neq 0$ is real numbers. In investigating the periodic flow in a rod, C. Sturm and J. Liouville

[1]kadriyeaydemr@gmail.com (Corresponding Author); [2]omukhtarov@yahoo.com
[1]Department of Mathematics, Faculty of Arts and Sciences, Amasya University, Amasya, Turkey
[2]Department of Mathematics, Faculty of Arts and Sciences, Tokat Gaziosmanpaşa University, Tokat, Turkey

in the first half of the 19th century were led to the definition of class of Sturm-Liouville problems consisting of self-adjoint linear differential equation of the form

$$-\frac{d}{dx}(K(x)\frac{dF(x)}{dx})+\ell(x)F(x)=\lambda q(x)F(x) \quad for\ x\in[a,b] \tag{8}$$

together with the boundary conditions of the form

$$K(a)F'(a)-hF(a)=0 \tag{9}$$

$$K(b)F'(b)-HF(b)=0 \tag{10}$$

They obtained some results that characterized by the general and qualitative nature of the solutions. They also proved that there exists infinitely countable number of values $\lambda_1,\lambda_2,...$ of spectral parameter λ with the corresponding non-trivial solutions $F_1(x),F_2(x),...$, the so- called eigenfunctions, and discussed the qualitative behavior of these eigenvalues and eigenfunctions, such as the asymptotics of eigenvalues, the zeros of the eigenfunctions that could be used in a variety of physical situations.These results have inspired much of branches of modern analysis and spectral theory of linear differential and integral operators, and continue to do so. The existence of periodic and oscillatory eigenfunctions important in the spectral theory of differential operators. We know that periodic boundary value problems of Sturm-Liouville type have been widely investigated due to their application in physics and engineering. For example, consider the heated string bent into a circle. Since the two ends of this string are physically the same, we would expect that the temperature and the temperature gradient to be equal at these endpoints. This situation is modelled by boundary conditions of the form

$$u(a)=u(b), \quad u'(a)=u'(b)$$

which are called periodic boundary conditions.

Periodic Sturm-Liouville problems for various type differential equations have been studied extensively in the literature(see, for example, [1–5] and references therein). In the paper [2], the authors considered the problem

$$\begin{cases} -u''+h(s)u=\lambda g(s,u), \quad 0\le s\le\pi \\ u(0)=u(2\pi), \quad u'(0)=u'(2\pi) \end{cases}$$

and

$$\begin{cases} u''+h(s)u=\lambda g(s,u), \quad 0\le s\le\pi \\ u(0)=u(2\pi), \quad u'(0)=u'(2\pi) \end{cases}$$

where $h\in L^1(0,2\pi), g:[0,2\pi]\times\mathbb{R}^+\to\mathbb{R}^+$ is continuous, λ is a positive parameter. In the work [3], a new existence theorems for a nonlinear periodic boundary value problem of first-order differential equations with impulses are established. In the article [4], the topological degree theory is applied to show the existence of positive solutions to the periodic Sturm-Liouville problem. In the paper [5] the eigenvalues of regular periodic and semi periodic Sturm-Liouville problems are considered. Binding and Rynne [6] considered the nonlinear Sturm-Liouville problem

$$\begin{cases} (-\rho y)''+\varrho y=ay^+-by^-+\lambda y \\ y(0)=y(2\pi), \quad (\rho y)'(0)=(\rho y)'(2\pi) \end{cases}$$

where $\frac{1}{\rho},\varrho\in L^1(0,2\pi)$ with $\rho>0$ on $(0,2\pi)$, $a,b\in L^1(0,2\pi)$ λ is a real parameter, and $y^{\pm}(t)=\max\{\pm y(t),0\}$ for $t\in[0,2\pi]$. It is showed that a sequence of half-eigenvalues exists and obtained degree theoretic properties associated with set of half-eigenvalues. In recent years, many spectral properties of periodic Sturm-Liouville problems have been studied and many techniques have been developed by many authors(see [7–16]).

Boundary value problems including transmission conditions appears in many fields of natural sciences. Recently, such type of transmission problems have been an important topic in theoretical and applied mathematics (see, [17–28]). In this study we will investigate some basic spectral properties of a new type periodic Sturm-Liouville problems. Namely, the differential equations are defined on three separated subintervals and the boundary conditions are set not only at the ends of the considered interval, but also at the internal points of interaction. We proved that the eigenvalues are real and the eigenfunctions belongs to distinct eigenvalues are orthogonal. We also defined a new type of characteristic function, the roots of which coincide with the eigenvalues.

2. Eigenvalues and Eigenfunctions of the Considered problem

Theorem 2.1. The eigenvalues of the three-interval periodic problem (1) – (7) are all real.

PROOF. Let λ be an eigenvalue of the considered problem (1) – (7) with an eigenfunction ψ. Taking the complex conjugate and note that the coefficient β is real, we arrive at

$$\overline{-\psi''(x)} = \overline{\lambda\psi}(x) \tag{11}$$

$$\overline{\psi(\daleth_1)} = \overline{\psi(\daleth_2)}, \quad \overline{\psi'(\daleth_1)} = \overline{\psi'(\daleth_2)} \tag{12}$$

$$\overline{\psi(c_1^-)} = \overline{\psi(c_1^+)}, \quad \overline{\psi'(c_1^-)} = \overline{\psi'(c_1^+)} \tag{13}$$

$$\overline{\psi(c_2^-)} = \beta\overline{\psi(c_2^+)}, \quad \overline{\psi'(c_2^-)} = \frac{1}{\beta}\overline{\psi'(c_2^+)} \tag{14}$$

This implies that $(\overline{\lambda}, \overline{\psi})$ is also an eigen pair for the problem (1) – (7). By the previous theorem we have

$$\begin{aligned} 0 &= (\lambda - \overline{\lambda})\Big(\int_{\daleth_1}^{c_1^-} \overline{\psi(x)}\psi(x)dx + \int_{c_1^+}^{c_2^-} \overline{\psi(x)}\psi(x)dx + \int_{c_2^+}^{\daleth_2} \overline{\psi(x)}\psi(x)dx\Big) \\ &= (\lambda - \overline{\lambda})\Big(\int_{\daleth_1}^{c_1^-} |\psi(x)|^2dx + \int_{c_1^+}^{c_2^-} |\psi(x)|^2dx + \int_{c_2^+}^{\daleth_2} |\psi(x)|^2dx\Big) \end{aligned} \tag{15}$$

Since ψ, being an eigenfunction, is not identically equal to zero on $[\daleth_1, c_1) \cup (c_1, c_2) \cup (c_2, \daleth_2]$

$$\int_{\daleth_1}^{c_1^-} |\psi(x)|^2dx + \int_{c_1^+}^{c_2^-} |\psi(x)|^2dx + \int_{c_2^+}^{\daleth_2} |\psi(x)|^2dx > 0$$

So, $\lambda = \overline{\lambda}$. Thus λ is real. The proof is complete. □

Remark 2.2. Since all eigenvalues of the considered problem (1) – (7) are real, without loss of generality we can now assume that the corresponding eigenfunctions are also real-valued.

Theorem 2.3. Let λ_k and λ_r are two distinct eigenvalues of the problem (1) – (7) on $[\daleth_1, c_1) \cup (c_1, c_2) \cup (c_2, \daleth_2]$, then their corresponding eigenfunctions ψ_k and ψ_r satisfy the following equality

$$\int_{\daleth_1}^{c_1^-} \psi_k(x)\psi_r(x)dx + \int_{c_1^+}^{c_2^-} \psi_k(x)\psi_r(x)dx + \int_{c_2^+}^{\daleth_2} \psi_k(x)\psi_r(x)dx = 0 \tag{16}$$

that is the eigenfunctions ψ_k and ψ_r are orthogonal in the Hilbert space $L_2(((\daleth_1, c_1) \oplus (c_1, c_2) \oplus (c_2, \daleth_2))$.

PROOF. Since ψ_k and ψ_r are eigenfunctions corresponding to the eigenvalues λ_k and λ_r respectively, we have

$$-\psi_k''(x) = \lambda_k\psi_k(x) \tag{17}$$

and

$$-\psi_r''(x) = \lambda_r \psi_r(x) \tag{18}$$

Multiplying (17) by ψ_r and (18) by ψ_k, then subtracting we get

$$(\lambda_k - \lambda_r)(\int_{\urcorner_1}^{c_1^-} \psi_k(x)\psi_r(x)dx + \int_{c_1^+}^{c_2^-} \psi_k(x)\psi_r(x)dx + \int_{c_2^+}^{\urcorner_2} \psi_k(x)\psi_r(x)dx)$$

$$= (\psi_k'\psi_r - \psi_r'\psi_k)|_{\urcorner_1}^{c_1^-} + (\psi_k'\psi_r - \psi_r'\psi_k)|_{c_1^+}^{c_2^-} + (\psi_k'\psi_r - \psi_r'\psi_k)|_{c_2^+}^{\urcorner_2}. \tag{19}$$

By using the boundary and transmission conditions we find

$$(\lambda_k - \lambda_r)(\int_{\urcorner_1}^{c_1^-} \psi_k(x)\psi_r(x)dx + \int_{c_1^+}^{c_2^-} \psi_k(x)\psi_r(x)dx + \int_{c_2^+}^{\urcorner_2} \psi_k(x)\psi_r(x)dx) = 0 \tag{20}$$

Since $\lambda_k \neq \lambda_r$ we get the equality (16). □

Theorem 2.4. The periodic problem $(1) - (7)$ is self-adjoint.

PROOF. Consider the periodic Sturm-Liouville problem $(1) - (7)$. Let $u,\ \vartheta \in C_2((\urcorner_1, c_1) \oplus (c_1, c_2) \oplus (c_2, \urcorner_2))$ that satisfies the periodic eigenvalue problem $(1) - (7)$. We shall prove that

$$\int_{\urcorner_1}^{c_1^-} [u\Xi_\lambda \vartheta - \vartheta \Xi_\lambda u]dx + \int_{c_1^+}^{c_2^-} [u\Xi_\lambda \vartheta - \vartheta \Xi_\lambda u]dx + \int_{c_2^+}^{\urcorner_2} [u\Xi_\lambda \vartheta - \vartheta \Xi_\lambda u]dx = 0.$$

By using the definition of the differential operator Ξ_λ we can show that

$$\vartheta \Xi_\lambda u - u\Xi_\lambda \vartheta = \frac{d}{dx}(\vartheta u' - u\vartheta')$$

Now integrating by parts over $[\urcorner_1, c_1) \cup (c_1, c_2) \cup (c_2, \urcorner_2]$ we obtain

$$\int_{\urcorner_1}^{c_1^-} [\vartheta \Xi_\lambda u - u\Xi_\lambda \vartheta]dx + \int_{c_1^+}^{c_2^-} [\vartheta \Xi_\lambda u - u\Xi_\lambda \vartheta]dx + \int_{c_2^+}^{\urcorner_2} [\vartheta \Xi_\lambda u - u\Xi_\lambda \vartheta]dx$$

$$= (\vartheta u' - u\vartheta')|_{\urcorner_1}^{c_1^-} + (\vartheta u' - u\vartheta')|_{c_1^+}^{c_2^-} + (\vartheta u' - u\vartheta')|_{c_2^+}^{\urcorner_2}. \tag{21}$$

To satisfy the conditions $(2) - (3)$ we get

$$u(\urcorner_1) = u(\urcorner_2),\ u'(\urcorner_1) = u'(\urcorner_2)$$

and

$$\vartheta(\urcorner_1) = \vartheta(\urcorner_2),\ \vartheta'(\urcorner_1) = \vartheta'(\urcorner_2).$$

By using this equalities we find

$$W(u, \vartheta; \urcorner_1) - W(u, \vartheta; \urcorner_2) = 0 \tag{22}$$

Similarly by using the transmission conditions $(4) - (7)$ we obtain

$$W(u, \vartheta; c_1^-) - W(u, \vartheta; c_1^+) = 0 \tag{23}$$

and

$$W(u,\vartheta;c_2^-)-W(u,\vartheta;c_2^+)=0 \tag{24}$$

Substituting the equalities (22), (23), (24) in (21) we get

$$\int_{\daleth_1}^{c_1^-}[\vartheta\Xi_\lambda u-u\Xi_\lambda\vartheta]dx+\int_{c_1^+}^{c_2^-}[\vartheta\Xi_\lambda u-u\Xi_\lambda\vartheta]dx+\int_{c_2^+}^{\daleth_2}[\vartheta\Xi_\lambda u-u\Xi_\lambda\vartheta]dx=0$$

which completes the proof. □

3. The Transmittal-Characteristic Function

Consider the initial value problem

$$-y''+q(x)y=\lambda y, x\in(\alpha_1,\alpha_2) \tag{25}$$

$$y(\alpha+0)=r(\lambda), y'(\alpha+0)=s(\lambda) \tag{26}$$

where $r,s:\mathbb{C}\to\mathbb{C}$ are given complex functions. Using the method in [29], we can prove the following Lemma.

Lemma 3.1. Assume that the real valued function $q(x)$ is continuous on (α_1,α_2) and the complex functions $r(\lambda),s(\lambda)$ are differentiable on whole complex plane $\mathbb{C}$(i.e. $r(\lambda)$ and $s(\lambda)$ are entire functions). Then, the initial value problem (25)-(26) has an unique solution $y=y(x,\lambda)$ which is an entire function of λ for each fixed $x\in(\alpha_1,\alpha_2)$.

Let us construct two basic solutions

$$\varphi(x,\lambda)=\begin{cases}\varphi_1(x,\lambda), & x\in[\daleth_1,c_1)\\ \varphi_2(x,\lambda), & x\in(c_1,c_2)\\ \varphi_3(x,\lambda), & x\in(c_2,\daleth_2]\end{cases},\ \chi(x,\lambda)=\begin{cases}\chi_1(x,\lambda), & x\in[\daleth_1,c_1)\\ \chi_2(x,\lambda), & x\in(c_1,c_2)\\ \chi_3(x,\lambda), & x\in(c_2,\daleth_2]\end{cases}$$

according to the following iterative technique. First, we define the solution $\varphi_1(x,\lambda)$. Let $\varphi_1(x,\lambda)$ be the solution of the equation (1) on $\Omega_1:=[\daleth_1,c_1)$ subject to the initial conditions

$$y(\daleth_1)=1,\quad y'(\daleth_1)=0 \tag{27}$$

Second, we shall define the solution $\varphi_2(x,\lambda)$ of Eq. (1) on $\Omega_2:=(c_1,c_2)$ by means of the solution $\varphi_1(x,\lambda)$ chosen so as to satisfy the initial conditions

$$y(c_1^+)=\varphi_1(c_1^-,\lambda),\quad y'(c_1^+)=\varphi_1'(c_1^-,\lambda) \tag{28}$$

Finally, we can define the solution $\varphi_3(x,\lambda)$ of Eq. (1) on $\Omega_3:=(c_2,\daleth_2]$ by means of the solution $\varphi_2(x,\lambda)$ satisfying the initial conditions

$$y(c_2^+)=\frac{1}{\beta}\varphi_2(c_2^-,\lambda),\quad y'(c_2^+)=\beta\varphi_2'(c_2^-,\lambda). \tag{29}$$

Using the same iterative technique as in defining the solutions $\varphi_1(x,\lambda)$, $\varphi_2(x,\lambda)$ and $\varphi_3(x,\lambda)$, we construct other solutions $\chi_1(x,\lambda)$, $\chi_2(x,\lambda)$ and $\chi_3(x,\lambda)$ as a solution to the Eq.(1) chosen as to satisfy the initial conditions

$$y(\daleth_1)=0,\quad y'(\daleth_1)=1 \tag{30}$$

$$y(c_1^+)=\chi_1(c_1^-,\lambda),\quad y'(c_1^+)=\chi_1'(c_1^-,\lambda). \tag{31}$$

and

$$y(c_2^+) = \frac{1}{\beta}\chi_2(c_2^-, \lambda), \quad y'(c_2^+) = \beta\chi_2'(c_2^-, \lambda) \tag{32}$$

respectively. By virtue of the Lemma 3.1, each of the solutions $\varphi_i(x, \lambda)$ and $\chi_i(x, \lambda)(i = 1, 2, 3)$ exists, unique for any fixed λ and is an entire function with respect to the complex variable λ for any fixed x.

Theorem 3.2. Each of the pair $\varphi_i(x, \lambda)$, $\chi_i(x, \lambda)$ is linearly independent solutions of Eq.(1) on the interval Ω_i, where $\Omega_1 = [\urcorner_1, c_1)$, $\Omega_2 = (c_1, c_2)$, $\Omega_3 = (c_2, \urcorner_2]$.

Proof. To prove it is sufficient to show that the Wronskians

$$W_\lambda(\varphi_i, \chi_i; x) =: \varphi_i(x, \lambda)\chi_i'(x, \lambda) - \varphi_i'(x, \lambda)\chi_i(x, \lambda)$$

are not equal to zero on Ω_i. □

Since the Wronskians $W_\lambda(\varphi_i, \chi_i; x)$ does not depend on variable x, Using the initial conditions (27 and (30) we have

$$W_\lambda(\varphi_1, \chi_1; x) = W_\lambda(\varphi_1, \chi_1; \urcorner_1) = 1 \neq 0. \tag{33}$$

Using (28), (31) and (33)

$$\begin{aligned} W_\lambda(\varphi_2, \chi_2; x) &= W_\lambda(\varphi_2, \chi_2; c_1^+) \\ &= \varphi_2(c_1^+, \lambda)\chi_2'(c_1^+, \lambda) - \varphi_2'(c_1^+, \lambda)\chi_2(c_1^+, \lambda) \\ &= \varphi_1(c_1^-, \lambda)\chi_1'(c_1^-, \lambda) - \varphi_1'(c_1^-, \lambda)\chi_1(c_1^-, \lambda) \\ &= W_\lambda(\varphi_1, \chi_1; c_1^-) = W_\lambda(\varphi_1, \chi_1; \urcorner_1) = 1 \neq 0. \end{aligned} \tag{34}$$

Similarly, using (29), (32) and 34) we get

$$\begin{aligned} W_\lambda(\varphi_3, \chi_3; x) &= W_\lambda(\varphi_3, \chi_3; c_2^+) \\ &= \varphi_3(c_2^+, \lambda)\chi_3'(c_2^+, \lambda) - \varphi_3'(c_2^+, \lambda)\chi_3(c_2^+, \lambda) \\ &= (\frac{1}{\beta}\varphi_2(c_2^-, \lambda))(\beta\chi_2'(c_2^-, \lambda)) - (\beta\varphi_2'(c_2^-, \lambda))(\frac{1}{\beta}\chi_2(c_2^-, \lambda)) \\ &= W_\lambda(\varphi_2, \chi_2; c_2^-) = 1 \neq 0. \end{aligned} \tag{35}$$

The proof is complete.

Theorem 3.3. A complex number λ is an eigenvalue of the transmittal-periodic problem (1)-(7) if and only if

$$\Delta(\lambda) := W_\lambda(\varphi_2, \chi_2; c_2^+)W_\lambda(\varphi_2, \chi_2; c_2^-)[W_\lambda(\varphi_3, \chi_3; \urcorner_1) + 1 - \varphi_3(\urcorner_2) - \chi_3'(\urcorner_2)] = 0.$$

Proof. Let $y_0(x, \lambda_0)$ be any eigenfunction belonging to the eigenvalue λ_0. It follows from the Theorem 3.2 that the solutions $\varphi_i(x, \lambda_0)$ and $\chi_i(x, \lambda_0)$ are linearly independent solutions of (1) on the Ω_i $i = 1, 2, 3$. Therefore the eigenfunction $y_0(x, \lambda_0)$ may be represented as

$$y_0(x, \lambda_0) = \begin{cases} \delta_1\varphi_1(x, \lambda_0) + \gamma_1\chi_1(x, \lambda_0) \text{ for } x \in \Omega_1 \\ \delta_2\varphi_2(x, \lambda_0) + \gamma_2\chi_2(x, \lambda_0) \text{ for } x \in \Omega_2 \\ \delta_3\varphi_2(x, \lambda_0) + \gamma_3\chi_2(x, \lambda_0) \text{ for } x \in \Omega_3 \end{cases} \tag{36}$$

where at least one of the coefficients $\delta_1, \delta_2, \delta_3, \gamma_1, \gamma_2, \gamma_3$ is not zero. Now applying the boundary and transmission conditions (2)-(7) we obtain

$$\ell_i y_0(x, \lambda_0) = 0, i = 1, 2, 3, 4, 5, 6 \tag{37}$$

These equalities forms a homogeneous linear system of algebraic equations with respect to the variables $\delta_1, \delta_2, \delta_3, \gamma_1, \gamma_2, \gamma_3$ whose determinant has the form

$$\Delta(\lambda) \;:=\; \begin{vmatrix} 1 & 0 & 0 & 0 & -\varphi_3(\urcorner_2) & -\chi_3(\urcorner_2) \\ 0 & 1 & 0 & 0 & -\varphi_3'(\urcorner_2) & -\chi_3'(\urcorner_2) \\ \varphi_2(c_1^+) & \chi_2(c_1^+) & -\varphi_2(c_1^+) & -\chi_2(c_1^+) & 0 & 0 \\ \varphi_2'(c_1^+) & \chi_2'(c_1^+) & -\varphi_2'(c_1^+) & -\chi_2'(c_1^+) & 0 & 0 \\ 0 & 0 & \varphi_2(c_2^-) & \chi_2(c_2^-) & -\varphi_2(c_2^-) & -\chi_2(c_2^-) \\ 0 & 0 & \varphi_2'(c_2^-) & \chi_2'(c_2^-) & -\varphi_2'(c_2^-) & -\chi_2'(c_2^-) \end{vmatrix}$$

It is easy to show that

$$\Delta(\lambda) = W_\lambda(\varphi_2, \chi_2; c_2^+) W_\lambda(\varphi_2, \chi_2; c_2^-)[W_\lambda(\varphi_3, \chi_3; \urcorner_2) + 1 - \varphi_3(\urcorner_2) - \chi_3'(\urcorner_2)]$$

Since the system of algebraic linear equations (37) has nontrivial solution, we have $\Delta(\lambda_0) = 0$. Now, show that any zero $\lambda = \lambda_0$ of the function $\Delta(\lambda)$ is an eigenvalue of the considered problem (1)-(7). Indeed, if $\Delta(\lambda_0) = 0$, then the system (37) has a nontrivial solution $(\delta_1, \gamma_1, \delta_2, \gamma_2, \delta_3, \gamma_3)$. Therefore the nonrivial function $y_0(x, \lambda_0)$ defined by (36) satisfies the equation (1) and the boundary and transmission conditions (2)-(7). This means, that λ_0 is an eigenvalue. □

Definition 3.4. The function $\Delta(\lambda)$ defined by

$$\Delta(\lambda) = W_\lambda(\varphi_2, \chi_2; c_2^+) W_\lambda(\varphi_2, \chi_2; c_2^-)[W_\lambda(\varphi_3, \chi_3; \urcorner_1) + 1 - \varphi_3(\urcorner_2) - \chi_3'(\urcorner_2)] \tag{38}$$

will be called the transmittal-characteristic function for the boundary value problem (1)-(7).

Corollary 3.5. The transmittal-characteristic function $\Delta(\lambda)$ is an entire function.

4. Conclusion

This work is devoted to the spectral analysis of Sturm-Liouville problems of a new type. In fact, we studied three different Sturm-Liouville equations for three unknown solutions, which are defined on three disjoint subintervals, at the common ends of which four interaction conditions are imposed, the so-called transmission conditions. We first established that the eigenvalues are real and the corresponding eigenfunctions are orthogonal in the appropriate Hilbert space. It is also shown that the considered boundary value problem generates a self-adjoint linear differential operator. Second, using our own approach, we constructed special one-interval solutions, in terms of which a characteristic function of a new type is defined, the so called the transmittal-characteristic function. Finally, we proved that the eigenvalues coincide with the zeros of this characteristic function, which is an entire function. The results obtained are a generalization of the analogous classical results, since in the particular case $\beta = 1$ our results are equivalent to the analogous results for the classical Sturm-Liouville problems.

Author Contributions

All the authors contributed equally to this work. They all read and approved the last version of the manuscript.

Conflicts of Interest

The authors declare no conflict of interest.

Acknowledgement

This work was supported by the Office of Scientific Research Projects Coordination at Amasya University, Grant number: FMB-BAP 20-0440.

References

[1] İ. Çelik, G. Gökmen, *Approximate Solution of Periodic Sturm-Liouville Problems with Chebyshev Collocation Method*, Applied Mathematics and Computation 170(1) (2005) 285–295.

[2] X. Haoa, L. Liu, Y. Wu, *Existence and Multiplicity Results for Nonlinear Periodic Boundary Value Problems*, Nonlinear Analysis: Theory, Methods and Applications 72(9-10) (2010) 3635–3642.

[3] J. Li, J. J. Nieto, J. Shen, *Impulsive Periodic Boundary Value Problems of First-Order Differential Equations*, Journal of Mathematical Analysis and Applications 325(1) (2007) 226–236.

[4] J. Qiu, *Positive Solutions for a Nonlinear Periodic Boundary-Value Problem with a Parameter*, Electronic Journal of Differential Equations 2012(133) (2012) 1–10.

[5] G. V. Berghe, M. V. Daele, H. D. Meyer, *A Modified Difference Scheme for Periodic and Semiperiodic Sturm-Liouville Problems*, Applied Numerical Mathematics 18(1-3) (1995) 69–78.

[6] P. A. Binding, P. B. Rynne, *Half-Eigenvalues of Periodic Sturm-Liouville Problems*, Journal of Differential Equations 206(2) (2004) 280–305.

[7] P. Binding, H. Volkmer, *A rüfer Angle Approach to the Periodic Sturm-Liouville Problem*, The American Mathematical Monthly 119(6) (2012) 477–484.

[8] A. Boumenir, *Eigenvalues of Periodic Sturm-Liouville Problems by the Shannon-Whittaker Sampling Theorem*, Mathematics of Computation of the American Mathematical Society 68(227) (1999) 1057–1066.

[9] F. Geng, Y. Xu, D. Zhu, *Periodic Boundary Value Problems for First-Order Impulsive Dynamic Equations on Time Scales*, Nonlinear Analysis: Theory, Methods and Applications 69(11) (2008) 4074–4087.

[10] K. V. Khmelnytskaya, H. Rosu, C. A. González, *Periodic Sturm-Liouville Problems Related to Two Riccati Equations of Constant Coefficients*, Annals of Physics 325(3) (2010) 596–606.

[11] V. A. Sadovnichii, Y. T. Sultanaev, A. M. Akhtyamov, *Inverse Sturm-Liouville Problem with Generalized Periodic Boundary Conditions*, Differential Equations 45(4) (2009) 526–538.

[12] A. A. Shkalikov, O. A. Veliev, *On the Riesz Basis Property of the Eigen-and Associated Functions of Periodic and Antiperiodic Sturm-Liouville Problems*, Mathematical Notes 85(5-6) (2009) 647–660.

[13] S. Somali, V. Oger, *Improvement of Eigenvalues of Sturm-Liouville Problem with t-Periodic Boundary Conditions*, Journal of Computational and Applied Mathematics 180(2) (2005) 433–441.

[14] Y. Yuan, J. Sun, A. Zettl, *Eigenvalues of Periodic Sturm Liouville Problems*, Linear Algebra and Its Applications 517 (2017) 148–166.

[15] Y. Wang, J. Li, Z. Cai. *Positive Solutions of Periodic Boundary Value Problems for the Second-Order Differential Equation with a Parameter*, Boundary Value Problems Article Number 49 2017(1) (2017) 1–11.

[16] Y. Zhao, H. Chen, B. Qin, *Periodic Boundary Value Problems for Second-Order Functional Differential Equations with Impulse*, Advances in Difference Equations Article Number 134 2014(1) (2014) 1–12.

[17] I. Akbarfam, A. Jodayree, *Resolvent Operator and Self-Adjointness of Sturm-Liouville Operators with a Finite Number of Transmission Conditions*, Mediterranean Journal Of Mathematics 11(2) (2014) 447–462.

[18] B. P. Allahverdiev, E. Bairamov, E. Ugurlu, *Eigenparameter Dependent Sturm-Liouville Problems in Boundary Conditions with Transmission Conditions*, Journal of Mathematical Analysis and Applications 401(1) (2013) 388–396.

[19] B. P. Allahverdiev, H. Tuna, *On the Resolvent of Singular Sturm-Liouville Operators with Transmission Conditions*, Mathematical Methods in The Applied Sciences 43(7) (2020) 388–396.

[20] J. Ao, J. Sun, *Eigenvalues of a Class of Fourth-Order Boundary Value Problems with Transmission Conditions Using Matrix Theory*, Linear and Multilinear Algebra 69(9) (2021) 1610–1624.

[21] K. Aydemir, H. Olğar, O. Sh. Mukhtarov, *Differential Operator Equations with Interface Conditions in Modified Direct Sum Spaces*, Filomat 32(3) (2018) 921–931.

[22] E. Bairamov, E. Uğurlu, *On the Characteristic Values of the Real Component of a Dissipative Boundary Value Transmission Problem*, Applied Mathematics and Computation 218(19) (2012) 9657–9663.

[23] H. Olğar, O. Sh. Mukhtarov, *Weak Eigenfunctions Of Two-Interval Sturm-Liouville Problems Together With Interaction Conditions*, Journal of Mathematical Physics 58(042201) (2017) DOI: 10.1063/1.4979615.

[24] H. Olğar, F. Muhtarov,*The Basis Property of the System of Weak Eigenfunctions of a Discontinuous Sturm-Liouville Problem*, Mediterranean Journal of Mathematics Article Number 114 14(3) (2017) 1–13.

[25] O. Sh. Mukhtarov, K. Aydemir, *Discontinuous Sturm-Liouville Problems Involving an Abstract Linear Operator*, Journal of Applied Analysis and Computation 10(4) (2020) 1545–1560.

[26] O. Sh. Mukhtarov, H. Olğar, K. Aydemir, I. Sh. Jabbarov, *Operator-Pencil Realization of One Sturm-Liouville Problem with Transmission Conditions*, Applied and Computational Mathematics 17(2) (2018) 284–294.

[27] O. Sh. Mukhtarov, M. Yücel, K. Aydemir, *A New Generalization of the Differential Transform Method for Solving Boundary Value Problems*, Journal of New Results in Science 10(2) (2021) 49–58.

[28] E. Şen, *Sturm-Liouville Problems With Retarded Argument and A Finite Number of Transmission Conditions*, Electronic Journal Of Differential Equations 2017(310) (2017) 1–8.

[29] E. C. Titchmarsh, *Eigenfunctions Expansion Associated with Second Order Differential Equations I*, Second edn. Oxford University Press, London, 1962.

Journal of New Theory
ISSN: 2149-1402

37 (2021) 35-44
Journal of New Theory
https://dergipark.org.tr/en/pub/jnt
Open Access

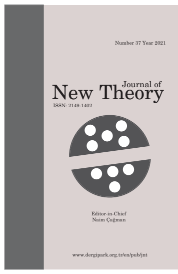

An Examination on to Find 5^{th} Order Bézier Curve in E^3

Şeyda Kılıçoğlu[1], Süleyman Şenyurt[2]

Article History
Received: 06 Nov 2021
Accepted: 21 Dec 2021
Published: 31 Dec 2021
10.53570/jnt.1020089
Research Article

Abstract — In this study, we have examined how to find any 5^{th} order Bézier curve with its known first, second and third derivatives, which are the 4^{th} order, the cubic and the quadratic Bézier curves, respectively, based on the control points of given the derivatives. Also we give an example to find the 5^{th} order Bézier curve with the given derivatives.

Keywords — *Bézier curves, derivatives of Bézier curve, cubic Bézier curves*

Mathematics Subject Classification (2020) — 53A04, 53A05

1. Introduction

As a tool of motion controller the Bézier curves are the most preferred ones in computer graphics for animation purposes. For example, Adobe Flash and Synfig are the applications of animation in which the Bézier curves are often integrated. Users sketched the desired path, and the application creates required frames for an object moving along the path. By being aware of the current importance of the Bézier curves, we have been motivated by the following studies. First Bézier-curves with curvature and torsion continuity has been examined in [1]. Also in [2] Bézier curves and surfaces has been studied in deep. In [3], Bézier curves are outlined deeply for Computer-Aided Geometric Design. In [4], Frenet apparatus of the cubic Bézier curves has been examined in E^3. We have already examine the cubic Bézier curves and involutes in [4] and [5], respectively. Before, 5^{th} order Bézier curve and its first, second, and third derivatives based on the control points are examined in [6, 7]. Futher involute, Bertrand mate and Mannheim partner of a cubic Bézier curve based on the control points with matrix form has been examined with Frenet apparatus in [8, 9]. In [10], the Bertrand pairs have also been examined by B-Spline curves. Last but not least, the Bézier curves have been associated to the alternative frame in [11].

2. How to Find 5^{th} Order Bézier Curve

In this study we have motivated by the following questions:

"How to find a 5^{th} order Bézier curve if we know the first, second and third derivatives?"

[1]seyda@baskent.edu.tr (Corresponding Author); [2]senyurtsuleyman52@gmail.com
[1]Department of Mathematics, Faculty of Education, Başkent University, Ankara, Turkey
[2]Department of Mathematics, Faculty of Arts and Sciences, Ordu University, Ordu, Turkey

Generally, Bézier curves can be defined by $n+1$ control points $P_0, P_1, ..., P_n$ with the parametrization

$$\mathbf{B}(t) = \sum_{i=0}^{n} \binom{n}{i} t^i (1-t)^{n-i} [P_i]$$

Definition 2.1. The 5^{th} order Bézier Curve has the following equation

$$\alpha(t) = \sum_{I=0}^{5} \binom{5}{I} t^I (1-t)^{5-I} [P_I] \qquad t \in [0,1]$$

and matrix representation

$$\alpha(t) = \begin{bmatrix} t^5 & t^4 & t^3 & t^2 & t & 1 \end{bmatrix} \begin{bmatrix} -1 & 5 & -10 & 10 & -5 & 1 \\ 5 & -20 & 30 & -20 & 5 & 0 \\ -10 & 30 & -30 & 10 & 0 & 0 \\ 10 & -20 & 10 & 0 & 0 & 0 \\ -5 & 5 & 0 & 0 & 0 & 0 \\ 1 & 0 & 0 & 0 & 0 & 0 \end{bmatrix} \begin{bmatrix} P_0 \\ P_1 \\ P_2 \\ P_3 \\ P_4 \\ P_5 \end{bmatrix}$$

with control points P_0, P_1, P_2, P_3, P_4, and P_5.

Theorem 2.2. The 5^{th} order Bézier curve with given the first derivative and the initial point P_0, has the following control points

$$\begin{aligned} P_1 &= P_0 + \frac{Q_0}{5} \\ P_2 &= P_0 + \frac{Q_0}{5} + \frac{Q_1}{5} \\ P_3 &= P_0 + \frac{Q_0}{5} + \frac{Q_1}{5} + \frac{Q_2}{5} \\ P_4 &= P_0 + \frac{Q_0}{5} + \frac{Q_1}{5} + \frac{Q_2}{5} + \frac{Q_3}{5} \\ P_5 &= P_0 + \frac{Q_0}{5} + \frac{Q_1}{5} + \frac{Q_2}{5} + \frac{Q_3}{5} + \frac{Q_4}{5} \end{aligned}$$

PROOF. If the first derivative of 5^{th} order Bézier curve is given,

$$\alpha'(t) = \begin{bmatrix} t^4 \\ t^3 \\ t^2 \\ t \\ 1 \end{bmatrix}^T [B\prime] \begin{bmatrix} Q_0 \\ Q_1 \\ Q_2 \\ Q_3 \\ Q_4 \end{bmatrix}$$

where $[B\prime]$ is the coefficient matrix of the 4^{th} order Bézier curve which is the derivative of the 5^{th} order Bézier curve, then the control points $Q_0, Q_1, ..., Q_4$ are given as in the following way,

$$\begin{aligned} Q_0 &= 5(P_1 - P_0) \\ Q_1 &= 5(P_2 - P_1) \\ Q_2 &= 5(P_3 - P_2) \\ Q_1 &= 5(P_4 - P_3) \\ Q_4 &= 5(P_5 - P_4) \end{aligned}$$

Let the 5^{th} order Bézier curve pass through from a given the initial point P_0.If we take each P_i and replace, we get all the control points based on the Q_i, $0 \le i \le 4$.

$$
\begin{aligned}
P_1 &= P_0 + \frac{Q_0}{5} \\
P_2 &= P_0 + \frac{Q_0}{5} + \frac{Q_1}{5} \\
P_3 &= P_0 + \frac{Q_0}{5} + \frac{Q_1}{5} + \frac{Q_2}{5} \\
P_4 &= P_0 + \frac{Q_0}{5} + \frac{Q_1}{5} + \frac{Q_2}{5} + \frac{Q_3}{5} \\
P_5 &= P_0 + \frac{Q_0}{5} + \frac{Q_1}{5} + \frac{Q_2}{5} + \frac{Q_3}{5} + \frac{Q_4}{5}
\end{aligned}
$$

Hence, this complete rhe proof. □

Corollary 2.3. The derivative of n^{th} order Bézier curve can not has the origin $(0,0,0)$ as a control point.

Proof. Let first derivative of n^{th} order Bézier curve has the origin $Q_0 = (0,0,0)$,

$$
\begin{aligned}
Q_i &= n\,(P_{i+1} - P_i) = (0,0,0) \\
P_{i+1} &= P_i
\end{aligned}
$$

Hence, Bézier curve has $n-1$ control points hence derivative of n^{th} order Bézier curve cannot has the origin $Q_i(0,0,0)$ as a control point. □

Corollary 2.4. If the first derivative of 5^{th} order Bézier curve with given control points Q_i, $0 < i < 4$, is given and 5^{th} order Bézier curve has initial point $P_0 = (0,0,0)$,has the following control points

$$
P_i = \frac{Q_0 + \cdots + Q_{i-1}}{5}, \ 1 \le i \le 5
$$

Proof. Since $P_i = P_0 + \frac{Q_0+Q_1+Q_2+\ldots+Q_{i-1}}{n}$, $1 \le i \le 5$ and $P_0 = (0,0,0)$, it is clear. □

Theorem 2.5. The 5^{th} order Bézier curve with given the end point P_5 and the first derivative, has the following control points as in the following ways

$$
\begin{aligned}
P_4 &= P_5 - \frac{Q_4}{5} \\
P_3 &= P_5 - \frac{Q_4}{5} - \frac{Q_3}{5} \\
P_2 &= P_5 - \frac{Q4}{5} - \frac{Q_3}{5} - \frac{Q_2}{5} \\
P_1 &= P_5 - \frac{Q_4}{5} - \frac{Q_3}{5} - \frac{Q_2}{5} - \frac{Q_1}{5} \\
P_0 &= P_5 - \frac{Q_4}{5} - \frac{Q_3}{5} - \frac{Q_2}{5} - \frac{Q_1}{5} - \frac{Q_0}{5}
\end{aligned}
$$

Proof. Let the first derivative of 5^{th} order Bézier curve with control points Q_0, Q_1, Q_2, Q_3, Q_4 be given as,

$$
\alpha'(t) = \begin{bmatrix} t^4 \\ t^3 \\ t^2 \\ t \\ 1 \end{bmatrix}^T [B\prime] \begin{bmatrix} Q_0 \\ Q_1 \\ Q_2 \\ Q_3 \\ Q_4 \end{bmatrix}
$$

where $[B\prime]$ is the coefficient matrix of the 4^{th} order Bézier curve which is the derivative of the 5^{th} order Bézier curve. Hence, the control points Q_0, Q_1, Q_2, Q_3, Q_4 are

$$\begin{aligned} Q_0 &= 5(P_1 - P_0) \\ Q_1 &= 5(P_2 - P_1) \\ Q_2 &= 5(P_3 - P_2) \\ Q_1 &= 5(P_4 - P_3) \\ Q_4 &= 5(P_5 - P_4) \end{aligned}$$

If the 5^{th} order Bézier curve passing through the end point P_5, then

$$\begin{aligned} P_4 &= P_5 - \frac{Q_4}{5} \\ P_3 &= P_4 - \frac{Q_3}{5} \\ P_2 &= P_3 - \frac{Q_2}{5} \\ P_1 &= P_0 - \frac{Q_1}{5} \\ P_0 &= P_1 - \frac{Q_0}{5} \end{aligned}$$

and we get all the control points P_i based on the Q_0, Q_1, Q_2, Q_3, Q_4

$$\begin{aligned} P_4 &= P_5 - \frac{Q_4}{5} \\ P_3 &= P_5 - \frac{Q_4}{5} - \frac{Q_3}{5} \\ P_2 &= P_5 - \frac{Q4}{5} - \frac{Q_3}{5} - \frac{Q_2}{5} \\ P_1 &= P_5 - \frac{Q_4}{5} - \frac{Q_3}{5} - \frac{Q_2}{5} - \frac{Q_1}{5} \\ P_0 &= P_5 - \frac{Q_4}{5} - \frac{Q_3}{5} - \frac{Q_2}{5} - \frac{Q_1}{5} - \frac{Q_0}{5} \end{aligned}$$

This complete the proof. □

Corollary 2.6. The 5^{th} order Bézier curve with given the end point $P_5 = (0,0,0)$ and the first derivative has the following control points as in the following ways

$$P_{i-1} = -\frac{Q_0 + \cdots + Q_{i-1}}{5}, 1 \leq i \leq 5$$

Theorem 2.7. The 5^{th} order Bézier curve with given any point P_k, $0 < k < n$, and the first derivative has the following control points

$$\begin{aligned} P_{k+1} &= P_k + \frac{Q_k}{5} \\ P_{k+2} &= P_k + \frac{Q_k}{5} + \frac{Q_{k+1}}{5} \\ &\cdots \\ P_5 &= P_k + \frac{Q_k}{5} + \frac{Q_{k+1}}{5} + \cdots + \frac{Q_4}{5} \end{aligned}$$

$$P_{k-1} = P_k - \frac{Q_{k-1}}{5}$$
$$P_{k-2} = P_{k-} - \frac{Q_{k-1}}{5} - \frac{Q_{k-2}}{5}$$
$$\cdots$$
$$P_0 = P_k - \frac{Q_{k-1}}{5} - \frac{Q_{k-2}}{5} - \cdots - \frac{Q_0}{5}$$

Theorem 2.8. The 5^{th} order Bézier curve with given the initial point P_0,the initial point Q_0 of the first derivative and the control points R_0, R_1, R_2, R_3 of the second derivative , has the following control points as in the following way

$$P_1 = P_0 + \frac{Q_0}{5}$$
$$P_2 = P_0 + 2\frac{Q_0}{5} + \frac{R_0}{20}$$
$$P_3 = P_0 + 3\frac{Q_0}{5} + 2\frac{R_0}{20} + \frac{R_1}{20}$$
$$P_4 = P_0 + 4\frac{Q_0}{5} + 3\frac{R_0}{20} + 2\frac{R_1}{20} + \frac{R_2}{20}$$
$$P_5 = P_0 + 5\frac{Q_0}{5} + \frac{4R_0}{20} + \frac{3R_1}{20} + \frac{2R_2}{20} + \frac{R_3}{20}$$

PROOF. The second derivative of 5^{th} order Bézier curve is a cubic Bézier curve with control points R_0, R_1, R_2, R_3. It has the following matrix representation

$$\alpha''(t) = \begin{bmatrix} t^3 \\ t^2 \\ t \\ 1 \end{bmatrix}^T [B''] \begin{bmatrix} R_0 \\ R_1 \\ R_2 \\ R_3 \end{bmatrix}$$

$$\alpha''(t) = \begin{bmatrix} t^3 \\ t^2 \\ t \\ 1 \end{bmatrix}^T [B''] \begin{bmatrix} (n-1)(Q_1 - Q_0) \\ (n-1)(Q_2 - Q_1) \\ (n-1)(Q_3 - Q_2) \\ (n-1)(Q_4 - Q_3) \end{bmatrix}$$

where $[B'']$ is the coefficient matrix of the *cubic* Bézier curve which is the second derivative of the 5^{th} order Bézier curve. Where control points R_0, R_1, R_2, R_3, and Q_0 are given, we can easily find the Q_1, Q_2, Q_3, Q_4.

$$Q_1 = Q_0 + \frac{R_0}{4}$$
$$Q_2 = Q_0 + \frac{R_0}{4} + \frac{R_1}{4}$$
$$Q_3 = Q_0 + \frac{R_0}{4} + \frac{R_1}{4} + \frac{R_2}{4}$$
$$Q_4 = Q_0 + \frac{R_0}{4} + \frac{R_1}{4} + \frac{R_2}{4} + \frac{R_3}{4}$$

Also if the initial control point P_0 is given we can find easly control points of 5^{th} order Bézier curve

$$
\begin{aligned}
P_1 &= P_0 + \frac{Q_0}{5} \\
P_2 &= P_0 + \frac{Q_0}{5} + \frac{Q_0 + \frac{R_0}{4}}{5} \\
P_3 &= P_0 + \frac{Q_0}{5} + \frac{Q_0 + \frac{R_0}{4}}{5} + \frac{Q_0 + \frac{R_0}{4} + \frac{R_1}{4}}{5} \\
P_4 &= P_0 + \frac{Q_0}{5} + \frac{Q_0 + \frac{R_0}{4}}{5} + \frac{Q_0 + \frac{R_0}{4} + \frac{R_1}{4}}{5} + \frac{Q_0 + \frac{R_0}{4} + \frac{R_1}{4} + \frac{R_2}{4}}{5} \\
P_5 &= P_0 + \frac{Q_0}{5} + \frac{Q_0 + \frac{R_0}{4}}{5} + \frac{Q_0 + \frac{R_0}{4} + \frac{R_1}{4}}{5} + \frac{Q_0 + \frac{R_0}{4} + \frac{R_1}{4} + \frac{R_2}{4}}{5} + \frac{Q_0 + \frac{R_0}{4} + \frac{R_1}{4} + \frac{R_2}{4} + \frac{R_3}{4}}{5}
\end{aligned}
$$

Hence, we have the proof. □

Theorem 2.9. The 5^{th} order Bézier curve with given the initial point P_0, the initial point Q_0 of the first derivative, the initial point R_0 of the second derivative and the control points S_0, S_1, S_2 of the third derivative has the following control points as in the following ways

$$
\begin{aligned}
P_1 &= P_0 + \frac{Q_0}{5} \\
P_2 &= P_0 + 2\frac{Q_0}{5} + \frac{R_0}{20} \\
P_3 &= P_0 + 3\frac{Q_0}{5} + 3\frac{R_0}{20} + \frac{S_0}{60} \\
P_4 &= P_0 + 4\frac{Q_0}{5} + 6\frac{R_0}{20} + 3\frac{S_0}{60} + \frac{S_1}{60} \\
P_5 &= P_0 + 5\frac{Q_0}{5} + 10\frac{R_0}{20} + 6\frac{S_0}{60} + 3\frac{S_1}{60} + \frac{S_2}{20}
\end{aligned}
$$

where P_0, Q_0, R_0, and S_0, S_1, S_2 must be given.

Proof. The third derivative of 5^{th} order Bézier curve is a quadratic Bézier curve with control points S_0, S_1, S_2 . Also it has the following matrix representation

$$
\alpha'''(t) = \begin{bmatrix} t^2 \\ t \\ 1 \end{bmatrix}^T \begin{bmatrix} B''' \end{bmatrix} \begin{bmatrix} S_0 \\ S_1 \\ S_2 \end{bmatrix}
$$

$$
\alpha'''(t) = \begin{bmatrix} t^2 \\ t \\ 1 \end{bmatrix}^T \begin{bmatrix} B''' \end{bmatrix} \begin{bmatrix} (n-2)(R_1 - R_0) \\ (n-2)(R_2 - R_1) \\ (n-2)(R_3 - R_2) \end{bmatrix}
$$

Where $[B''']$ is the coefficient matrix of the quadratic Bézier curve which is the second derivative of the 5^{th} order Bézier curve. Since te control points S_0, S_1, S_2, and R_0 are given, by solving the following system

$$
\begin{aligned}
R_1 &= R_0 + \frac{S_0}{3} \\
R_2 &= R_0 + \frac{S_0}{3} + \frac{S_1}{3} \\
R_3 &= R_0 + \frac{S_0}{3} + \frac{S_1}{3} + \frac{S_2}{3}
\end{aligned}
$$

We can easily find the R_1, R_2, R_3. Also if the initial control point Q_0 of first derivative is given we can find easly Q_i control points of 5^{th} order Bézier curve

$$\begin{aligned}
Q_1 &= Q_0 + \frac{R_0}{4} \\
Q_2 &= Q_0 + 2\frac{R_0}{4} + \frac{S_0}{12} \\
Q_3 &= Q_0 + 3\frac{R_0}{4} + 2\frac{S_0}{12} + \frac{S_1}{12} \\
Q_4 &= Q_0 + 4\frac{R_0}{4} + 3\frac{S_0}{12} + 2\frac{S_1}{12} + \frac{S_2}{12}
\end{aligned}$$

Hence,

$$\begin{aligned}
P_1 &= P_0 + \frac{Q_0}{5} \\
P_2 &= P_0 + 2\frac{Q_0}{5} + \frac{R_0}{20} \\
P_3 &= P_0 + 3\frac{Q_0}{5} + 2\frac{R_0}{20} + \frac{R_1}{20} \\
&= P_0 + 3\frac{Q_0}{5} + 2\frac{R_0}{20} + \frac{R_0 + \frac{S_0}{3}}{20} \\
&= P_0 + 3\frac{Q_0}{5} + 3\frac{R_0}{20} + \frac{S_0}{60} \\
P_4 &= P_0 + 4\frac{Q_0}{5} + 3\frac{R_0}{20} + 2\frac{R_1}{20} + \frac{R_2}{20} \\
&= P_0 + 4\frac{Q_0}{5} + 3\frac{R_0}{20} + 2\frac{R_0 + \frac{S_0}{3}}{20} + \frac{R_0 + \frac{S_0}{3} + \frac{S_1}{3}}{20} \\
&= P_0 + 4\frac{Q_0}{5} + 6\frac{R_0}{20} + 3\frac{S_0}{60} + \frac{S_1}{60} \\
P_5 &= P_0 + 5\frac{Q_0}{5} + 4\frac{R_0}{20} + 3\frac{R_1}{20} + 2\frac{R_2}{20} + \frac{R_3}{20} \\
&= P_0 + 5\frac{Q_0}{5} + 4\frac{R_0}{20} + 3\frac{R_0 + \frac{S_0}{3}}{20} + 2\frac{R_0 + \frac{S_0}{3} + \frac{S_1}{3}}{20} + \frac{R_0 + \frac{S_0}{3} + \frac{S_1}{3} + \frac{S_2}{3}}{20} \\
&= P_0 + 5\frac{Q_0}{5} + 10\frac{R_0}{20} + 6\frac{S_0}{60} + 3\frac{S_1}{60} + \frac{S_2}{20}
\end{aligned}$$

This complete the proof. □

2.1. An Example to Find 5^{th} Order Bézier Curve with Given First Derivative

In this section, we will give an example to find 5^{th} order Bézier curves which are defined in E^3. For more detail, see [3].

Example 2.10. Let $\alpha(t) = \big(74t^5 - 210t^4 + 180t^3 - 50t^2 + 5t + 1, -79t^5 + 185t^4 - 130t^3 + 10t^2 + 10t + 1, -63t^5 + 95t^4 - 30t^3 - 5t + 2\big)$ be an example of a 5^{th} order Bézier curve with control points, $P_0 = (1,1,2), P_1 = (2,3,1), P_2 = (-2,6,0), P_3 = (7,-3,-4), P_4 = (5,0,5), P_5 = (0,-3,-1)$.

The control points of the first derivative of 5^{th} order of a Bézier curve are

$$\begin{aligned}
Q_0 &= 5(P_1 - P_0) = 5((2,3,1) - (1,1,2)) = (5,10,-5) \\
Q_1 &= 5(P_2 - P_1) = 5((-2,6,0) - (2,3,1)) = (-20,15,-5) \\
Q_2 &= 5(P_3 - P_2) = 5((7,-3,-4) - (-2,6,0)) = (45,-45,-20) \\
Q_3 &= 5(P_4 - P_3) = 5((5,0,5) - (7,-3,-4)) = (-10,15,45) \\
Q_4 &= 5(P_5 - P_4) = 5((0,-3,-1) - (5,0,5)) = (-25,-15,-30)
\end{aligned}$$

5^{th} order Bézier curve with given the first derivative and the initial point P_0, has the following control points

$$
\begin{aligned}
P_1 &= P_0 + \frac{Q_0}{5}\\
P_2 &= P_0 + \frac{Q_0}{5} + \frac{Q_1}{5}\\
P_3 &= P_0 + \frac{Q_0}{5} + \frac{Q_1}{5} + \frac{Q_2}{5}\\
P_4 &= P_0 + \frac{Q_0}{5} + \frac{Q_1}{5} + \frac{Q_2}{5} + \frac{Q_3}{5}\\
P_5 &= P_0 + \frac{Q_0}{5} + \frac{Q_1}{5} + \frac{Q_2}{5} + \frac{Q_3}{5} + \frac{Q_4}{5}
\end{aligned}
$$

P_0 and $Q_0, Q_1, \ldots, Q_4$ *are given*

$$
\begin{aligned}
P_1 &= (1,1,2) + \frac{(5,10,-5)}{5} = (2,3,1)\\
P_2 &= (1,1,2) + \frac{(5,10,-5)}{5} + \frac{(-20,15,-5)}{5} = (-2,6,0)\\
P_3 &= (1,1,2) + \frac{(5,10,-5)}{5} + \frac{(-20,15,-5)}{5} + \frac{(45,-45,-20)}{5} = (7,-3,-4)\\
P_4 &= (1,1,2) + \frac{(5,10,-5)}{5} + \frac{(-20,15,-5)}{5} + \frac{(45,-45,-20)}{5} + \frac{(-10,15,45)}{5} = (5,0,5)\\
P_5 &= (1,1,2) + \frac{(5,10,-5)}{5} + \frac{(-20,15,-5)}{5} + \frac{(45,-45,-20) + (-10,15,45) + (-25,-15,-30)}{5}\\
&= (0,-3,-1)
\end{aligned}
$$

The second derivative of 5^{th} order of a Bézier curve as a 3^{rd} order Bézier curve with control points R_0, R_1, R_2, R_3 are given as in the following way

$$
\begin{aligned}
R_0 &= 4\left(Q_1 - Q_0\right) = 4\left((-20,15,-5) - (5,10,-5)\right) = (-100,20,0)\\
R_1 &= 4\left(Q_2 - Q_1\right) = 4\left((45,-45,-20) - (-20,15,-5)\right) = (260,-240,-60)\\
R_2 &= 4\left(Q_3 - Q_2\right) = 4\left((-10,15,45) - (45,-45,-20)\right) = (-220,240,260)\\
R_3 &= 4\left(Q_4 - Q_3\right) = 4\left((-25,-15,-30) - (-10,15,45)\right) = (-60,-120,-300)
\end{aligned}
$$

The 5^{th} order Bézier curve with given the initial point P_0,the initial point Q_0 of the first derivative and the control points R_0, R_1, R_2, R_3 of the second derivation , has the following control points as in the following ways

$$
\begin{aligned}
P_1 &= P_0 + \frac{Q_0}{5}\\
P_2 &= P_0 + 2\frac{Q_0}{5} + \frac{R_0}{20}\\
P_3 &= P_0 + 3\frac{Q_0}{5} + 2\frac{R_0}{20} + \frac{R_1}{20}\\
P_4 &= P_0 + 4\frac{Q_0}{5} + 3\frac{R_0}{20} + 2\frac{R_1}{20} + \frac{R_2}{20}\\
P_5 &= P_0 + 5\frac{Q_0}{5} + \frac{4R_0}{20} + \frac{3R_1}{20} + \frac{2R_2}{20} + \frac{R_3}{20}
\end{aligned}
$$

where P_0, Q_0, R_0, R_1, R_3 are given.

$$\begin{aligned}
P_1 &= (1,1,2) + \tfrac{(5,10,-5)}{5} = (2,3,1) \\
P_2 &= (1,1,2) + 2\tfrac{(5,10,-5)}{5} + \tfrac{(-100,20,0)}{20} = (-2,6,0) \\
P_3 &= (1,1,2) + 3\tfrac{(5,10,-5)}{5} + 2\tfrac{(-100,20,0)}{20} + \tfrac{(260,-240,-60)}{20} = (7,-3,-4) \\
P_4 &= (1,1,2) + 4\tfrac{(5,10,-5)}{5} + 3\tfrac{(-100,20,0)}{20} + 2\tfrac{(260,-240,-60)}{20} + \tfrac{(-220,240,260)}{20} = (5,0,5) \\
P_5 &= (1,1,2) + \tfrac{5(5,10,-5)}{5} + \tfrac{4(-100,20,0)}{20} + \tfrac{3(260,-240,-60)}{20} + \tfrac{2(-220,240,260)}{20} + \tfrac{(-60,-120,-300)}{20} \\
&= (0,-3,-1)
\end{aligned}$$

The third derivative of 5^{th} order of a Bézier curve using the control points S_0, S_1, and S_2 of 5^{th} order Bézier Curve are

$$\begin{aligned}
S_0 &= 3(R_1 - R_0) = 3((260,-240,-60) - (-100,20,0)) = (1080,-780,-180) \\
S_1 &= 3(R_2 - R_1) = 3((-220,240,260) - (260,-240,-60)) = (-1440,1440,960) \\
S_2 &= 3(R_3 - R_2) = 3((-60,-120,-300) - (-220,240,260)) = (480,-1080,-1680)
\end{aligned}$$

3. Conclusion

We know that the first derivative of a 5^{th} order Bézier curve is 4^{th} order Bézier curve with 5 control points,in this study we have examined that, when any 4^{th} order Bézier curve with 5 control points is given, how to find 5^{th} order Bézier curve. Also, the second derivative of a 5^{th} order Bézier curve is cubic Bézier curve with 4 control points, we have examined that, when any cubic Bézier curve with 4 control points is given, how to find 5^{th} order Bézier curve. Further the third derivative of a 5^{th} order Bézier curve is a quadratic Bézier curve with 3 control points. We have examined that, when any cubic Bézier curve with three control points is given, how to find 5^{th} order Bézier curve. As a result we can choose any initial or end control points except origin of any order derivatives and we can write which we want exactly the 5^{th} order Bézier curve.

Author Contributions

All the authors contributed equally to this work. They all read and approved the last version of the manuscript.

Conflicts of Interest

The authors declare no conflict of interest.

References

[1] H. Hagen, *Bézier-Curves with Curvature and Torsion Continuity*, The Rocky Mountain Journal of Mathematics 16(3) (1986) 629–638.

[2] F. Taş, K. Ilarslan, *A New Approach to Design the Ruled Surface*, International Journal of Geometric Methods in Modern Physics 16(6) (2019).

[3] G. Farin, *Curves and Surfaces for Computer-Aided Geometric Design*, Academic Press, 1996.

[4] Ş. Kılıçoğlu, S. Şenyurt, *On the Cubic Bézier Curves in E^3*, Ordu University Journal of Science and Technology 9(2) (2019) 83–97.

[5] Ş. Kılıçoğlu, S. Şenyurt, *On the Involute of the Cubic Bézier Curve by Using Matrix Representation in E^3*, European Journal of Pure and Applied Mathematics 13 (2020) 216–226.

[6] Ş. Kılıçoğlu, S. Şenyurt, *On the Matrix Representation of 5th order Bézier Curve and derivatives*, Communications Faculty of Sciences University of Ankara Series A1 Mathematics and Statistic (2021) In press.

[7] Ş. Kılıçoğlu, S. Şenyurt, *On the Matrix Representation of Bézier Curves and Derivatives in E^3*, Sigma Journal of Engineering and Natural Sciences (2021) In press.

[8] Ş. Kılıçoğlu, S. Şenyurt, *On the Bertrand Mate of a Cubic Bézier Curve by Using Matrix Representation in E^3*, 18^{th} International Geometry Symposium in Honour of Prof. Dr. Sadık Keleş, Malatya, Turkey, 2021, pp. 129.

[9] Ş. Kılıçoğlu, S. Şenyurt, *On the Mannheim Partner of a Cubic Bézier Curve in E^3*, 10^{th} International Eurasian Conference on Mathematical and Applications, Sakarya, Turkey, 2021, pp. 154.

[10] M. Incesu, S. Y. Evren, *The Selection of Control Points for Two Open Non Uniform B-Spline Curves to Form Bertrand Pairs*, Tblisi Journal of Mathematics, Special Issue 8 (2021) 195–208.

[11] H. K. Samanci, M. Incesu, *Investigating a Quadratic Bézier Curve Due to NCW and N-Bishop Frames*, Turkish Journal of Mathematics and Computer Science 12(2) (2020) 120–127.

Journal of New Theory
ISSN: 2149-1402

37 (2021) 45-57
Journal of New Theory
https://dergipark.org.tr/en/pub/jnt
Open Access

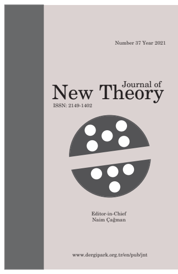

A New Method to Obtain PH-Helical Curves in $\mathbb{E}^{n+1}$

Ahmet Mollaoğulları[1], **Mehmet Gümüş**[2], **Kazım İlarslan**[3], **Çetin Camcı**[4]

Article History
Received: 23 Nov 2021
Accepted: 26 Dec 2021
Published: 31 Dec 2021
10.53570/jnt.1027564
Research Article

Abstract — Helical curves are constructed by the property that their unit tangents make a constant angle with a chosen constant direction. There are relations between polynomial planar curves, helices and Pythagorean-hodograph or shortly PH-curves. The aim of this paper is to obtain a method which generate PH-curves and PH-helical curves from a planar curve in Euclidean Space $\mathbb{E}^{n+1}$. Furthermore, some examples are given in $\mathbb{E}^4$ and $\mathbb{E}^5$ to explain the method neatly.

Keywords — *PH-curve, helical curve, PH-helical curve, planar curve, polynomial curve*

Mathematics Subject Classification (2020) — 53A04, 53A05

1. Introduction

Helix is an interesting curve which has been studied by many mathematicians in differential geometry. We can see helices or its various types of general helix in many areas such as nature, physics, kinematic motion, design of architectural building and the structure of the DNA. A curve is a general helix (or constant slope curve) if its tangent vector field makes a constant angle with a fixed straight line in Euclidean space $\mathbb{E}^3$. In 1802, Lancret [1] introduced the famous result on helices and it was proved in 1845 by B. de Saint Venant that the ratio of its curvature to torsion is constant. Indeed, helix is a geometric curve whose curvature and torsion are non-vanishing constants [2]. In addition, if the curvature and the torsion of a curve are non-zero constants then the curve is a general helix. So it is clear that helix is a special case of general helix. Furthermore, straight lines and circles are degenerate-helices.

In the curve theory, another important curves are Pythagorean-Hodograph curves, or shortly PH-curves. These curves have many applications such as CNC machining, offseting, computer aided geometric design and motion planning. They were first introduced in Farouki et al. [3]. Because they are characterized by their arclength which is a polynomial function, they have attracted the attention of researchers and have been widely studied in [4–11].

In [12], Izumiya and Takeuchi show that cylindrical helices can be obtained from planar curves. They give a method to obtain a helical curve from a planar curve in their study. Moreover, there are well-known two methods for constructing PH-curves: One of them is by using complex numbers representation [4] and the other method is quaternion representation [5, 7]. Via the point of view

[1]ahmet_m@comu.edu.tr (Corresponding Author); [2]mehmetgumus@comu.edu.tr; [3]kilarslan@yahoo.com, [4]ccamci@comu.edu.tr
[1,4] Department of Mathematics, Faculty of Arts and Sciences, Onsekiz Mart University, Çanakkale, Turkey
[2]Department of Accounting and Tax Treatment, Lapseki Vocational School, Onsekiz Mart University, Çanakkale, Turkey
[3]Department of Mathematics, Faculty of Arts and Sciences, Kırıkkale University, Kırıkkale, Turkey

of these studies Camcı and İlarslan give a new method for construction of PH-helical curves in 3-dimensional Euclidean space in [13]. In this paper, we extend their theory to the Euclidean space $\mathbb{E}^{n+1}$.

2. Basic Concepts and Notions

Let $\alpha : I \subset \mathbb{R} \to \mathbb{E}^n$ be a regular curve in Euclidean space $\mathbb{E}^n$. It is well known that the curve α is said to be of unit speed (or parameterized by arclength function s) if $\langle \alpha'(s), \alpha'(s) \rangle = 1$, where $\langle , \rangle$ is the standard inner product of $\mathbb{E}^n$ given by

$$\langle X, Y \rangle = \sum_{i=1}^{n} x_i y_i,$$

where $X = (x_1, x_2, ..., x_n)$, $Y = (y_1, y_2, ..., y_n) \in \mathbb{E}^n$. Let $\{V_1, V_2, ..., V_n\}$ be the moving Frenet frame along a space curve α, where V_i $(i = 1, 2, ..., n)$ denote ith Frenet vector field of α. Then, the Frenet formulas are given by

$$\begin{cases} V_1'(t) = & \nu(t) k_1(t) V_2(t) \\ V_i'(t) = & \nu(t) \left(-k_{i-1}(t) V_{i-1}(t) + k_i(t) V_{i+1}(t) \right), \quad 2 \leq i \leq n-1 \\ V_n'(t) = & -\nu(t) k_{n-1}(t) V_{n-1}(t) \end{cases} \tag{1}$$

where $\nu(t) = \left\| \alpha'(t) \right\|$ and k_i $(i = 1, 2, ..., n-1)$ denote the i-th curvature function of the curve (see [2,14]). If the curve lies in a hyperplane of $\mathbb{E}^n$, then it is said that α is a $(n-1)$-flat curve. It is well known that α is $(n-1)$-flat curve in $\mathbb{E}^n$ if and only if $k_{n-1}(t) = 0$ [15]. Harmonic curvature functions were defined by Özdamar and Hacısalihoğlu in [16] as follow:

Definition 2.1. Let α be a regular curve in $\mathbb{E}^n$. Harmonic curvatures of the curve α are defined by $H_i : I \subset \mathbb{R} \to \mathbb{R}$ such that

$$H_i = \begin{cases} 0, & i = 1 \\ \frac{k_1}{k_2}, & i = 2 \\ \{V_1[H_{i-1}] + k_i H_{i-2}\} \frac{1}{k_{i+1}}, & i = 3, 4, ..., n-2 \end{cases}$$

Characterizations for generalized helices by using the harmonic curvatures of the curve were studied by Camcı et al. in [17]. They obtained some important results for generalized helix in n-dimensional Euclidean space $\mathbb{E}^n$.

Theorem 2.2. [17] Let α be a non-degenerate curve in n-dimensional Euclidean space $\mathbb{E}^n$. Let $\{V_1, V_2, ..., V_n\}$ and $\{H_1, H_2, ..., H_{n-2}\}$ be the Frenet frame and harmonic curvatures of the curve, respectively. Then, α is a general helix if and only if $H_{n-2}' + \nu k_{n-1} H_{n-3} = 0$.

Definition 2.3. [17] Let α be a unit speed, non-degenerate curve in n-dimensional Euclidean space $\mathbb{E}^n$. Let $\{V_1, V_2, ..., V_n\}$ and $\{H_1, H_2, ..., H_{n-2}\}$ be the Frenet frame and harmonic curvatures of the curve, respectively. The vector

$$D = V_1 + H_1 V_3 + ... + H_{n-2} V_n$$

is called the generalized Darboux vector of the curve α.

The relationship between the generalized Darboux vector D and the general helix is given by the following theorem.

Theorem 2.4. [17] Let α be a unit speed, non-degenerate curve in Euclidean space $\mathbb{E}^n$. Let $\{V_1, V_2, ..., V_n\}$ and $\{H_1, H_2, ..., H_{n-2}\}$ be the Frenet frame and harmonic curvatures of the curve, respectively. Then α is a generalized helix if and only if D is a constant vector.

Definition 2.5. [3] Let $\alpha : I \subset \mathbb{R} \to \mathbb{E}^{n+1}\,(t \to \alpha(t))$ be a polynomial curve. If the speed of the curve $v(t) = \left\|\dot{\alpha}(t)\right\|$ is polynomial, then it is called a Pythagorean-hodograph or shortly PH-curve.

One of the well-known equations in mathematics history is the Pythagorean equation, i.e., $a^2+b^2 = c^2$. General solution of this equation is [18] :

$$a = t(u^2 - v^2), \quad b = 2tuv, \quad c = t(u^2 + v^2) \tag{2}$$

where t is a scale parameter. It can be deduced from Equation (2) that rational solution of the Pythagorean n-tuple $a_1^2 + a_2^2 + ... + a_n^2 = \sigma^2$ can be given as follows:

$$\begin{aligned} a_1 &= t(u_1^2 - u_2^2 - ... - u_n^2) \\ a_i &= 2ta_1a_i, i = 2,,,n \\ \sigma &= t(u_1^2 + u_2^2 + ... + u_n^2) \end{aligned}$$

where u_i $(i = 1, 2, ..., n)$ are integers and t is scaling parameter.

3. The Construction of a Helix in $\mathbb{E}^{n+1}$

In Euclidean space $\mathbb{E}^{n+1}$, let H^n be a $n-$hyperplane and $\gamma : I \to H^n \subset \mathbb{E}^{n+1}$ be a regular curve. Hence, we can define a curve such that

$$\beta(t) = \gamma(t) + \left(\cot\theta \int_0^t \left\|\dot{\gamma}(u)\right\| du\right) \overrightarrow{a} + \overrightarrow{c} \tag{3}$$

where $\|\overrightarrow{a}\| = 1$, $\langle \overrightarrow{a}, \dot{\gamma}(t) \rangle = 0$, $\theta \in \mathbb{R}$, $\overrightarrow{a}$ and $\overrightarrow{c}$ is a constant vector. Therefore, from Equation (3),

$$\dot{\beta}(t) = \dot{\gamma}(t) + \left(\cot\theta \left\|\dot{\gamma}(t)\right\|\right) \overrightarrow{a} \tag{4}$$

and from Equation (4),

$$\left\|\dot{\beta}(t)\right\| = \frac{1}{\sin\theta} \left\|\dot{\gamma}(t)\right\| \tag{5}$$

Thus, from Equations (4) and (5), we have

$$T_\beta = \sin\theta T_\gamma + \cos\theta \overrightarrow{a}, \langle T_\beta, \overrightarrow{a} \rangle = \cos\theta \tag{6}$$

where T_β (resp. T_γ) is a tangent of the curve β (resp. γ). From Equation (6), it can be observed that β is a helix.

Theorem 3.1. All helix curves in Euclidean space $\mathbb{E}^{n+1}$ can be obtained from a regular curve which lies in a hyperplane $H^n \subset \mathbb{E}^{n+1}$.

Proof. Let $\beta : I \to \mathbb{E}^{n+1}$ be a unit speed helix curve. Hence, the generalized Darboux vector $D(s)$ of the curve β is a constant where

$$D(s) = V_1 + H_1V_3 + .. + H_{n-1}V_{n+1} \tag{7}$$

In this case, unit axes of the curve β is equal to

$$\overrightarrow{a} = \frac{D(s)}{\|D(s)\|} = \frac{V_1 + H_1V_3 + .. + H_{n-1}V_{n+1}}{\sqrt{1 + H_1^2 + H_2^2 + .. + H_{n-1}^2}}$$

and we have $\langle T_\beta, \overrightarrow{a}\rangle = \cos\theta$ where $\beta'(s) = T_\beta$. Hence we can see that

$$\langle \beta', \overrightarrow{a}\rangle = \cos\theta.$$

If we consider the curve

$$\gamma(s) = \beta(s) - \langle \beta(s), \overrightarrow{a}\rangle \overrightarrow{a}, \tag{8}$$

then we have $\langle \gamma(s), \overrightarrow{a}\rangle = 0$. This means that the curve γ lies in H^n. Moreover, we can see that

$$\left\|\gamma'(s)\right\| = \left\|\beta'(s) - \langle \beta'(s), \overrightarrow{a}\rangle \overrightarrow{a}\right\| = \sin\theta \tag{9}$$

From Equations (8) and (9), we have

$$\gamma(s) + \left(\cot\theta \int_0^s \left\|\dot{\gamma}(u)\right\| du\right)\overrightarrow{a} = \beta(s) - s\cos\theta\overrightarrow{a} + s\cot\theta\sin\theta\overrightarrow{a} = \beta(s)$$

□

From Equation (5), we can see that if the curve α is a polynomial curve, then the curve β is a polynomial curve. Hence, from Theorem 3.1, we can give following theorem.

Theorem 3.2. Under the above notation, if the curve α is a PH-curve, then the curve β is a PH-helical curve. Moreover, all PH-helical curves in Euclidean space $\mathbb{E}^{n+1}$ can be obtained from a PH-curve $\gamma : I \to H^n \subset \mathbb{E}^{n+1}$

The following theorems are given in [13] for obtaining PH-curves and PH-helical curves from planar curves in $\mathbb{E}^3$.

Theorem 3.3. [13] Let $H^2(a, b, c) = \left\{(p_1, p_2, p_3) \in \mathbb{E}^3 : ap_1 + bp_2 + cp_1 + d = 0\right\}$ be a plane in $\mathbb{E}^3$. If the curve $\gamma : I \to H^2$, $\gamma(t) = (\gamma_1(t), \gamma_2(t), \gamma_3(t))$ is a PH-curve, then

$$\begin{aligned}
\gamma_1(t) &= \int \left(b\sqrt{a^2+b^2+c^2}\left(u^2(t) - v^2(t)\right) - 2acu(t)v(t)\right) dt \\
\gamma_2(t) &= \int \left(-a\sqrt{a^2+b^2+c^2}\left(u^2(t) - v^2(t)\right) - 2bcu(t)v(t)\right) dt \\
\gamma_3(t) &= \int 2\left(a^2+b^2\right) u(t)v(t)\, dt \\
\sigma(t) &= \sqrt{a^2+b^2}\sqrt{a^2+b^2+c^2}\left(u^2(t) + v^2(t)\right)
\end{aligned}$$

where $u(t)$ and $v(t)$ are polynomials and

$$\sigma^2(t) = \left(\gamma_1'(t)\right)^2 + \left(\gamma_2'(t)\right)^2 + \left(\gamma_3'(t)\right)^2$$

Theorem 3.4. [13] Let $H^2(a, b, c)$ be a plane in $\mathbb{E}^3$ where

$$H^2(a, b, c) = \{(p_1, p_2, p_3) : ap_1 + bp_2 + cp_3 + d = 0\}$$

In this case, we get all PH- helical curves from planes $H^2(a, b, c)$ in $\mathbb{E}^3$ such that

$$\gamma_{(a,b,c)}(\gamma, t) = \beta(t) = (\beta_1(t), \beta_2(t), \beta_3(t))$$

where

$$\beta_1(t) = \int \left[b\sqrt{a^2+b^2+c^2}\left(u^2(t) - v^2(t)\right) - 2acu(t)v(t) + a\left(a^2+b^2\right)\cot\theta\left(u^2(t) + v^2(t)\right)\right] dt$$

$$\beta_2(t) = \int \left(-a\sqrt{a^2+b^2+c^2}\left(u^2(t) - v^2(t)\right) - 2bcu(t)v(t) + b\left(a^2+b^2\right)\cot\theta\left(u^2(t) + v^2(t)\right)\right) dt$$

$$\beta_3(t) = \int \left[2\left(a^2+b^2\right) u(t)v(t) + c\left(a^2+b^2\right)\cot\theta\left(u^2(t) + v^2(t)\right)\right] dt$$

Hence, axis of the curve β is equal to

$$\overrightarrow{a} = \left(\frac{a}{\sqrt{a^2+b^2+c^2}}, \frac{b}{\sqrt{a^2+b^2+c^2}}, \frac{c}{\sqrt{a^2+b^2+c^2}}\right)$$

4. PH-Helical Curves in $\mathbb{E}^{n+1}$

In this section we give a method to obtain a PH curve in $H^n \subset \mathbb{E}^{n+1}$. Then, we give a theorem in $\mathbb{E}^4$ for the given method. After then, using Theorem 3.2, we give a theorem to construct a PH-helical curve in $\mathbb{E}^4$. Finally, we support these theorems by some examples.

For $a_1, a_2, ..., a_{n+1}, a_{n+2} \in \mathbb{R}$, let

$$H^n(a_1, a_2, ..., a_{n+1}) = \left\{ (p_1, p_2, , ..., p_{n+1}) \in \mathbb{E}^{n+1} | \sum_{i=1}^{n+1} (a_i p_i) + a_{n+2} = 0 \right\}$$

be a hyperplane of $\mathbb{E}^{n+1}$. Assume that $\gamma : I \to H^n(a_1, a_2, ..., a_{n+1}), \gamma(t) = (\gamma_1(t), \gamma_2(t), ..., \gamma_{n+1}(t))$ is a $PH - curve$ with the speed of a polynomial such as $\sigma(t)$. Therefore, we have

$$\sum_{i=1}^{n+1} (\gamma_i^{'}(t))^2 = \sigma^2(t) \tag{10}$$

Since γ lies in $H^n(a_1, a_2, ..., a_{n+1})$ we write

$$\sum_{i=1}^{n+1} (a_i \gamma_i(t)) + a_{n+2} = 0 \tag{11}$$

From Equation (10), we get

$$\sum_{i=1}^{n} \left(\frac{\gamma_i^{'}(t)}{\gamma_{n+1}^{'}(t)} \right)^2 + 1 = \left(\frac{\sigma(t)}{\gamma_{n+1}^{'}(t)} \right)^2 . \tag{12}$$

Differentiation Equation (11) give us

$$\sum_{i=1}^{n+1} a_i \gamma_i^{'}(t) = 0$$

Applying the following substitutions

$$\begin{aligned} X_i &= \frac{\gamma_i^{'}(t)}{\gamma_{n+1}^{'}(t)}, \ i = 1, 2, ..., n \\ \omega &= \frac{\sigma(t)}{\gamma_{n+1}^{'}(t)} \end{aligned}$$

we have

$$\sum_{i=1}^{n} \left(X_i^2\right) + 1 = \omega^2 \tag{13}$$

and

$$\sum_{i=1}^{n} (a_i X_i) + a_{n+1} = 0 \tag{14}$$

From Equation (14), X_n can be written as

$$X_n = \sum_{i=1}^{n-1} (b_i X_i) + b_n \tag{15}$$

where

$$b_i = -\frac{a_i}{a_n}, i = 1, 2, ..., n-1$$

and

$$b_n = -\frac{a_{n+1}}{a_n}$$

Considering Equations (13) and (15), we get

$$\sum_{i=1}^{n-1}(1+b_i^2)X_i^2 + \sum_{\substack{i,j=1\\ i\neq j}}^{n}(b_ib_jX_iX_j) + \sum_{i=1}^{n}2(b_ib_{n+1}X_i) = \omega^2 \tag{16}$$

If we apply the following transformations in Equation (16),

$$X_i = Y_i - \frac{b_ib_{n+1}}{1+b_1^2+b_2^2+...b_n^2}, i = 1,2,...,n$$

then we find

$$\sum_{i=1}^{n-1}(1+b_i^2)Y_i^2 + \sum_{\substack{i,j=1\\ i\neq j}}^{n}(b_ib_jY_iY_j) + \left(\frac{1+b_1^2+b_2^2+...+b_n^2}{1+b_1^2+b_2^2+...+b_{n-1}^2}\right) = \omega^2$$

We can rewrite this quadratic form as

$$Y^tAY + \left(\frac{1+b_1^2+b_2^2+...+b_n^2}{1+b_1^2+b_2^2+...+b_{n-1}^2}\right) = \omega^2 \tag{17}$$

where

$$Y = \begin{pmatrix} Y_1 \\ Y_2 \\ \vdots \\ Y_{n-1} \end{pmatrix} \text{ and } A = \begin{bmatrix} 1+b_1^2 & b_1b_2 & ... & b_1b_{n-1} \\ b_1b_2 & 1+b_2^2 & ... & b_2b_{n-1} \\ \vdots & \vdots & \vdots & \vdots \\ b_1b_{n-1} & b_2b_{n-1} & ... & 1+b_{n-1}^2 \end{bmatrix}$$

One can calculate the eigenvalues of A as $\lambda_1 = 1, \lambda_2 = 1, ..., \lambda_{n-2} = 1, \lambda_{n-1} = 1+b_1^2+b_2^2+...b_{n-1}^2$ and the corresponding eigenvectors of A as columns of the following matrix:

$$A = \begin{bmatrix} -\frac{b_2}{b_1} & -\frac{b_3}{b_1} & \cdots & -\frac{b_{n-1}}{b_1} & -\frac{b_{n-2}}{b_1} & \frac{b_1}{b_{n-1}} \\ 1 & 0 & \cdots & 0 & 0 & \frac{b_2}{b_{n-1}} \\ 0 & 1 & \cdots & 0 & 0 & \frac{b_3}{b_{n-1}} \\ \vdots & \vdots & \ddots & \vdots & \vdots & \vdots \\ 0 & 0 & \cdots & 1 & 0 & \frac{b_{n-2}}{b_{n-1}} \\ 0 & 0 & \cdots & 0 & 1 & 1 \end{bmatrix}$$

Here I_{n-2} is the Idendity matrix of dimension $(n-2)$. We define the index set

$$S_{n-j} = \{1, n-j+1, n-j+2, ..., n-1\}$$

so that we can give a general form of the orthonormal matrix Q obtained by eigenvectors of A which diagonalize Equation (17) and satisfies $Z = QY$ where

$$Q=\begin{bmatrix}
\frac{-b_{n-1}}{\sqrt{\sum\limits_{i\in S_{n-k-1}} b_i^2}} & \frac{-b_1b_{n-2}}{\sqrt{\sum\limits_{i\in S_{n-k}} b_i^2\sum\limits_{i\in S_{n-k-1}} b_i^2}} & \frac{-b_1b_{n-3}}{\sqrt{\sum\limits_{i\in S_{n-k}} b_i^2\sum\limits_{i\in S_{n-k-1}} b_i^2}} & \cdots & \frac{-b_1b_2}{\sqrt{\sum\limits_{i\in S_{n-k}} b_i^2\sum\limits_{i\in S_{n-k-1}} b_i^2}} & \frac{b_1}{\sqrt{\sum\limits_{i\in S_{n-1}} b_i^2}} \\
0 & 0 & 0 & \cdots & \frac{\sqrt{\sum\limits_{i\in S_{n-k}} b_i^2}}{\sqrt{\sum\limits_{i\in S_{n-k-1}} b_i^2}} & \frac{b_2}{\sqrt{\sum\limits_{i\in S_{n-1}} b_i^2}} \\
0 & 0 & 0 & \cdots & \frac{-b_2b_3}{\sqrt{\sum\limits_{i\in S_{n-k}} b_i^2\sum\limits_{i\in S_{n-k-1}} b_i^2}} & \frac{b_3}{\sqrt{\sum\limits_{i\in S_{n-1}} b_i^2}} \\
\vdots & \vdots & \vdots & \ddots & \vdots & \vdots \\
0 & 0 & \frac{\sqrt{\sum\limits_{i\in S_{n-k}} b_i^2}}{\sqrt{\sum\limits_{i\in S_{n-k-1}} b_i^2}} & \cdots & \frac{-b_2b_{n-3}}{\sqrt{\sum\limits_{i\in n-k} b_i^2\sum\limits_{i\in S_{n-k-1}} b_i^2}} & \frac{b_{n-3}}{\sqrt{\sum\limits_{i\in S_{n-1}} b_i^2}} \\
0 & \frac{\sqrt{\sum\limits_{i\in S_{n-k}} b_i^2}}{\sqrt{\sum\limits_{i\in S_{n-k-1}} b_i^2}} & \frac{-b_{n-2}b_{n-3}}{\sqrt{\sum\limits_{i\in S_{n-k}} b_i^2\sum\limits_{i\in S_{n-k-1}} b_i^2}} & \cdots & \frac{-b_2b_{n-2}}{\sqrt{\sum\limits_{i\in S_{n-k}} b_i^2\sum\limits_{i\in S_{n-k-1}} b_i^2}} & \frac{b_{n-2}}{\sqrt{\sum\limits_{i\in S_{n-1}} b_i^2}} \\
\frac{b_1}{\sqrt{\sum\limits_{i\in S_{n-k-1}} b_i^2}} & \frac{b_{n-1}b_{n-2}}{\sqrt{\sum\limits_{i\in S_{n-k}} b_i^2\sum\limits_{i\in S_{n-k-1}} b_i^2}} & \frac{b_{n-1}b_{n-3}}{\sqrt{\sum\limits_{i\in S_{n-k}} b_i^2\sum\limits_{i\in S_{n-k-1}} b_i^2}} & \cdots & \frac{b_2b_{n-1}}{\sqrt{\sum\limits_{i\in S_{n-k}} b_i^2\sum\limits_{i\in S_{n-k-1}} b_i^2}} & \frac{b_{n-1}}{\sqrt{\sum\limits_{i\in S_{n-1}} b_i^2}}
\end{bmatrix}$$

Here k stands for the k-th column of Q. To clarify Q, we give the following examples for spacial cases $n=3$ and 4 respectively:

$$Q=\begin{bmatrix}
\frac{-b_3}{\sqrt{b_1^2+b_3^2}} & \frac{-b_1b_2}{\sqrt{b_1^2+b_3^2}\sqrt{b_1^2+b_2^2+b_3^2}} & \frac{b_1}{\sqrt{b_1^2+b_2^2+b_3^2}} \\
0 & \frac{\sqrt{b_1^2+b_3^2}}{\sqrt{b_1^2+b_2^2+b_3^2}} & \frac{b_2}{\sqrt{b_1^2+b_2^2+b_3^2}} \\
\frac{b_1}{\sqrt{b_1^2+b_3^2}} & \frac{-b_2b_3}{\sqrt{b_1^2+b_3^2}\sqrt{b_1^2+b_2^2+b_3^2}} & \frac{b_3}{\sqrt{b_1^2+b_2^2+b_3^2}}
\end{bmatrix}$$

$$Q=\begin{bmatrix}
\frac{-b_4}{\sqrt{b_1^2+b_4^2}} & \frac{-b_1b_3}{\sqrt{b_1^2+b_4^2}\sqrt{b_1^2+b_2^2+b_3^2+b_4^2}} & \frac{-b_1b_2}{\sqrt{b_1^2+b_3^2+b_4^2}\sqrt{b_1^2+b_2^2+b_3^2+b_4^2}} & \frac{b_1}{\sqrt{b_1^2+b_2^2+b_3^2+b_4^2}} \\
0 & 0 & \frac{\sqrt{b_1^2+b_3^2+b_4^2}}{\sqrt{b_1^2+b_2^2+b_3^2+b_4^2}} & \frac{b_2}{\sqrt{b_1^2+b_2^2+b_3^2+b_4^2}} \\
0 & \frac{\sqrt{b_1^2+b_4^2}}{\sqrt{b_1^2+b_3^2+b_4^2}} & \frac{-b_2b_3}{\sqrt{b_1^2+b_3^2+b_4^2}\sqrt{b_1^2+b_2^2+b_3^2+b_4^2}} & \frac{b_3}{\sqrt{b_1^2+b_2^2+b_3^2+b_4^2}} \\
\frac{-b_1}{\sqrt{b_1^2+b_4^2}} & \frac{-b_3b_4}{\sqrt{b_1^2+b_4^2}\sqrt{b_1^2+b_2^2+b_3^2+b_4^2}} & \frac{-b_2b_4}{\sqrt{b_1^2+b_3^2+b_4^2}\sqrt{b_1^2+b_2^2+b_3^2+b_4^2}} & \frac{b_4}{\sqrt{b_1^2+b_2^2+b_3^2+b_4^2}}
\end{bmatrix}$$

Applying $Z=QY$ in Equation (17) we get

$$\sum_{i=1}^{n-2}(Z_i^2)+(1+b_1^2+b_2^2+...+b_{n-1}^2)Z_{n-1}^2+\frac{1+b_1^2+b_2^2+b_3^2+...+b_n^2}{1+b_1^2+b_2^2+...+b_{n-1}^2}=\omega^2 \tag{18}$$

Because Equation (18) is a Pythagorean (n+2)-tuple, rational solution for this equation is

$$
\begin{aligned}
Z_1(t) &= \frac{r(t)}{s(t)}\left(u_1^2(t) - \sum_{i=2}^{n-1} u_i^2(t)\right)\\
Z_i(t) &= \frac{2r(t)}{s(t)} u_1(t)u_i(t), \quad i = 2, 3, ..., n-1\\
\sqrt{\frac{1 + b_1^2 + b_2^2 + b_3^2 + ... + b_n^2}{1 + b_1^2 + b_2^2 + ... + b_{n-1}^2}} &= \frac{2r(t)}{s(t)} u_1(t)u_n(t)\\
\omega(t) &= \frac{r(t)}{s(t)}\sum_{i=1}^{n} u_i^2(t)
\end{aligned}
$$

where $u_1(t), u_2(t), ..., u_n(t)$ are arbitrary polynomials and

$$
s(t) = \frac{2\sqrt{1 + b_1^2 + b_2^2 + ... + b_n^2}}{\sqrt{1 + b_1^2 + b_2^2 + b_3^2 + ... + b_{n+1}^2}} r(t)u_1(t)u_n(t)
$$

Hence, the components of (γ) can be written with arbitrary polynomials $u_1(t), u_2(t), ..., u_n(t)$ and the reals $a_1, a_2, ..., a_{n+1}$.

For $n = 3$, we give the following theorem in $\mathbb{E}^4$.

Theorem 4.1. For the hyperplane,

$$
H^3(a_1, a_2, a_3, a_4) = \{(p_1, p_2, p_3, p_4) : a_1p_1 + a_2p_2 + a_3p_3 + a_4p_4 + a_5 = 0, p_1, p_2, p_3, p_4 \in \mathbb{R}\}
$$

let $\gamma : I \to H^3$,$\gamma(t) = (\gamma_1(t), \gamma_2(t), \gamma_3(t), \gamma_4(t))$ lies in H^3. Then, γ is a PH-curve in $\mathbb{E}^4$ with the followings:

$$
\gamma_1 = \int \begin{pmatrix} a_2\left(a_1^2 + a_2^2 + a_3^2\right)\sqrt{a_1^2 + a_2^2 + a_3^2 + a_4^2}\left(u_1^2 - u_2^2 - u_3^2\right) \\ -2a_1a_3\sqrt{a_1^2 + a_2^2 + a_3^2}\sqrt{a_1^2 + a_2^2 + a_3^2 + a_4^2}u_1u_2 - 2a_1a_4\sqrt{a_1^2 + a_2^2}\sqrt{a_1^2 + a_2^2 + a_3^2}u_1u_3 \end{pmatrix} dt
$$

$$
\gamma_2 = \int \begin{pmatrix} -a_1\left(a_1^2 + a_1^2 + a_3^2\right)\sqrt{a_1^2 + a_2^2 + a_3^2 + a_4^2}\left(u_1^2 - u_2^2 - u_3^2\right) \\ -2a_2a_3\sqrt{a_1^2 + a_2^2 + a_3^2}\sqrt{a_1^2 + a_2^2 + a_3^2 + a_4^2}u_1u_2 - 2a_1a_4\sqrt{a_1^2 + a_2^2}\sqrt{a_1^2 + a_2^2 + a_3^2}u_1u_3 \end{pmatrix} dt
$$

$$
\gamma_3 = \int \left(2\left(a_1^2 + a_2^2\right)\sqrt{a_1^2 + a_2^2 + a_3^2}\sqrt{a_1^2 + a_2^2 + a_3^2 + a_4^2}u_1u_2 - 2a_3a_4\sqrt{a_1^2 + a_2^2}\sqrt{a_1^2 + a_2^2 + a_3^2}u_1u_3\right) dt
$$

$$
\gamma_4 = \int \left(2\sqrt{a_1^2 + a_2^2}\left(a_1^2 + a_2^2 + a_3^2\right)^{3/2} u_1u_3\right) dt
$$

$$
\sigma = \left(a_1^2 + a_2^2\right)\sqrt{a_1^2 + a_2^2 + a_3^2 + a_4^2}\left(a_1^2 + a_1^2 + a_3^2\right)\left(u_1^2 + u_2^2 + u_3^2\right)
$$

where u_1, u_2 and u_3 are arbitrary polynomials of parameter "t" and $\sigma(t) = \|\dot{\gamma}(t)\|$.

PROOF. Assume that $\gamma : I \to H^3(a_1, a_2, a_3, a_4)$,$\gamma(t) = (\gamma_1(t), \gamma_2(t), \gamma_3(t), \gamma_4(t))$ be a $PH-curve$ with the speed of a polynomial such as $\sigma(t)$ in $H^3(a_1, a_2, a_3, a_4)$. So we have

$$
(\gamma_1'(t))^2 + (\gamma_2'(t))^2 + (\gamma_3'(t))^2 + (\gamma_4'(t))^2 = \sigma^2(t). \tag{19}
$$

Since γ lies in $H^3(a_1, a_2, a_3, a_4)$ we write

$$
a_1\gamma_1(t) + a_2\gamma_2(t) + a_3\gamma_3(t) + a_4\gamma_4(t) + a_5 = 0. \tag{20}
$$

From Equation (19), we get

$$\left(\frac{\gamma_1'(t)}{\gamma_4'(t)}\right)^2+\left(\frac{\gamma_2'(t)}{\gamma_4'(t)}\right)^2+\left(\frac{\gamma_3'(t)}{\gamma_4'(t)}\right)^2+1=\left(\frac{\sigma(t)}{\gamma_4'(t)}\right)^2. \tag{21}$$

Differentiating Equation (20), we find

$$a_1\gamma_1'(t)+a_2\gamma_2'(t)+a_3\gamma_3'(t)+a_4\gamma_4'(t)=0. \tag{22}$$

If we make the following substitutions in Equations (21) and (22),

$$X_1=\frac{\gamma_1'}{\gamma_4'},\ X_2=\frac{\gamma_2'}{\gamma_4'},\ X_3=\frac{\gamma_3'}{\gamma_4'},\ \omega=\frac{\sigma}{\gamma_4'}.$$

we have

$$X_1^2+X_2^2+X_3^2+1=\omega^2 \tag{23}$$

and

$$a_1X_1+a_2X_2+a_3X_3+a_4=0. \tag{24}$$

From Equation (24) X_3 can be written as

$$X_3=b_1X_1+b_2X_2+b_3 \tag{25}$$

where $b_1=-\frac{a_1}{a_3}$, $b_2=-\frac{a_2}{a_3}$, $b_3=-\frac{a_4}{a_3}$. Considering Equations (23) and (25), we get

$$(1+b_1^2)X_1^2+(1+b_2^2)X_2^2+2b_1b_2X_1X_2+2b_1b_3X_1+2b_2b_3X_2+1+b_3^2=\omega^2 \tag{26}$$

Applying the following transformations in Equation (26)

$$X_1=Y_1-\frac{b_1b_3}{1+b_1^2+b_2^2}$$

$$X_2=Y_2-\frac{b_2b_3}{1+b_1^2+b_2^2}$$

we find

$$(1+b_1^2)Y_1^2+(1+b_2^2)Y_2^2+2b_1b_2Y_1Y_2+\left(\frac{1+b_1^2+b_2^2+b_3^2}{1+b_1^2+b_2^2}\right)=\omega^2$$

We can write this quadratic form as

$$\begin{bmatrix}Y_1 & Y_2\end{bmatrix}.\begin{bmatrix}1+b_1^2 & b_1b_2\\ b_1b_2 & 1+b_2^2\end{bmatrix}.\begin{bmatrix}Y_1\\ Y_2\end{bmatrix}+\left(\frac{1+b_1^2+b_2^2+b_3^2}{1+b_1^2+b_2^2}\right)=\omega^2 \tag{27}$$

and if we diagonalize Equation (27) with the matrix Q we get

$$Z_1^2+\left(\sqrt{1+b_1^2+b_2^2}Z_2\right)^2+\left(\sqrt{\frac{1+b_1^2+b_2^2+b_3^2}{1+b_1^2+b_2^2}}\right)^2=\omega^2 \tag{28}$$

here

$$Q=\begin{bmatrix}\frac{-b_2}{\sqrt{b_1^2+b_2^2}} & \frac{b_1}{\sqrt{b_1^2+b_2^2}}\\ \frac{b_1}{\sqrt{b_1^2+b_2^2}} & \frac{b_2}{\sqrt{b_1^2+b_2^2}}\end{bmatrix}$$

and satisfies $Z=Q^{-1}Y$. It is seen that Equation (28) is a Pythagorean Quaternary and its solution is

$$Z_1(t)=\frac{r(t)}{s(t)}(u_1^2(t)-u_2^2(t)-u_3^2(t))$$

$$Z_2(t) = \frac{2r(t)}{\sqrt{1+b_1^2+b_2^2}s(t)}u_1(t)u_2(t)$$

$$\sqrt{\frac{1+b_1^2+b_2^2+b_3^2}{1+b_1^2+b_2^2}} = \frac{2r(t)}{s(t)}u_1(t)u_3(t)$$

$$\omega(t) = \frac{r(t)}{s(t)}(u_1^2(t)+u_2^2(t)+u_3^2(t))$$

$$s(t) = \frac{2\sqrt{1+b_1^2+b_2^2}}{\sqrt{1+b_1^2+b_2^2+b_3^2}}r(t)u_1(t)u_3(t)$$

where u_1, u_2 and u_3 are arbitrary polynomials. So, by the backward operations we find $\gamma_1, \gamma_2, \gamma_3$ and γ_4 as declared. □

By means of Theorem 3.1, we give the following theorem:

Theorem 4.2. For the hyperplane

$$H^3(a_1,a_2,a_3,a_4) = \{(p_1,p_2,p_3,p_4) : a_1p_1+a_2p_2+a_3p_3+a_4p_4+a_5 = 0, a_1,a_2,a_3,a_4,a_5 \in \mathbb{R}\}$$

let $\gamma : I \to H^3, \gamma(t) = (\gamma_1(t), \gamma_2(t), \gamma_3(t), \gamma_4(t))$ be a PH-curve in H^3. Then, the curve $\beta : I \to \mathbb{E}^4, \beta(t) = (\beta_1(t), \beta_2(t), \beta_3(t), \beta_4(t))$ is a PH-helical curve in $\mathbb{E}^4$ where

$$\beta_1 = \int \left(\begin{array}{c} a_2\left(a_1^2+a_2^2+a_3^2\right)\sqrt{a_1^2+a_2^2+a_3^2+a_4^2}\left(u_1^2-u_2^2-u_3^2\right) \\ -2a_1a_3\sqrt{a_1^2+a_2^2+a_3^2}\sqrt{a_1^2+a_2^2+a_3^2+a_4^2}u_1u_2 - 2a_1a_4\sqrt{a_1^2+a_2^2}\sqrt{a_1^2+a_2^2+a_3^2}u_1u_3 \\ +a_1\left(a_1^2+a_2^2\right)\left(a_1^2+a_1^2+a_3^2\right)\cot\theta\left(u_1^2+u_2^2+u_3^2\right) \end{array} \right) dt$$

$$\beta_2 = \int \left(\begin{array}{c} -a_1\left(a_1^2+a_1^2+a_3^2\right)\sqrt{a_1^2+a_2^2+a_3^2+a_4^2}\left(u_1^2-u_2^2-u_3^2\right) \\ -2a_2a_3\sqrt{a_1^2+a_2^2+a_3^2}\sqrt{a_1^2+a_2^2+a_3^2+a_4^2}u_1u_2 - 2a_1a_4\sqrt{a_1^2+a_2^2}\sqrt{a_1^2+a_2^2+a_3^2}u_1u_3 \\ +a_2\left(a_1^2+a_2^2\right)\left(a_1^2+a_1^2+a_3^2\right)\cot\theta\left(u_1^2+u_2^2+u_3^2\right) \end{array} \right) dt$$

$$\beta_3 = \int \left(\begin{array}{c} 2\left(a_1^2+a_2^2\right)\sqrt{a_1^2+a_2^2+a_3^2}\sqrt{a_1^2+a_2^2+a_3^2+a_4^2}u_1u_2 - 2a_3a_4\sqrt{a_1^2+a_2^2}\sqrt{a_1^2+a_2^2+a_3^2}u_1u_3 \\ +a_3\left(a_1^2+a_2^2\right)\left(a_1^2+a_1^2+a_3^2\right)\cot\theta\left(u_1^2+u_2^2+u_3^2\right) \end{array} \right) dt$$

$$\beta_4 = \int \left(2\sqrt{a_1^2+a_2^2}\left(a_1^2+a_2^2+a_3^2\right)^{3/2}u_1u_3 + a_4\left(a_1^2+a_2^2\right)\left(a_1^2+a_1^2+a_3^2\right)\cot\theta\left(u_1^2+u_2^2+u_3^2\right) \right) dt$$

Hence, the unit axis of the curve (β) is

$$\overrightarrow{d} = \left(\frac{a_1}{\sqrt{a_1^2+a_2^2+a_3^2+a_4^2}}, \frac{a_2}{\sqrt{a_1^2+a_2^2+a_3^2+a_4^2}}, \frac{a_3}{\sqrt{a_1^2+a_2^2+a_3^2+a_4^2}}, \frac{a_4}{\sqrt{a_1^2+a_2^2+a_3^2+a_4^2}} \right)$$

Example 4.3. For the hyperplane $H^3(3,4,12,84)$, from Theorem 4.1, it is easy to see that by putting $u_1(t) = 1, u_2(t) = t$ and $u_3(t) = 1+t$ we obtain a PH-curve $\gamma : I \to H^3, \gamma(t) = (\gamma_1(t), \gamma_2(t), \gamma_3(t), \gamma_4(t))$ with the followings:

$$\begin{aligned} \gamma_1(t) &= -\tfrac{114920}{3}t^3 - 113620t^2 - 32760t - \tfrac{57460}{3} \\ \gamma_2(t) &= 2830t^3 - 31785t^2 - 43680t + 14365 \\ \gamma_3(t) &= -37895t^2 - 131040t \\ \gamma_4(t) &= 10985t^2 + 21970t \end{aligned}$$

We can check that $\|\dot{\gamma}(t)\| = 143650(t^2+t+1)$ which is equal to $\sigma(t)$ given in Theorem 4.1 as well. Also by the way of Theorem 4.2, assuming $\cot\theta = 1$ we get a PH-helix curve from the curve γ such as $\beta : I \to \mathbb{E}^4, \beta(t) = (\beta_1(t), \beta_2(t), \beta_3(t), \beta_4(t))$ with the followings:

$$\begin{aligned}
\beta_1(t) &= -\tfrac{109850}{3}t^3 - 111085t^2 - 27690t - \tfrac{54925}{3} \\
\beta_2(t) &= \tfrac{92950}{3}t^3 - 28405t^2 - 36920t + \tfrac{46475}{3} \\
\beta_3(t) &= 6760t^3 - 27755t^2 - 110760t + 3380 \\
\beta_4(t) &= 47320t^3 + 81965t^2 + 163930t + 23660
\end{aligned}$$

Furthermore it can be calculated that $\left\|\dot{\beta}(t)\right\| = 143650\sqrt{2}(t^2+t+1)$ that means β is also a PH-curve. At the same time, since $< \dot{\beta}(t), \vec{a} >= \frac{85\sqrt{2}}{2}$ for the constant vector $\vec{a} = \left(\frac{3}{85}, \frac{4}{85}, \frac{12}{85}, \frac{84}{85}\right)$, it's seen that β is a helical curve in $\mathbb{E}^4$.

Example 4.4. $\gamma : I \to H^4(3, 12, 4, 84, 132)$,$\gamma(t) = (\gamma_1(t), \gamma_2(t), \gamma_3(t), \gamma_4(t), \gamma_5(t))$ is a PH-curve components below:

$$\begin{aligned}
\gamma_1(t) &= -58984900t^3 - 55462500t^2 - 96990100t \\
\gamma_2(t) &= -30149075t^2 - 152020800t \\
\gamma_3(t) &= 44238675t^3 - 73950000t^2 - 6434925t \\
\gamma_4(t) &= 72537725t^3 - 99969350t \\
\gamma_5(t) &= -39918125t^2 + 79836250t
\end{aligned}$$

It can be calculated that $\|\dot{\gamma}(t)\| = 221193375(t^2+1)$. Also the curve β which is obtained from γ by using Theorem 3.2 is a PH-helical curve in $\mathbb{E}^5$ with the followings

$$\begin{aligned}
\beta_1(t) &= -\tfrac{231712975}{4}t^3 - 55462500t^2 - \tfrac{375280525}{4}t \\
\beta_2(t) &= 4226625t^3 - 30149075t^2 - 139340925t \\
\beta_3(t) &= 45647550t^3 - 73950000t^2 - 2208300t \\
\beta_4(t) &= 29586375t^3 + 72537725t^2 - 11210225t \\
\beta_5(t) &= 46492875t^3 - 39918125t^2 + 219314875t
\end{aligned}$$

Furthermore it can be calculated that $\left\|\dot{\beta}(t)\right\| = \frac{1105966875}{4}(t^2+1)$ that means β is also a PH-curve. At the same time, since $< \dot{\beta}(t), \vec{a} >= \frac{471}{5}$ for the constant vector $\vec{a} = \left(\frac{3}{157}, \frac{12}{157}, \frac{4}{157}, \frac{84}{157}, \frac{132}{157}\right)$, it's seen that β is a helical curve in $\mathbb{E}^5$.

5. Conclusion

In this paper, we give a method to obtain PH-curves from arbitrary planar curves. And then we show that there are PH-helical curves which are obtained from PH-curves that we constructed. We give the derivation of the method in $\mathbb{E}^4$ as an application in details and another PH-helical curve in $\mathbb{E}^5$ without detailed computations. Changing the coefficients and the polynomials used in examples, one can obtain any PH-helical curves whose components are of any degrees. Of course, it's possible to extend Theorem 4.1 and and 4.2 to any dimension of $\mathbb{E}^{n+1}$. In addition, because we consider only the rational solutions of $(n+1)$-tuples of Pythagorean equation, we can say that it may not be possible to obtain all PH-helical curves with our method given in the paper. So this is an open problem in the literature.

Author Contributions

All the authors contributed equally to this work. They all read and approved the final version of the manuscript.

Conflicts of Interest

The authors declare no conflict of interest.

Acknowledgment

This work was supported by the Office of Scientific Research Projects Coordination at Çanakkale Onsekiz Mart University, Grant number: FHD-2020-3452.

References

[1] M. A. Lancret, *M' emoire sur les courbes 'a double courbure*, M'emoires pr'esent'es 'a l'Institut des Sciences, Letters et arts par divers savants, Tome 1(1802) 416–454.

[2] W. Kuhnel, Differential Geometry: Curves-Surfaces-Manifolds, Braunchweig, Friedr. Vieweg & Sohn, 1999.

[3] R. T. Farouki, T. Sakkalis, *Pythagorean Hodographs*, IBM Journal of Research and Development 34(5) (1999) 736–752.

[4] R. T. Farouki, T. Sakkalis, *Pythagorean-Hodograph Space Curves*, Advances in Computational Mathematics 2(1) (1994) 41–66.

[5] R. T. Farouki, C. Y. Han., C. Manni, A. Sestini, *Characterization and Construction of Helical Polynomial Space Curves*, Journal of Computational and Applied Mathematics 162(2) (2004) 365–392.

[6] R. T. Farouki, Pythagorean-Hodograph Curves: Algebra and Geometry Inseparable, Springer, Berlin, Heidelberg, 2008.

[7] R. T. Farouki, C. Giannelli, A. Sestini, *Helical Polynomial Curves and Double Pythagorean Hodographs I Quaternion and Hopf map representations*, Journal of Symbolic Computation 44(2) (2009) 161–179.

[8] R. T. Farouki, C. Giannelli, A. Sestini, *Helical Polynomial Curves and Double Pythagorean Hodographs II. Enumeration of Low-Degree Durves*, Journal of Symbolic Computation 44(4) (2009) 307–332.

[9] R. T. Farouki, M. Al-Kandari, T. Sakkalis, *Structural Invariance of Spatial Pythagorean Hodographs*, Computer Aided Geometric Design 19(6) (2002) 395–407.

[10] R. T. Farouki, Z. Sír, *Rational Pythagorean-Hodograph Space Curves*, Computer Aided Geometric Design 28(2) (2011) 78–88.

[11] H. Pottman, *Curve Design with Rational Pythagorean-Hodograph Curves*, Advances in Computational Mathematics 3 (1995) 147–170.

[12] S. Izumiya, N. Takeuchi, *Generic Properties of Helices and Bertrand Curves*, Journal of Geometry 74 (2002) 97–109.

[13] Ç. Camcı K. İlarslan, *A New Method for Construction of PH-Helical Curves in* $\mathbb{E}^3$, Comptes Rendus De L Academıe Bulgare Des Scıences, 72(3) (2019) 301–308.

[14] H. Gluck, *Higher Curvatures of Curves in Euclidean Space*, The American Mathematical Monthly 37 (1966) 699–704.

[15] M. C. Romero-Fuster, E. Sanabria-Codesal, *Generalized Helices Twistings and Flattenings of Curves in n-Space*, Matematica Contemporanea 17 (1999) 267–280.

[16] E. Ödamar, H. H. Hacısalihoğlu, *A Characterization of Inclined Curves in Euclidean n-Space*, Communications Faculty of Sciences University of Ankara Series A1-Mathematics and Statistics 24 (1975) 15–23.

[17] Ç. Camcı K. İlarslan, L. Kula, H. H. Hacısalihoğlu, *Harmonic Cuvature and General Helices*, Chaos Solitons Fractals 40 (2009) 2590–2596.

[18] K. K. Kubota, *Pythagorean Triples in Unique Factorization Domains*, The American Mathematical Monthly 79 (1972) 503–505.

Journal of
New Theory
ISSN: 2149-1402

37 (2021) 58-67
Journal of New Theory
https://dergipark.org.tr/en/pub/jnt
Open Access

Efficiency Analysis and Estimation of Factors Affecting the Efficiency with Decision Trees in Imbalanced Data: A Case of Turkey's Environmental Sustainability

Selin Ceren Turan[1], Emre Dünder[2], Mehmet Ali Cengiz[3]

Article History
Received: 08 Dec 2021
Accepted: 28 Dec 2021
Published: 31 Dec 2021
10.53570/jnt.1034246
Research Article

Abstract − Cities have proliferated and experienced increasing environmental issues in the modern world. The concept of environmental sustainability is one of the main problems to solve. Therefore, it is fundamental to establish statistical methods to measure environmental sustainability. The first aim of this study is to measure the environmental sustainability performance of 42 cities in Turkey by Data Envelopment Analysis. The second aim is to solve the imbalance in the efficiency values obtained using Synthetic Minority Oversampling Technique methods. After all, we expose the multiple relationships between input and output variables and efficiency using the Decision trees classifiers approach. As a result of the analyses, three internal factors were found to influence the environmental efficiency levels: residential sales, population intensity, and the number of completed industrial sites. It has been determined that the number of completed industrial sites and the increase in residential sales distorted environmental efficiency.

Keywords − *Classification, decision trees, DEA, environmental sustainability, imbalanced data, SMOTE*

Mathematics Subject Classification (2020) − 62H30, 62P99

1. Introduction

The world has become a situation in which natural resources are depleted rapidly. Besides, it has become difficult to compensate for depleted resources. Factors such as an increase in consumption and population, excessive consumption of natural resources, unplanned urbanization, and industrialization have caused environmental problems to reach serious levels. As a result of all this, an increase in water, soil, and air pollution occurs. Thus, problems arise that threaten the health of living things. This situation, which impacts the lives of all living things, has led people to develop solutions. In this context, the concept of environmental sustainability is tried to be expanded.

In the simplest terms, the concept of sustainability can be defined as developing without harming resources to transfer them to future generations while making use of today's resources. With environmental issues gaining a global dimension, states that have entered the path of developing policies based on the concept of environmental sustainability have signed international protocols and agreements. Besides, the number of established non-governmental organizations has increased, and various studies have been initiated to protect the environment. The United Nations Environment Conference in Stockholm in 1972, the United Nations

[1]scturan1@gmail.com (Corresponding Author); [2]emre.dunder@omu.edu.tr; [3]macengiz@omu.edu.tr
[1,2,3] Department of Statistics, Faculty of Arts and Sciences, Ondokuz Mayıs University, Samsun, Turkey

Environment and Development Conference in 1992, and the Sustainable Development Summit in 2002 are global conferences on environmental issues. In these conferences, political approaches were handled to realize sustainable development, which prevents environmental issues.

Countries and organizations use different methodologies to evaluate the performance of their policies to improve the quality of life and reduce pollution sustainably. Data Envelopment Analysis (DEA) is one of those methods. DEA is a non-parametric statistical method used to define the effectiveness limits of decision-making units (DMUs) with more than input and output. There are some studies about environmental sustainability performance comparisons such as Marshall and Shortle [1], Siong and Hussein [2], Yu and Wen [3], Yoshino et al. [4], Xiaoping et al. [5]. However, all these and similar studies are only on environmental performance measurement.

The imbalance is one of the problems that can be encountered in datasets. It can be defined as the number of observations belonging to classes is not equal. While working with such datasets, the near-perfect accuracy values in the analysis results do not mean that the model is very successful. Therefore, while performing performance evaluation, considering measures such as sensitivity, determination, negative/positive predictive value will also provide a healthier performance evaluation. To improve this gap in performance values, methods such as oversampling, under-sampling, and Synthetic Minority Oversampling Technique (SMOTE) are used to change the sample structure in the dataset. The concept of environmental sustainability has become an important part of scientific studies day by day. However, in the studies in the literature, it has been determined that there is no study that deals with the situation of encountering the imbalance problem in the data sets used. Adebayo et al. [6] investigated coal consumption and environmental sustainability in South Africa by examining the role of financial development and globalization by using a dataset covering the period from 1980 to 2017. Kimhombo et al. [7] investigated by panel analysis whether there is a trade-off between financial globalization, economic growth, and environmental sustainability. Khan et al. [8] investigated how environmental technology contributes to wastewater improvement in 16 selected OECD countries during 2000–2019.

There are some studies for examining the performance analysis of classifiers on imbalanced datasets in the literature. Akbani et al. [9] investigated how Support Vector Machines (SVM) should be implemented in such datasets. They investigated the cause of the classic SVM classifier's failures and proposed the SMOTE method for high success. It was observed that they achieved higher success with the method they proposed compared to classical methods. In a study conducted by He [10], the most appropriate approaches and performance analysis criteria for imbalanced datasets were examined. They identified what vital areas are encountered with imbalanced datasets. They have determined which vital areas are encountered with imbalanced datasets. They also examined the statistical structures of datasets and mentioned what algorithms the information discovery could take place in such situations.

Inspired by all this information, this study includes an empirical application on DEA related to the environmental sustainability concept. This study consists of two stages. The first stage of this study is the environmental sustainability performance of 42 cities in Turkey is evaluated using the DEA method. For this purpose, input and output variables were selected among the environmental sustainability indicators used in the study conducted by Yu and Wen [3]. Then, it aims to balance the data by using SMOTE and some other types of SMOTE methods, which is one of the resampling methods to solve the imbalance problem in the obtained performance values. The second stage of this study ensures that the relations between the environmental sustainability performance of 42 cities in Turkey and other factors are determined by the Decision Trees classifier. Unlike past studies, this study investigates the solve the imbalance in the efficiency values obtained using SMOTE methods.

The rest of our study includes four more main sections. In the next section, data envelopment analysis, transforming imbalanced data into the balanced dataset, decision trees classifier, and performance criteria are included. While the findings are included in the third section, some comments and studies can be made in the fourth section.

2. Preliminary

2.1. Data Envelopment Analysis

It is of great importance for countries and institutions to know how much production can increase by increasing efficiency due to the rational use of resources. In this context, efficiency measurements of units have become a critical necessity today. DEA can be defined as a linear programming-based method that produces consistent results in the presence of many inputs and outputs. It is used to evaluate their relative effectiveness. Efficiency measurement in this method is carried out as the weighted sum of the outputs divided by the weighted sum of the inputs. In classical DEA models, the unit with the highest efficiency in the observation set is determined by considering the input and output variables of homogeneous DMUs. Then, an efficiency limit is created according to this unit. Efficiency rankings are performed by calculating the distances of other DMUs according to this limit. In this way, it is possible to mathematically interpret how ineffective DMUs can increase or decrease the input/output levels to be effective and which decision points can be used as a reference. The basic assumption in these models is that all DMUs have similar strategic objectives, and in this context, the same type of output is produced using the same kind of input.

One of the most used models of DEA is the model described as the CCR model developed by Charnes et al. [11] based on the assumption of a continuous return to scale (CRS). The second model is the model known as the BCC model, which was expanded by Banker et al. [12] with the assumption of variable returns to scale, see [13]. The model selection for input-oriented or output-oriented is discussed while using CCR and BCC models in DEA studies [1,14]. In the technical efficiency measurement made using the input-oriented efficiency, the minimum input level required to produce the fixed output amount is tried to be obtained. The input oriented CCR model obtained from Charnes et al. [15] is as follows:

$$E_k = \min\theta - \varepsilon\left(\sum_{i=1}^{m} S_i^- + \sum_{r=1}^{s} S_r^+\right)$$

constraints,

$$\sum_{j=1}^{n} x_{ij}\,\lambda_j - \theta x_{ik} + S_i^- = 0, i = 1,2,\dots,m$$

$$\sum_{j=1}^{n} y_{rj}\,\lambda_j - y_{rk} - S_r^+ = 0, r = 1,2,\dots,s$$

$$\lambda\_j, S\_i\text{^}-, S\_r\text{^}+ \geq 0;\ r = 1,2,\dots,s; i = 1,2,\dots,m; j = 1,2,\dots,n \tag{1}$$

Here, E_k is k[th] DMU's efficiency value. *i* and *r*, respectively, is the number of inputs and outputs. *j* indicates the number of DMU. θ represents how much the input amount can be reduced without modifying the output and λ_j is the variable used in the determination of the reference set. Decision units with $\lambda_j > 0$ are called effective, and these effective units are obtained as a reference set for ineffective decision units. S_i^- and S_r^+ show the excess in the input variables and the lack of the output variables, respectively. In the case that θ = 1 and $S_i^- = S_r^+ = 0$ for each input and output variable, DMU is considered effective. In this study, an output oriented CCR model was used. The output oriented CCR model aims to maximize the output value without the need for more than the current input values. The output oriented CCR model obtained from Cooper et al. [16] is as follows:

$$E_k = \max\gamma - \varepsilon\left(\sum_{i=1}^{m} S_i^- + \sum_{r=1}^{s} S_r^+\right)$$

constraints,

$$\sum_{j=1}^{n} x_{ij}\,\beta_j - x_{ik} + S_i^- = 0, i = 1,2, \dots, m$$

$$\sum_{j=1}^{n} y_{rj}\,\beta_j - \gamma y_{rk} - S_r^+ = 0, r = 1,2, \dots, s$$

$$\beta\_j, S\_i\text{^}-, S\_r\text{^}+ \geq 0; r = 1,2, \dots, s; i = 1,2, \dots, m;\ j = 1,2, \dots, n \quad (2)$$

Here, γ represents the expansion coefficient that determines how radially the output of decision-makers can be increased. β_j is the variable used in the determination of the reference set.

2.2. Transforming Imbalanced Data into Balanced Datasets

While making the classification, it is tried to be guessed which units will be included in different classes or groups depending on some input variables. Samples of courses in a dataset can have an imbalanced distribution and are frequently encountered with such datasets. Datasets such as fraud detection and delayed invoice estimation are widely known examples of imbalanced datasets.

Applying methods such as increasing the sample rate by collecting more samples, trying different machine learning algorithms, changing class weights, and punishing models help to make the imbalanced datasets more balanced. In addition, there are many suggested methods in the literature to eliminate the effect of imbalanced datasets on classification. Under-sampling and oversampling methods are the most used of these methods. Under-sampling can be defined as approximating the number of majority classes to the number of minority classes in the dataset. In oversampling methods, the number of observations of the minority class increases, or the number of observations of the majority class is reduced. Thus, it is made to achieve balance. The most important disadvantages are that the under-sampling method causes loss of information by decreasing the number of samples in the dataset.

In contrast, the oversampling method may increase the number of samples and cause an overfitting problem. On the other hand, the under-sampling method reduces training time significantly with this sample reduction in the dataset and significantly saves memory. An increase in training time is observed since the oversampling method greatly increases the size of the data set. Also, the memory used occupies a considerable amount of space.

Synthetic Minority Oversampling Technique (SMOTE), which is based on the principle of operation of the oversampling method, is among the recommended methods to eliminate the effect of imbalanced datasets on classification. In this study, SMOTE algorithms are focused on. SMOTE method selects the most recent neighbours by applying the K-nearest neighbours (KNN) algorithm and then combines them. Thus, synthetically replicates the class type where the available imbalanced data distribution. The algorithm calculates distances between vectors using feature vectors and their closest neighbours. These differences are multiplied by the random number between 0 and 1 and added back to the dataset. Thus, the data becomes balanced [17]. The SMOTE algorithm is a pioneering algorithm for algorithms such as ADAptive SYNthetic (ADASYN), Density-Based SMOTE (DBSMOTE), Relocating Safe-level SMOTE (RSLS).

2.3. Decisions Trees

Tree-based learning algorithms are one of the most used supervised learning algorithms. This is because they can generally be adapted to the solution of all classification and regression problems. Decision trees are a basic data mining classification algorithm used for classifying data. It is used in many different datasets due to its ease of creating and interpreting results, transparency, and sensitivity to noisy data. The decision tree is used to break data sets containing many records into smaller sets by applying decision rules. That is, a tree structure is taken as an example in this method. In this structure, while going from the stem to the leaves, there is a query in each node and the answers given to the queries connected to the nodes. Each query process starts from the body of the decision tree and repeats towards the leaves recursively [18]. There are class labels on the leaves of the tree. Commonly known decision tree classification methods are C4.5, Iterative Dichotomiser 3 (ID3), and Classification and Regression Trees (CART).

2.4. Performance Measurement Criteria

In classification applications, consistency criteria are considered to measure model performances in general. But the consistency criterion may show bias towards the majority class in imbalanced classification problems. For this reason, the F-score, G-mean, and the area under the ROC curve (AUC) criteria, which are more suitable for measuring model performances, were used in this study.

3. Results and Discussion

In the application part, we implemented DEA on 42 different cities existing in Turkey to measure the environmental efficiency levels. Water consumption, electricity consumption, practising nurses, fuel consumption and total environmental public expenditure, are used as input variables, while $(S02)^{-1}$, $(\text{PM10})^{-1}$, $(\text{Water waste})^{-1}$, and $(\text{Solid Waste})^{-1}$ are used as an output variable for the DEA approach in the study. These input and output variables were selected among the variables used in environmental sustainability analysis in the literature. The data sets were taken from the Turkey Statistical Institute (TURKSTAT) (https://data.tuik.gov.tr/) and the Ministry of Environment and Urbanization (https://csb.gov.tr/).

We obtained the efficiency values in the first phase and then carried out the decision tree algorithm by handling the class-imbalanced problem. We selected one of the most popular CART algorithms. Following this way, we conducted a two-stage approach to identify the potential internal factors on the efficiencies. Statistical analyses in this study were carried out using MaxDEA 8 Basic (available at http://maxdea.com/MaxDEA.htm) and R-Project softwares [19]. We utilized Benchmark [20] and rpart [21] packages existing in R-Project.

Table 1 shows the definitions of the inputs, outputs, and internal factors considered in the analysis part.

Table 1. Definition of the variables

Type	Variables	Explanation
Inputs	i_1	Water Consumption
	i_2	Electricity consumption
	i_3	Fuel consumption
	i_4	Total environmental public expenditure
Outputs	o_1	$(\text{S02})^{-1}$
	o_2	$(\text{PM10})^{-1}$
	o_3	$(\text{Water waste})^{-1}$
	o_4	$(\text{Solid Waste})^{-1}$
Internal factors	x_1	Residential sales
	x_2	Population in the cities
	x_3	Population density
	x_4	Farming areas
	x_5	Number of completed industrial sites
	x_6	Number of cars (per thousand)
	x_7	Number of motor vehicles by cities
	x_8	GDP per capita ($)

Table 2 denotes the descriptive statistics of the inputs, outputs, and internal factors. The mean, standard deviation, maximum and minimum values are given for each variable.

Table 2. Descriptive statistics of the variables

Type	V	Mean	SD	Min	Max
Inputs	i_1	74840.595	144731.774	4633.000	931885.000
	i_2	2070006.167	4125846.530	69057.000	25304170.000
	i_3	239729.690	445398.485	18360.000	2824675.000
	i_4	135730601.690	384771460.557	6672868.000	2450908325.000
Outputs	o_1	0.070	0.044	0.007	0.167
	o_2	0.016	0.006	0.008	0.033
	o_3	0.002	0.006	0.000	0.033
	o_4	0.000	0.000	0.000	0.000
Internal factors	x_1	9383.476	24208.458	146.000	153897.000
	x_2	1159361.643	2056903.741	74412.000	13255685.000
	x_3	153.931	385.930	19.360	2551.133
	x_4	3233593.714	2447038.310	143688.000	12591457.000
	x_5	1416.595	1065.354	26.000	5147.000
	x_6	81.429	33.517	18.000	147.000
	x_7	236638.262	448382.847	9247.000	2794236.000
	x_8	18975527.071	52964266.728	726575.000	343536128.000

V: Variables, **SD**: Standard deviation, **Min**: Minimum, **Max**: Maximum

As seen from Table 1, we used four inputs and four outputs with the complete data set. Because of the opposite nature of the data, we used the reciprocal of the outputs. The sample size assumption is satisfied since the sample size is relatively large, at least three times higher ($n = 42 > p = 24$).

Table 3 reports the environmental efficiency values of all the cities.

Table 3. The efficiency values of the cities

City	Efficiency	Decision
Adana	0.182	Not efficient
Adıyaman	0.418	Not efficient
Afyonkarahisar	0.146	Not efficient
Antalya	0.037	Not efficient
Balıkesir	0.162	Not efficient
Bayburt	1.000	**Efficient**
Bilecik	1.000	**Efficient**
Bitlis	0.704	Not efficient
Burdur	0.661	Not efficient
Bursa	0.075	Not efficient
Çanakkale	0.382	Not efficient
Çorum	0.201	Not efficient
Diyarbakır	0.152	Not efficient
Edirne	0.261	Not efficient
Elazığ	0.207	Not efficient
Erzincan	0.419	Not efficient
Eskişehir	0.616	Not efficient
Gaziantep	0.066	Not efficient
Giresun	0.653	Not efficient
Hatay	0.215	Not efficient
Isparta	0.275	Not efficient
İstanbul	0.021	Not efficient
İzmir	0.033	Not efficient

Table 4. (Continued) The efficiency values of the cities

City	Efficiency	Decision
Kars	1.000	**Efficient**
Kırklareli	1.000	**Efficient**
Kütahya	0.263	Not efficient
Malatya	0.174	Not efficient
Manisa	0.247	Not efficient
Ordu	0.280	Not efficient
Osmaniye	1.000	**Efficient**
Rize	0.553	Not efficient
Samsun	0.214	Not efficient
Siirt	0.369	Not efficient
Sivas	0.663	Not efficient
Şanlıurfa	0.198	Not efficient
Tekirdağ	0.089	Not efficient
Tokat	0.354	Not efficient
Trabzon	0.224	Not efficient
Uşak	0.515	Not efficient
Van	0.276	Not efficient
Yalova	1.000	**Efficient**
Yozgat	0.462	Not efficient

According to table 3, only a few cities (seven cities) are efficient in terms of environmental sustainability, and the ratio of the efficient units is 14.3%.

We labelled the units as efficient and not efficient and implemented the decision tree algorithms using eight internal factors in the second stage. We have two purposes of conducting decision trees: 1) To determine the important variables that affect environmental efficiency 2) To construct reasonable rules for proposing further suggestions.

However, the data mining algorithms are rather sensitive to the distribution of the response variable, especially in the presence of a class imbalanced problem. Our DEA results clearly point out the class-imbalanced problem because of the ratio of the efficient units. To overcome this difficulty, we applied four different oversampling techniques such as SMOTE, DBSMOTE, RSLS, and ADASYN. We checked three performance metrics: AUC, F-score, and G-mean of the decision tree results.

Table 4 presents the results of the AUC, F-score and G-mean for each oversampling method and when there is no oversampling.

Table 5. The results of the performance metrics for oversampling methods

Method	AUC	G-mean	F-score
No oversampling	0.500	0.000	0.000
SMOTE	**0.990**	0.039	0.028
DBSMOTE	0.975	**0.060**	0.031
RSLS	0.938	0.051	**0.036**
ADASYN	**0.990**	0.039	0.028

According to the metrics, the oversampling methods obviously improve the performance of the decision tree algorithms. When compared with the raw efficiency data, the over-sampled data sets overcome the class-imbalanced problem by increasing AUC, G-mean, and F-scores. However, there is no absolute discrimination among oversampling methods in achievement. Because of that reason, we interpret the decision tree results and struggle to make inferences on general findings.

Table 5 shows the variable selection results for each oversampling method.

Table 6. The selected variables by decision tree algorithm

Oversampling method	x_1	x_2	x_3	x_4	x_5	x_6	x_7	x_8
No oversampling	NS	NS	NS	NS	NS	NS	NS	NS
SMOTE	+	NS	+	NS	+	NS	NS	NS
DBSMOTE	+	NS	NS	NS	+	NS	NS	NS
RSLS	+	NS	NS	NS	NS	NS	NS	NS
ADASYN	+	NS	+	NS	+	NS	NS	NS

NS: Not selected

The "+" symbol in Table 5 indicates that the relevant variables were selected. When the class-imbalanced problem was not solved, i.e., the decision tree algorithm did not select any variables when the oversampling was not applied. The variable of residential sales (x_1) was commonly selected by all the algorithms. Besides, the variables of the population intensity (x_3) and the number of completed industrial sites (x_5) was selected by the other algorithms. We can observe that the residential sales, population intensity, and completed industrial sites significantly affect the environmental efficiency levels.

Table 6 reports the extracted rules and the ratios from the decision tree algorithms with the oversampling methods.

Table 7. The extracted rules from decision trees

Tree	Rules	Inference	Ratio
SMOTE	1	If x_5>=713 then inefficient	42
+	2	If x_5<713 and x_3 ≥83 then efficient	31
CART	3	If x_5<713 and x_3<83 and x_1<883 then efficient	18
	4	If x_5<713 and x_3<83 and x_1 ≥883 then efficient	10
DBSMOTE +	1	If x_5 ≥713 then inefficient	45
CART	2	If x_5<713 and x_1<1241 then efficient	42
	3	If x_5<713 and x_1 ≥1241 then inefficient	13
RSLS + CART	1	If x_1<972 then efficient	65
	2	If x_1 ≥972 then inefficient	35
ADASYN	1	If x_5 ≥713 then inefficient	41
+	2	If x_5<713 and x_3 ≥84 then efficient	32
CART	3	If x_5<713 and x_3<84 and x_1<782 then efficient	18
	4	If x_5<713 and x_3<84 and x_1 ≥782 then efficient	10

According to the rules, higher residential sales leads to environmental inefficiency for all the cases. Mostly, the rules point out the environmental inefficiency when the number of completed industrial sites becomes high, singly. The environmental efficiency is observed simultaneously when residential sales are relatively lower, and the population intensity is more elevated. Even though the threshold values differ among the trees, they are rather similar. Also, the rules containing the number of completed industrial sites have the highest frequency in general.

4. Conclusion

It is crucial to provide efficient management in environmental issues in worldwide. Due to the importance of this topic, we should understand the main determinants and possible effects of these determinants that may affect environmental efficiency. Within this purpose, we attempted to identify the related factors on the environmental efficiency levels of Turkish cities. We followed a three-way approach using DEA, oversampling methods, and decision tree algorithms to reach our purpose. First, we obtained the efficiencies of the cities and then applied one of the decision trees, the CART algorithm, with oversampling procedures.

We utilized the capacity of data mining with the CART algorithm for selecting the most relevant factors and making further inferences with the extracted rule sets. The imbalance of the distribution of the efficiency levels led us to use oversampling methods. Also, the use of oversampling methods proved the rightness of our way since the raw efficiency data did not produce any rules. One of the most benefits of this paper is to demonstrate how reasonable results can be obtained by handling the class-imbalanced problem in second stage DEA.

According to the results, three internal factors were found to influence the environmental efficiency levels: residential sales, population intensity, and the number of completed industrial sites. Mainly, the increment of the residential sales and the number of completed industrial sites distort environmental efficiency. However, environmental efficiency can be ensured, even in high population intensity, when the residential sales are relatively low.

Our findings give insight into the improvement of the environmental efficiency process. We propose to decrease the residential and industrial buildings, together with the population intensity

Author Contributions

S.C.T: designing the study, providing data and statistical analyses, and writing the manuscript. E.D: statistical analyses and interpreting the results. M.A.C: literature research and discussed the results.

Conflict of Interest

The authors declare no conflict of interest.

References

[1] E. Marshall, J. Shortle, *Using DEA and VEA to evaluate quality of life in the Mid-Atlantic States*, Agricultural and Resource Economics Review 34(2) (2005) 185–203.

[2] H. C. Siong, M. Z. S. M Hussein, *Modeling Urban Quality of Life with Data Envelopment Analysis Methods*, Research Result Report, *Universiti Teknologi Malaysia*, VOT78513, 2008.

[3] Y. Yu, Z. Wen, *Evaluating China's Urban Environmental Sustainability with Data Envelopment Analysis*, Ecological Economics (69) (2010) 1748–1755.

[4] D. Yoshino, A. Fujiwara, J. Zhang, *Environmental Efficiency Model Based on Data Envelopment Analysis and Its Application to Environmentally Sustainable Transport Policies*, Transportation Research Record 2163(1) (2010) 112–123.

[5] Z. Xiaoping, L. Yuanfang, W. Wenjia, *Evaluation of Urban Resource and Environmental Efficiency in China Based on The DEA Model*, Journal of Resources and Ecology 5(1) (2014) 11–19.

[6] T. S. Adebayo, D. Kirikkaleli, I. Adeshola, D. Oluwajana, G. D. Akinsola, O. S. Osemeahon, *Coal Consumption and Environmental Sustainability in South Africa: The Role of Financial Development and Globalization*, International Journal of Renewable Energy Development 10(3) (2021) 527–536.

[7] S. Kihombo, A. I. Vaseer, Z. Ahmed, S. Chen, D. Kirikkaleli, T. S. Adebayo, *Is There a Trade-Off Between Financial Globalization, Economic Growth, and Environmental Sustainability? An Advanced panel Analysis*, Environmental Science and Pollution Research (2021) 1–11.

[8] S. A. R. Khan, P. Ponce, Z. Yu, H. Golpîra, M. Mathew, *Environmental Technology and Wastewater Treatment: Strategies to Achieve Environmental Sustainability*, Chemosphere 286 (2022) 131532.

[9] R. Akbani, S. Kwek, N. Japkowicz, *Applying Support Vector Machines to Imbalanced Datasets*, Machine Learning: ECML of the series Lecture Notes in Computer Science 3201 (2004) 39–50.

[10] H. He, *Learning from Imbalanced Data*, IEEE Transactions on Knowledge and Data Engineering 21(9) (2009) 1263–1284.

[11] A. Charnes, W. W. Cooper, E. Rhodes, *Measuring the Efficiency of Decision-Making Units*, European Journal of Operations Research 2(6) (1978) 429–444.

[12] R. D. Banker, A. Charnes, W. Cooper, *Some Models for Estimating Technical and Scale Inefficiencies in Data Envelopment Analysis*, Management Science 30(9) (1984) 1078–1092.

[13] T. Coelli, *A Guide to DEAP Version 2.1: A Data Envelopment Analysis (Computer) Program*, Centre for Efficiency and Productivity Analysis, University of New England, Australia 96(08) (1996) 1–49.

[14] R. Fare, S. Grosskopf, *Modeling Undesirable Factors in Efficiency Evaluation: Comment*, European Journal of Operational Research 157(1) (2004) 242–245.

[15] A. Charnes, W. Cooper, A. Y. Lewin, L. M. Seiford, *Data Envelopment Analysis Theory, Methodology and Applications*, Journal of the Operational Research Society 48(3) (1997) 332–333.

[16] W. W. Cooper, L. M. Seiford, K. Tone, *Data Envelopment Analysis: A Comprehensive Text with Models, Applications, References and DEA-Solver Software*, Journal of the Operational Research Society 52(12) (2001) 1408–1409.

[17] S. Kotsiantis, D. Kanellopoulos, P. Pintelas, *Handling Imbalanced Datasets: A Review*, GESTS International Transactions on Computer Science and Engineering 30(1) (2006) 25–36.

[18] R. S. Mitchell, J. G. Michalski, T. M. Carbonell, *An Artificial Intelligence Approach*, Berlin, Germany, Springer, 2013.

[19] R Core Team (2021). R: A language and environment for statistical computing. R Foundation for Statistical Computing, Vienna, Austria, https://www.R-project.org/

[20] P. Bogetoft, L. Otto, Benchmarking with Dea, Sfa, and r (Vol. 157). Springer Science & Business Media, 2010.

[21] T. Therneau, B. Atkinson, (2019). rpart: Recursive Partitioning and Regression Trees. R package version 4.1-15. https://CRAN.R-project.org/package=rpart

Journal of
New Theory
ISSN: 2149-1402

37 (2021) 68-75
Journal of New Theory
https://dergipark.org.tr/en/pub/jnt
Open Access

On Fuzzy Differential Inequalities with Upper and Lower Solutions

Ali Yakar[1], **Seda Çağlak**[2]

Article History
Received: 08 Dec 2021
Accepted: 23 Dec 2021
Published: 31 Dec 2021
10.53570/jnt.1034452
Research Article

Abstract — In this article, by using the technique of upper and lower solutions, some comparison results for first-order fuzzy differential equations are established. Hukuhara derivative, Hukuhara difference, and partial orderings are used for proving theorems. We extend our results to initial time difference case as well. Also, the practicality of these comparison results is demonstrated by giving an example.

Keywords — *Fuzzy number, upper and lower solutions, Hukuhara derivative*

Mathematics Subject Classification (2020) — 28E10, 26D10

1. Introduction

Fuzzy mathematics is an interesting part of mathematics. It could be said a new branch of mathematics since it emerged in the 1960s. It was proposed to explain real-life in mathematical language. We use relative concepts a lot in our daily lives. Situations that can vary from person to person such as good and bad, young and old, beautiful and ugly, had taken place in our lives. Classical mathematics is not sufficient to explain such notions. Everything is certain in classical mathematics, something is either black or white. Classical mathematics does not allow gray color. At this point where classical mathematics is insufficient, Lutfi Askerzade Zadeh's fuzzy mathematical theory comes into play. He showed in his theory that he revealed in 1965, fuzzy logic constitutes a good model of real-life [1]. Although his theory was not accepted in the scientific community at first, it is now used in different branches of science and engineering.

The fuzzy theory attracted great attention and spread very commonly among scientists from various fields of science. Fuzzy systems can also be used in predicting, decision making, air conditioning, mechanical control systems such as automobile control systems and intelligent structures, as well as industrial process control systems, and so on. See [2–4] and the references cited therein.

In fuzzy mathematics, arithmetical operations are valid like in classical mathematics. There are two methods. One is Zadeh Extension Principle and the other is interval arithmetic with level sets. These methods are explained in [5]. There are some differences between fuzzy mathematics and classical mathematics. For example, if u is a fuzzy number, $u - u$ may not be 0 in fuzzy mathematics. As a result of this issue, a new difference known as the Hukuhara difference is defined, as shown in [6]. By using Hukuhara difference, Hukuhara derivative is defined [7]. On the other hand, it is possible to compare two fuzzy numbers or two fuzzy functions. How to compare two fuzzy notions are mentioned in [8]. Besides, it is possible solving fuzzy differential equations. Many methods were developed to solve fuzzy differential equations. How to solve first-order fuzzy differential equations are explained

[1]ali.yakar@gop.edu.tr; [2]caglakseda@gmail.com (Corresponding Author)
[1,2]Department of Mathematics, Tokat Gaziosmanpaşa University, Tokat, Turkey

in [5]. Besides this, the definition of fuzzy upper and lower solutions are located in [9]. In this study, by using all the knowledge mentioned above, some comparison results are proved and one example is introduced to support the results.

2. Preliminaries

Hukuhara difference is a useful operation for the difference between fuzzy notions and also, interval arithmetic via level sets is an easy method for arithmetical operations in fuzzy cases. In the following, definitions of fuzzy numbers, level sets of a fuzzy number, Hukuhara difference, and Hukuhara derivative are given.

Definition 2.1. [5] A fuzzy set U (fuzzy subset of E) is defined as a mapping (E is universal set)

$$\mu_u : E \to [0,1]$$

where $\mu_u(x)$ is the membership degree of x the fuzzy set U.

Definition 2.2. [10] A fuzzy membership function $u : \mathbb{R} \to [0,1]$ is called a fuzzy number if it has the following conditions:

i. u is normal. It means there is at least a real member $x_0 \in \mathbb{R}$ such that $u(x_0) = 1$.

ii. u is fuzzy convex. It means for two arbitrary real points $x_1, x_2 \in \mathbb{R}$ and $t \in [0,1]$, we have

$$u(tx_1 + (1-t)x_2) \geq \min\{u(x_1), u(x_2)\}$$

iii. u is upper semi-continuous on $\mathbb{R}$. It means if we increase its value at a certain point x_0 to $f(x_0)+\varepsilon$ (for some positive constant ε), then the result is upper-semicontinuous; if we decrease its value to $f(x_0)-\varepsilon$ then the result is lower-semi-continuous.

iv. u is compactly supported. It means the closure of the set $\{x \in \mathbb{R}; u(x) > 0\}$, as a support set, is compact set.

Remark 2.3. The space of fuzzy numbers will be denoted by $\mathbb{R}_{\mathcal{F}}$.

Definition 2.4. Let $U : E \to [0,1]$ be a fuzzy set. The level sets of U are defined as the classical sets.

$$U_r = [u_r^-, u_r^+] = \{x \in E : \mu_U(x) \geq r\}, \qquad 0 < r < 1$$

Remark 2.5. There are numerous fuzzy numbers. However, in our investigation, we only mention triangular and trapezoidal numbers. As a result, we define these fuzzy numbers as follows:
A trapezoidal fuzzy number u can be shown with an ordered pair of functions $(a,b,c,d) \in \mathbb{R}^4$,

$$u(x) = \begin{cases} 0, & t < a \\ \frac{t-a}{b-a}, & a \leq t \leq b \\ 1, & b \leq t \leq c \\ \frac{d-t}{d-c}, & c < t \leq d \\ 0, & d < t \end{cases}$$

Employing r-cut approach, we find the level set with the endpoints calculated by

$$u_r^- = a + r(b-a), u_r^+ = d - r(d-c)$$

where $r \in [0,1]$. When $b = c$ is in the form (a,b,c,d), the fuzzy number is referred to as a triangular fuzzy number. The fuzzy number may thus be represented by a triplet $(a,b,c) \in \mathbb{R}^3$, $a \leq b \leq c$.

Definition 2.6. [6] The Hukuhara difference (H-difference $\ominus_H$) defined by

$$u \ominus_H v = w \Leftrightarrow u = v + w,$$

being + the standard fuzzy addition.

If $u \ominus_H v$ exists, its level-sets are

$$[u \ominus_H v]_r = [u_r^- - v_r^-, u_r^+ - v_r^+]$$

Definition 2.7. [11] A function $\psi : (a,b) \to \mathbb{R}_{\mathcal{F}}$ is called Hukuhara differentiable if for sufficiently small $h > 0$ the H-differences $\psi(u+h) \ominus \psi(u)$ and $\psi(u) \ominus \psi(u-h)$ exist and if there exists an element $\psi'(u) \in \mathbb{R}_{\mathcal{F}}$ such that

$$\lim_{h \to 0} \frac{\psi(u+h) \ominus \psi(u)}{h} = \lim_{h \to 0} \frac{\psi(u) \ominus \psi(u-h)}{h} = \psi'(u)$$

The fuzzy number $\psi(u)$ is called the Hukuhara derivative of ψ at u.

Lemma 2.8. Let u be Hukuhara differentiable and $u(t) = (x(t), y(t), z(t)))$ be triangular number valued function then we get $u' = (x', y', z')$.

Definition 2.9. [8] Let $u, v \in \mathbb{R}_{\mathcal{F}}$. It is said $u \leq v$ if only if $u_r^- \leq v_r^-$ and $u_r^+ \leq v_r^+$ for each $r \in [0,1]$.

Definition 2.10. [8] Let $u, v \in \mathbb{R}_{\mathcal{F}}$. It is said $u \preceq v$ if only if $u_r^- \geq v_r^-$ and $u_r^+ \leq v_r^+$ for each $r \in [0,1]$, that is $u_r \subseteq v_r, \forall r \in [0,1]$.

Lemma 2.11. [8] If $u, v, w \in \mathbb{R}_{\mathcal{F}}$ are such that Hukuhara differences $u \ominus_H w$ and $v \ominus_H w$ exist, then

$$u \leq v \Leftrightarrow u \ominus_H w \leq v \ominus_H w$$

Definition 2.12. [9] Let $\Psi \in C([t_0, T] \times \mathbb{R}_{\mathcal{F}}, \mathbb{R}_{\mathcal{F}})$, $T > t_0$ and $x' = \Psi(t, x)$, $x(t_0) = x_0$ be fuzzy initial value problem.

A function $q \in C^1([t_0, T], \mathbb{R}_{\mathcal{F}})$ is an upper solution for fuzzy initial value problem above, if

$$\begin{cases} q'(t) \geq \Psi(t, q(t)), & t \in [t_0, T] \\ q(t_0) \geq x_0 \end{cases}$$

A function $p \in C^1([t_0, T], \mathbb{R}_{\mathcal{F}})$ is a lower solution for fuzzy initial value problem above, if

$$\begin{cases} p'(t) \leq \Psi(t, p(t)), & t \in [t_0, T] \\ p(t_0) \leq x_0 \end{cases}$$

Remark 2.13. Analogous definitions can be given for $\preceq$ partial ordering.

3. Main Results

In this section, several comparison results are given by using upper and lower solutions and, it is also proved that the solution of fuzzy differential equation exists between corresponding lower and upper solutions.

Let us consider the following first order fuzzy differential equation

$$x' = \Psi(t, x), x(t_0) = x_0 \tag{1}$$

where $\Psi \in C([t_0, T] \times \mathbb{R}_{\mathcal{F}}, \mathbb{R}_{\mathcal{F}})$ and $T > t_0$.

Theorem 3.1. Let the functions $p, q \in C^1([t_0, T], \mathbb{R}_{\mathcal{F}})$ satisfy the following inequalities

$$q' > \Psi(t, q(t)), \quad p' \leq \Psi(t, p(t)) \tag{2}$$

If $p(t_0) < q(t_0)$, then $p(t) < q(t)$ for all $t \in [t_0, T]$.

Proof. Since we are going to prove $p(t) < q(t)$ by Definition 2.9, we must show that $p_r^-(t) < q_r^-(t)$ and $p_r^+ < q_r^+$ on $t \in [t_0, T]$. If it was wrong, there would exists a $t_1 \in (t_0, T]$ such that

$$p_r^-(t_1) = q_r^-(t_1), p_r^+(t_1) = q_r^+(t_1)$$

and

$$p_r^-(t) < q_r^-(t), p_r^+(t) < q_r^+(t)$$

for $t \in [t_0, t_1)$. Therefore, for sufficiently small $h > 0$, we obtain

$$\begin{cases} p_r^-(t_1 - h) < q_r^-(t_1 - h) \\ p_r^+(t_1 - h) < q_r^+(t_1 - h) \end{cases}$$

i.e. $p(t_1 - h) < q(t_1 - h)$. By using Lemma 2.11 , we have

$$p(t_1 - h) \ominus p(t_1) < q(t_1 - h) \ominus q(t_1)$$

By dividing inequality with $-h$ and limiting for $h \to 0$, we arrive at

$$\lim_{h \to 0} \frac{p(t_1 - h) \ominus p(t_1)}{-h} \geq \lim_{h \to 0} \frac{q(t_1 - h) \ominus q(t_1)}{-h}$$

which implies that

$$p'(t_1) \geq q'(t_1)$$

As a result, we get a contradiction

$$\Psi(t_1, p(t_1)) \geq p'(t_1) \geq q'(t_1) > \Psi(t_1, q(t_1)) = \Psi(t_1, p(t_1))$$

So we conclude that $p(t) < q(t)$ on $[t_0, T]$. □

Similarly it can be shown that the result of the theorem holds even when we change $\leq$ by $<$ and $\geq$ by $>$ in the assumptions of theorem 3.1.

We are in position to show that the existence of the solution of the problem (1) located between corresponding lower and upper solutions.

Theorem 3.2. Let the functions $p, q \in C^1([t_0, T], \mathbb{R}_{\mathcal{F}})$ satisfy the strict inequalities $p' < \Psi(t, p)$ and $q' > \Psi(t, q)$ on $[t_0, T]$. Furthermore, y is the solution of the problem (1). Then, $p(t_0) \leq y(t_0) \leq q(t_0)$ implies that $p(t) < y(t) < q(t)$ for $[t_0, T]$.

Proof. We shall only give a proof for $y(t) < q(t)$ on $[t_0, T]$. If $y(t_0) < q(t_0)$, then the result follows from Theorem 3.1. We now suppose that $y(t_0) = q(t_0)$ and, we define the function z such as $z(t) = q(t) \ominus y(t)$ on $[t_0, T]$. Then, the level sets of this function can be written as $Z_r = [z_r^-, z_r^+]$, that is,

$$\begin{cases} z_r^- = q_r^- - y_r^- \\ z_r^+ = q_r^+ - y_r^+ \end{cases}$$

If we differentiate the both sides of the real function z_r^-, we find that

$$(z_r^-)'(t_0) = (q_r^-)'(t_0) - (y_r^-)'(t_0) > \Psi(t_0, (q_r^-)'(t_0)) - \Psi(t_0, (y_r^-)'(t_0)) = 0$$

It is easy to observe that $z_r^-(t)$ is increasing on the interval $[t_0, t_0 + h]$ for sufficiently small $h > 0$. For this reason, we obtain

$$y_r^-(t_0 + h) < q_r^-(t_0 + h)$$

If we utilize Theorem 3.1, we can easily see that $y_r^-(t) < q_r^-(t)$, for all $t \in [t_0 + h, T]$. Analogously,

$$\begin{aligned}(z_r^+)'(t_0) &= (q_r^+)'(t_0) - (y_r^+)'(t_0) \\ &> \Psi(t_0, (q_r^+)'(t_0)) - \Psi(t_0, (y_r^+)'(t_0)) \\ &= 0\end{aligned}$$

We can easily see that z_r^+ is increasing to the right of t_0 in a sufficiently small interval $[t_0, t_0 + h]$. Hence,

$$y_r^+(t_0 + h) < q_r^+(t_0 + h), y_r^-(t) < q_r^-(t)$$

for all $t \in [t_0 + h, T]$. Since we have chosen sufficiently small h, we obtain $y(t) < q(t)$ on $[t_0, T]$ due to

$$\begin{cases} y_r^-(t) < q_r^-(t) \\ y_r^+(t) < q_r^+(t) \end{cases}$$

In a similar way, we can prove $p(t) < y(t)$ on $[t_0, T]$. Thus, we have

$$p(t) < y(t) < q(t) \text{ on } [t_0, T]$$

□

Theorem 3.3. Let $\Psi \in C([t_0, T] \times \mathbb{R}_\mathcal{F}, \mathbb{R}_\mathcal{F})$ and the functions $p, q \in C^1([t_0, T], \mathbb{R}_\mathcal{F})$ be lower and upper solutions of (1) respectively. Suppose that Hukuhara differences $\Psi(t, x) \ominus \Psi(t, y)$ and $x \ominus y$ exist and for $x \geq y$, there exist a positive constant L such that

$$\Psi(t, x) \ominus \Psi(t, y) \leq L(x \ominus y) \tag{3}$$

Then, $p(t) \leq q(t)$ on $[t_0, T]$ provided that $p(t_0) \leq q(t_0)$.

Proof. Firstly, we define the function $\tilde{q}(t) = q(t) + \varepsilon \cdot e^{2Lt}$ for some $\varepsilon > 0$. Let the level sets be $\tilde{q}_r = [\tilde{q}_r^-(t), \tilde{q}_r^+(t)]$, i.e.

$$\begin{cases} \tilde{q}_r^-(t) = q_r^-(t) + \varepsilon \cdot e^{2Lt} \\ \tilde{q}_r^+(t) = q_r^+(t) + \varepsilon \cdot e^{2Lt} \end{cases}$$

Observe that $p_r^-(t_0) \leq q_r^-(t_0) < \tilde{q}_r^-(t_0)$. Now, taking derivatives of both sides of $q_r^-(t)$, we get

$$\begin{aligned}\frac{d}{dt}(\tilde{q}_r^-(t)) &= \frac{d}{dt}(q_r^-(t)) + 2L\varepsilon \cdot e^{2Lt} \\ &\geq \Psi(t, q_r^-(t)) + 2L\varepsilon e^{2Lt} \\ &\geq \Psi(t, q_r^-(t)) - \Psi(t, \tilde{q}_r^-(t)) + 2L\varepsilon e^{2Lt} + \Psi(t, \tilde{q}_r^-(t))\end{aligned}$$

By using one sided Lipschitz type inequality (3.3), it follows

$$\frac{d}{dt}(\tilde{q}_r^-(t)) \geq -L(\tilde{q}_r^-(t) - q_r^-(t)) + \Psi(t, \tilde{q}_r^-(t)) + L\varepsilon e^{2Lt} > \Psi(t, \tilde{q}_r^-(t))$$

An application of Theorem 3.1 gives that $p_r^-(t) < \tilde{q}_r^-(t)$. Letting $\varepsilon \to 0$, we obtain $p_r^-(t) \leq q_r^-(t)$ on $[t_0, T]$. Analogously,

$$\begin{aligned}\frac{d}{dt}(\tilde{q}_r^+(t)) &= \frac{d}{dt}(q_r^+(t)) + 2L\varepsilon e^{2Lt} \\ &\geq \Psi(t, q_r^+(t)) + 2L\varepsilon e^{2Lt} \\ &\geq \Psi(t, q_r^+(t)) - \Psi(t, \tilde{q}_r^+(t)) + 2L\varepsilon e^{2Lt} + \Psi(t, \tilde{q}_r^+(t)) \\ &\geq -L(\tilde{q}_r^+(t) - q_r^+(t)) + \Psi(t, \tilde{q}_r^+(t)) + L\varepsilon e^{2Lt} \\ &> \Psi(t, \tilde{q}_r^+(t))\end{aligned}$$

Also by Theorem 3.1 and the fact that $p_r^+(t_0) \leq q_r^+(t_0) < \tilde{q}_r^+(t_0)$, we conclude that $p_r^+(t) < \tilde{q}_r^+(t)$, meaning that $p_r^+(t) \leq q_r^+(t)$ when ε goes to zero. According to Definition 2.9, we deduce that $p(t) \leq q(t)$ on $[t_0, T]$ which completes the proof. □

Remark 3.4. The same conclusions are valid for $\preceq$ partial ordering

Example 3.5. Consider fuzzy initial value problem $x' = x, x(0) = (2, 3, 4)$ where $\Psi(t, x) = x$. We consider the functions $p(t) = (-t^2 + 1)(0, 1, 2)$ and $w(t) = e^t(5, 6, 7)$ for $t \in [0, 1]$. Let us try to examine that whether the inequality $p'(t) \leq \Psi(t, p)$ holds for $t \in [0, 1]$. Here, $p'(t) = -2t(0, 1, 2)$ and $\Psi(t, p) = (-t^2+1)(0, 1, 2)$. Since $p'(t) = (0, -2t, -4t)$ then by Lemmma 2.8 and Remark 2.5 ,the level sets can be written as

$$[p'(t)]_r = [(p'(t))^-_r, (p'(t))^+_r] = [-2tr, -2t(2 + r)]$$

and we also have $\Psi(t, p) = (0, -t^2 + 1, -2t^2 + 2)$. On the other hand, we acquire

$$[\Psi(t, p)]_r = [(\Psi(t, p))^-_r], (\Psi(t, p))^+_r] = [(-t^2 + 1)r, (-t^2 + 1)(2 - r)]$$

It is easily observe that

$$(p'(t))^-_r \leq (\Psi(t, p))^-_r \quad \text{and} \quad (p'(t))^+_r \leq (\Psi(t, p))^+_r$$

for $r \in [0, 1]$, i.e., $p' \leq \Psi(t, p)$ on $[0, 1]$. Now, looking for that whether $p(0) \leq x(0)$ is true. Since $p(0) = (0, 1, 2)$, its level set $[p(0)]_r] = [r, 2 - r]$ and since $x(0) = (2, 3, 4)$, its level sets $[x(0)]_r = [2 + r, 4 - r]$. Therefore, we can see that

$$((p(0))^-_r \leq ((x(0))^-_r \quad \text{and} \quad ((p(0))^+_r \leq ((x(0))^+_r$$

So, $p(0) \leq x(0)$. Finally, p is the lower solution of fuzzy differential equation. Like mentioned above, if we take $q(t) = e^t(5, 6, 7)$ and $\Psi(t, q) = e^t(5, 6, 7)$, then we can similarly show that

$$q'(t) \geq \Psi(t, q), q(0) \geq x(0)$$

Consequently, q is the upper solution of the given fuzzy differential equation. It is obvious that the fuzzy differential equation satisfies the one sided Lipschitz condition given in (3.3) for $L > 1$. Moreover, by comparing the following level sets that we have just found

$$[p(0)]_r = [r, 2 - r] \quad \text{and} \quad [q(0)]_r = [5 + r, 7 - r]$$

We see that

$$[p(0)]^-_r \leq [q(0)]^-_r \quad \text{and} \quad [p(0)]^+_r \leq [q(0)]^+_r$$

for $r \in [0, 1]$, so the inequality $p(0) \leq q(0)$ holds. As a consequence, we obtain $p(t) \leq q(t)$ on $[0, 1]$ by Theorem 3.3. Actually, we can check directly whether the result holds. To do so, let us construct the level sets of $p(t)$ and $q(t)$:

$$[p(t)]_r = [(-t^2 + 1)r, (-t^2 + 1)(2 - r)] \quad \text{and} \quad [q(t)]_r = [e^t(5 + r), e^t(7 - r)]$$

and it can be easily seen that

$$[p(t)]^-_r \leq [q(t)]^-_r \quad \text{and} \quad [p(t)]^+_r \leq [q(t)]^+_r$$

for all $r \in [0, 1]$. Thus, $p(t) \leq q(t)$ on $[0, 1]$ is obtained. Furthermore, one can get the exact solution of the problem as follows:

$$y = e^t(2, 3, 4)$$

Observe that, $p(t) \leq y(t) \leq q(t)$, $t \in [0, 1]$, it's represented in Figure 1.

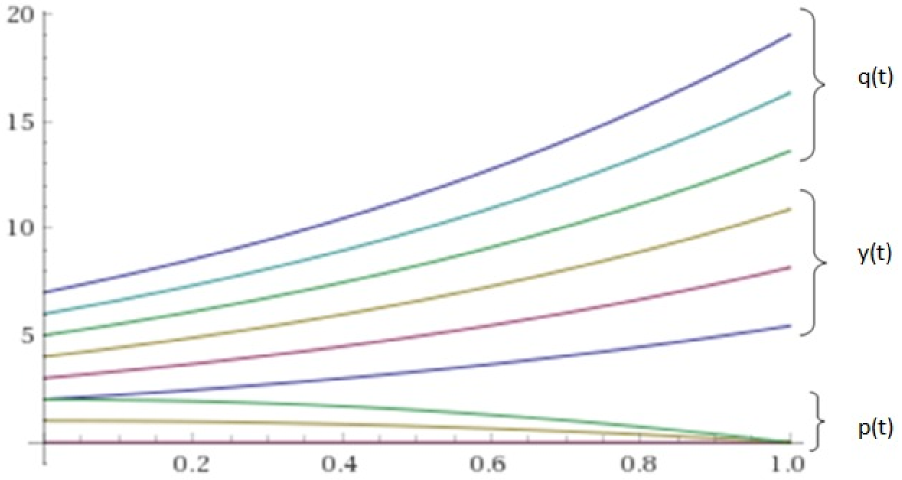

Fig. 1

In some cases, lower and upper solutions may differ at initial points. In such instances, we need to make some changes to the previous theorem and add extra conditions to achieve the similar results.

Theorem 3.6. Assume that

(H1) $\Psi \in C([t_0, \tau_0 + T] \times \mathbb{R}_{\mathcal{F}}, \mathbb{R}_{\mathcal{F}}), \tau_0 \geq t_0, T > 0$ and the functions $p \in C^1([t_0, t_0 + T], \mathbb{R}_{\mathcal{F}})$, $q \in C^1([\tau_0, \tau_0 + T], \mathbb{R}_{\mathcal{F}})$ such that

$$p' \leq \Psi(t, p), p(t_0) \leq x_0,$$
$$q' \geq \Psi(t, q), q(\tau_0) \geq x_0,$$

(H2) $\Psi(t, x) \ominus \Psi(t, y) \leq L(x \ominus y), x \geq y, L > 0$

(H3) $\Psi(t, x)$ is non decreasing in t for each x.

Then we have

(i) $p(t) \leq q(t + \gamma)$ on $[t_0, t_0 + T]$ or

(ii) $p(t - \gamma) \leq q(t)$ on $[\tau_0, \tau_0 + T]$
where $\gamma = \tau_0 - t_0$.

Proof.

(i) Define the function $q_0(t) = q(t + \gamma)$ thus we get

$$q_0(t_0) = q(t_0 + \gamma) = q(\tau_0) \geq x_0 \geq p(t_0)$$

and

$$q'(t) = q'(t + \gamma) \geq \Psi(t + \gamma, q(t + \gamma)) = \Psi((t + \gamma), q_0(t)) > \Psi(t, q_0(t))$$

So, q is an upper solution. By using Theorem 3.3 the proof is completed.

(ii) Define the function $p_0(t) = p(t - \gamma), t \geq \tau_0$. It can be written as before

$$p_0(\tau_0) = p_0(\tau_0 - \gamma) = p_0(t_0) \leq x_0 \leq q(\tau_0)$$

and

$$p_0'(t) = p'(t - \gamma) \leq \Psi(t - \gamma, p(t - \gamma)) = \Psi(t - \gamma, p_0(t))$$

which leads to the fact p is a lower solution. As a result, by using the previous Theorem, (ii) is proved.

□

4. Conclusion

In this paper, it is aimed to prove some comparison theorems by utilizing upper and lower solutions for fuzzy differential equations of first order. Our results have been refined to initial time difference case where upper and lower solutions start different points in time. In addition, an example has been given for illustration.

Author Contributions

All the authors contributed equally to this work. They all read and approved the final version of the manuscript.

Conflicts of Interest

The authors declare no conflict of interest.

References

[1] L. A. Zadeh, Fuzzy sets, World Scientific, 1996.

[2] C.-W. Chen, *Stability Conditions of Fuzzy Systems and Its Application to Structural and Mechanical Systems*, Advances in Engineering Software 37 (9) (2006) 624–629.

[3] Q. Shen, B. Jiang, V. Cocquempot, *Fault-Tolerant Control for T–S Fuzzy Systems with Application to Near-Space Hypersonic Vehicle with Actuator Faults*, IEEE Transactions on Fuzzy Systems 20 (4) (2011) 652–665.

[4] T. Terano, K. Asai, M. Sugeno, Fuzzy Systems Theory and Its Applications, Academic Press Professional, Inc., 1992.

[5] B. Bede, Fuzzy Sets, Springer, 2013.

[6] M. Hukuhara, *Integration des Applications Mesurables dont la Valeur est un Compact Convexe*, Funkcialaj Ekvacioj 10 (3) (1967) 205–223.

[7] P. Diamond, P. Kloeden, Metrics of Fuzzy Sets: Theory and Applications, World Scientific, 1994.

[8] R. Rodríguez-López, *Comparison Results for Fuzzy Differential Equations*, Information Sciences 178 (6) (2008) 1756–1779.

[9] R. Rodríguez-López, *Monotone Method for Fuzzy Differential Equations*, Fuzzy Sets and Systems 159 (16) (2008) 2047–2076.

[10] T. Allahviranloo, Fuzzy Fractional Differential Operators and Equations, Vol. 397, Springer, 2020.

[11] M. L. Puri, D. A. Ralescu, Differentials of Fuzzy Functions, De Gruyter Mouton, 2011.

Journal of New Theory
ISSN: 2149-1402

37 (2021) 76-85
Journal of New Theory
https://dergipark.org.tr/en/pub/jnt
Open Access

Bianchi VI_0 Universe with Magnetized Strange Quark Matter in $f(R,T)$ Theory

Sinem Kalkan[1], **Can Aktaş**[2]

Article History
Received: 11 Dec 2021
Accepted: 26 Dec 2021
Published: 31 Dec 2021
10.53570/jnt.1035548
Research Article

Abstract — This study discusses $f(R,T)$ theory, one of the alternative theories. It then studies magnetized strange quark matter in the universe model Bianchi VI_0, homogeneous and anisotropic. Afterwards, it has determined whether the energy conditions are provided by using the deceleration parameter while obtaining the solutions. Moreover, the evolution of the cosmic universe is examined with the help of graphics and tables.

Keywords — *$f(R,T)$ theory, Bianchi VI_0, deceleration parameter*

Mathematics Subject Classification (2020) — 83C05, 83C15

1. Introduction

Recent observations have shown that the universe is accelerating and expanding [1–3]. The reasons for this acceleration and expansion still remain a mystery. Einstein's General Relativity theory has tried to explain the universe in general. However, it has fallen short of explaining acceleration and expansion. Therefore, alternative theories to this theory have been put forward by many scientists. Among these alternative theories, there are theories such as $f(R)$ theory [4], $f(G)$ theory [5], and Lyra theory [6]. In this study, we have discussed the $f(R,T)$ theory put forward by Harko et al. in 2011 [4]. $f(R,T)$ theory has also been studied by many scientists [7–16]. Although it is known that the magnetic field played an important role in the formation of structures in the early universe, its cause has still not fully understood. The magnetic field is thought to affect the formation of galaxies [17]. Strange quark matter (SQM) with a magnetic field provides information about the accelerating expansion of the universe according to Supernova-type Ia observations [18]. One of the reasons we have studied quark matter with magnetic field is because quark-gluon matter must be stable and it must ensure charge neutrality [19]. Moreover, Singh and Beesham have studied SQM with the cosmological term in $f(R,T)$ theory [20]. Besides, Katore et al. have studied in Bianchi VI_0 universe model [21]. In addition, Aktaş has investigated magnetized strange quark matter (MSQM) in $f(R,T)$ theory [22]. Further, Nagpal et al. have studied MSQM and SQM distribution in $f(R,T)$ theory [17]. Furthermore, Pradhan and Bali have studied magnetized Bianchi VI_0 universe model [23]. Additionally, Aktaş et al. have studied MSQM distribution for the Marder universe model in $f(R,T)$ theory [24]. Moreover, Sahoo et al. have investigated MSQM in $f(R,T)$ theory [18]. Besides, some scientists have investigated MSQM and SQM [25–30].

[1]sinemkalkan@stu.comu.edu.tr (Corresponding Author); [2]canaktas@comu.edu.tr
[1]Institute of Graduate Education, Çanakkale Onsekiz Mart University, Çanakkale, Turkey
[2]Department of Mathematics, Faculty of Arts and Sciences, Çanakkale Onsekiz Mart University, Çanakkale, Turkey

The Section 2 of this study presents basic equations in the $f(R,T)$ theory with cosmological term by considering MSQM. The Section 3 obtains modified field equations by using an equation of state and a decelaration parameter. Finally, the graphs of the obtained solutions are interpreted and the energy states of the MSQM in this universe are examined. This study is a part of the first author's master's thesis.

2. Field Equations in $f(R,T)$ Modified Gravition Theory

In 2011, Harko et al. suggested a new theory as a function $f(R,T)$ connected to R and T instead of Ricci scalar R in the Einstein-Hilbert type action function [4]. The action in the modified gravitational theories is as follows.

$$S = \frac{1}{16\pi}\int (f(R,T)+2\Lambda)\sqrt{-g}d^4x + \int L_m\sqrt{-g}d^4x \tag{1}$$

where T is the trace of $T_{ik} = -2\frac{\delta(\sqrt{-g}L_m)}{\sqrt{-g}\delta g^{ik}}$, R is Ricci scaler, g is the determinant of the metric tensor g_{ik}, and L_m is matter Lagrangian. Here, assume that the Lagrangian L_m depends only on the metric tensor component g_{ik} rather than derivatives [4]. By changing the action S in the Equation (1) regarding g_{ik}, the $f(R,T)$ gravitational field equations are obtained as follows [4,31]:

$$f_R(R,T)R_{ik} - \frac{1}{2}f(R,T)g_{ik} + (g_{ik}\Box - \nabla_i\nabla_k)f_R(R,T) = 8\pi T_{ik} - f_T(R,T)T_{ik} - f_T(R,T)\Theta_{ik} + \Lambda g_{ik} \tag{2}$$

here Θ_{ik} is defined by [4]

$$\Theta_{ik} = -2T_{ik} + g_{ik}L_m - 2\frac{\partial^2 L_m}{\partial g^{ik}\partial^{lm}}g^{lm}$$

where $f_T(R,T)$ and $f_R(R,T)$ indicate partial derivatives of $f(R,T)$ in regard to T and R, respectively, ∇_i is the covariant derivative, and $\Box = \nabla_i\nabla^i$ [4].

Contracting the Equation (2), we get

$$3\Box f_R(R,T) + f_R(R,T)R - 2f(R,T) = \big(8\pi - f_T(R,T)\big)T - f_T(R,T)\Theta + 4\Lambda \tag{3}$$

where $\Theta = g^{ik}\Theta_{ik}$. From Equations (2) and (3), we have

$$\begin{aligned} f_R(R,T)(R_{ik} - \frac{1}{3}Rg_{ik}) + \frac{1}{6}f(R,T)g_{ik} &= 8\pi\big(T_{ik} - \frac{1}{3}Tg_{ik}\big) - f_T(R,T)(T_{ik} - \frac{1}{3}Tg_{ik}) \\ &\quad -f_T(R,T)\big(\Theta_{ik} - \frac{1}{3}\Theta g_{ik}\big) + \nabla_i\nabla_k f_R(R,T) + \Lambda g_{ik} \end{aligned}$$

In this study, we consider $f(R,T) = R+2f(T)$. The gravitational field equation is as follows [4,31]:

$$R_{ik} - \frac{1}{2}Rg_{ik} = 8\pi T_{ik} - 2f'(T)T_{ik} - 2f'(T)\Theta_{ik} + (f(T)+\Lambda)g_{ik}$$

In addition, in this study, $f(T) = \mu T$ such that μ is an arbitrary constant [4]. Moreover, in this theory, the field equation (3) with cosmological term Λ is given by

$$G_{ik} = (2\mu + 8\pi)T_{ik} + \big(\mu(\rho - p) + \Lambda\big)g_{ik} \tag{4}$$

such that ρ and p are the energy density and pressure, respectively.

The energy momentum tensor in MSQM is considered as

$$T_{ik} = h^2(u_iu_k - \frac{1}{2}g_{ik}) + u_iu_k(\rho+p) - pg_{ik} - h_ih_k \tag{5}$$

where h^2 is magnetic field [32,33]. Further, $u^i = \delta_i^4$ that satisfies the condition $u_iu^i = 1$.

3. Modified Einstein Field Equations and Solutions in Bianchi VI_0 Universe

The Bianchi universe VI_0, a homogeneous-anisotropic metric, is

$$ds^2 = dt^2 - A^2dx^2 - B^2e^{-2m^2x}dy^2 - C^2e^{2m^2x}dz^2 \tag{6}$$

where A, B, and C are functions of t and m is constant. Besides, the coordinates: (x, y, z, t). From Equations (4)-(6), the collection of modified field equations for the Bianchi universe VI_0 are acquired as follows:

$$\frac{m^4}{A^2} + \frac{\ddot{C}}{C} + \frac{\ddot{B}}{B} + \frac{\dot{C}\dot{B}}{CB} = 4h^2\pi + h^2\mu - 3p\mu + \mu\rho - 8p\pi + \Lambda \tag{7}$$

$$-\frac{m^4}{A^2} + \frac{\ddot{C}}{C} + \frac{\ddot{A}}{A} + \frac{\dot{C}\dot{A}}{CA} = -4h^2\pi - h^2\mu - 3p\mu + \mu\rho - 8p\pi + \Lambda \tag{8}$$

$$-\frac{m^4}{A^2} + \frac{\ddot{B}}{B} + \frac{\ddot{A}}{A} + \frac{\dot{B}\dot{A}}{BA} = -4h^2\pi - h^2\mu - 3p\mu + \mu\rho - 8p\pi + \Lambda \tag{9}$$

$$-\frac{m^4}{A^2} + \frac{\dot{C}\dot{B}}{CB} + \frac{\dot{C}\dot{A}}{CA} + \frac{\dot{A}\dot{B}}{AB} = 8\pi\rho + 3\mu\rho + 4h^2\pi + h^2\mu - p\mu + \Lambda \tag{10}$$

$$-\frac{m^2\dot{C}}{C} + \frac{m^2\dot{B}}{B} = 0 \tag{11}$$

here "$\cdot$" indicates the derivative with respect to t.

In this study, there are five $f(R,T)$ field equations and seven unknowns. The unknowns are p, Λ, h, A, B, C, and ρ. To solve this system of the equations, auxiliary equations must be considered. First, the following MSQM's equation of state is used to completely solve the system.

$$p = \frac{\rho - 4B_c}{3} \tag{12}$$

where B_c is a bag constant [19,34]. Furthermore, deceleration parameter can be taken as follows [35]:

$$q = -1 + \frac{d}{dt}\left(\frac{1}{H}\right) = -1 + \frac{1}{2\beta\sqrt{t+\alpha}} \tag{13}$$

where α and β are constants and H is Hubble parameter. Using Equation (11),

$$B = c_1 C \tag{14}$$

such that c_1 is a constant. Later on, if we use Equation (13), then we obtain the equation

$$C = \frac{c_2 e^{2\beta\sqrt{t+\alpha}}}{\sqrt{c_3}} \tag{15}$$

where c_2 and c_3 are constants. From Equations (7)-(15), the metric potential A, magnetic field h^2, energy density ρ, pressure p, and cosmological term Λ are obtained as follows:

$$A = c_3 e^{2\beta\sqrt{t+\alpha}}$$

$$h^2 = \frac{m^4}{(4\pi + \mu)c_3^2(e^{2\beta\sqrt{\alpha+t}})^2}$$

$$\rho = \frac{3}{8(4\pi + \mu)}\left(\frac{\beta}{(\alpha + t)^{\frac{3}{2}}} - \frac{2m^4}{c_3^2 e^{4\beta\sqrt{\alpha+t}}}\right) + B_c$$

$$p = \frac{1}{8(4\pi+\mu)}\left(\frac{\beta}{(\alpha+t)^{\frac{3}{2}}} - \frac{2m^4}{c_3^2 e^{4\beta\sqrt{\alpha+t}}}\right) - B_c$$

and

$$\Lambda = -\frac{2\pi m^4}{c_3^2(4\pi+\mu)e^{4\beta\sqrt{\alpha+t}}} - \frac{\beta(3\pi+\mu)}{(4\pi+\mu)(\alpha+t)^{\frac{3}{2}}} + \frac{3\beta^2}{\alpha+t} - 4(2\pi+\mu)B_c$$

Phase transition have realized while $q(t_{tr}) = 0$. Here,

$$t_{tr} = \frac{1}{4\beta^2}\left(1 - 4\beta^2\alpha\right)$$

As the phase transition in our universe happens after the Big Bang, $t_{tr} > 0 \Rightarrow \beta\sqrt{\alpha} < 0.5$ [35]. Moreover, because $q > 0$ for, $t = 0$, the cosmic universe passes from deceleration to acceleration [35]. Given the fact that $\beta\sqrt{\alpha} < 0.5$, different values q_0 are given in Table 1 for different constants.

Table 1. Values of the deceleration parameter q_0 corresponding to β values for $\alpha = 0.05$

β	$\beta\sqrt{\alpha}$	$q_0 = q(t_0)$
0.15	$0.03354101966 < 0.5$	-0.62
0.25	$0.05590169942 < 0.5$	-0.46
0.35	$0.0782623792 < 0.5$	-0.104

t_0 is the age of the universe and is taken as 13.8 billion years.

4. Conclusion

This section provides the graphs A, B, C, h^2, p, Λ, ρ, and q corresponding to different q_0 values. Table 2 shows that the examined universe model satisfies the energy conditions (EC), that is, the energy conditions preserve the properties of the substance.

Table 2. Analyze of energy conditions

q_0	Null EC $\{p+\rho \geq 0\}$	Weak EC $\{p+\rho \geq 0 \ \& \ 0 \leq \rho\}$	Dominant EC $\{-p+\rho \geq 0 \ \& \ -\lvert p\rvert+\rho \geq 0\}$	Strong EC $\{p+\rho \geq 0 \ \& \ 3p+\rho \geq 0\}$
-0.62	$\oplus$	$\oplus$	$\oplus$	$\oplus$
-0.46	$\oplus$	$\oplus$	$\oplus$	$\oplus$
-0.104	$\oplus$	$\oplus$	$\oplus$	$\oplus$

$\bigoplus$: Energy condition is provided.

Figure 1 provides that as accepted in today's models, the transition of the considered universe model is from deceleration to acceleration. Further, the evolution of the metric potential A, B, and C are presented in Figures 2-4, respectively.

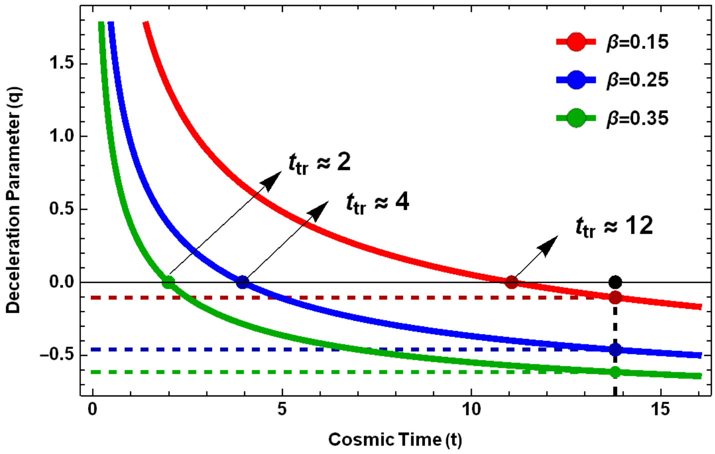

Fig. 1. The evolution of the deceleration parameter with respect to cosmic time for $\alpha = 0.05$

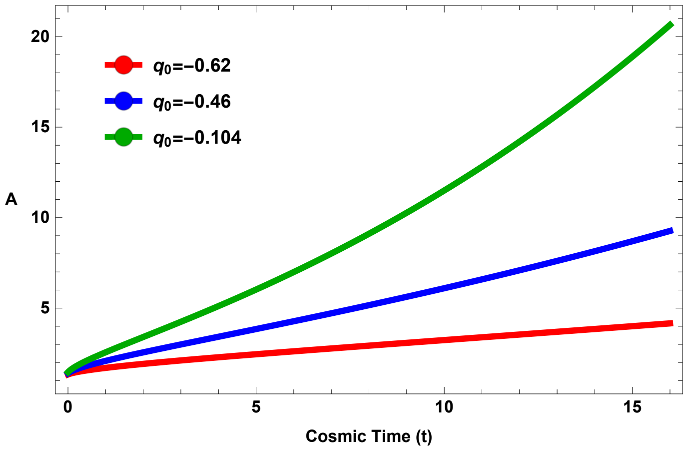

Fig. 2. The evolution of the metric potential A with respect to cosmic time for $m = 0.4$, $c_3 = 1.25$, and $\alpha = 0.05$

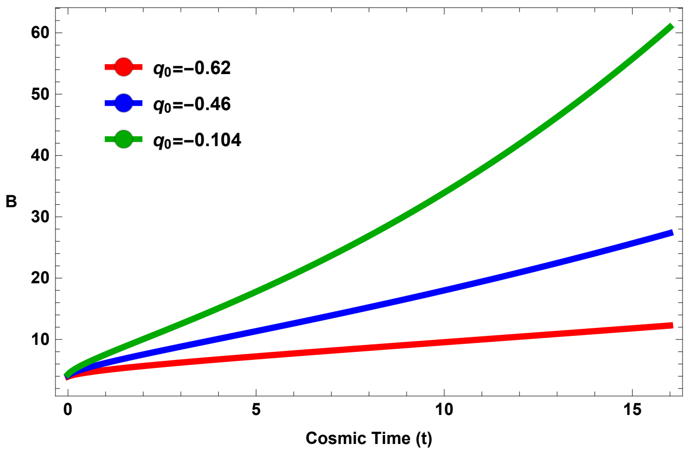

Fig. 3. The evolution of the metric potential B with respect to cosmic time for $c_1 = 1.5$, $c_2 = 2.75$, $c_3 = 1.25$, and $\alpha = 0.05$

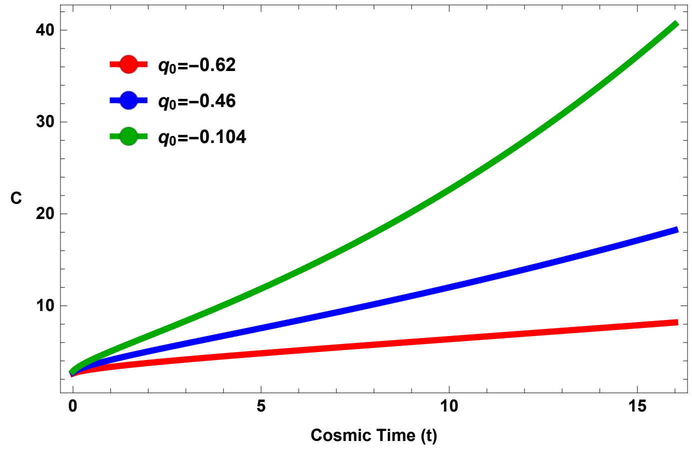

Fig. 4. The evolution of the metric potential C with respect to cosmic time for $c_2 = 2.75$, $c_3 = 1.25$, and $\alpha = 0.05$

Figures 2-4 show that the metric potentials increases over time. Moreover, for $q_0 = -0.62$, smaller than the other q_0 values, the increase is less. Similarly, for $q_0 = -0.104$, larger than the other q_0 values, the increase is more.

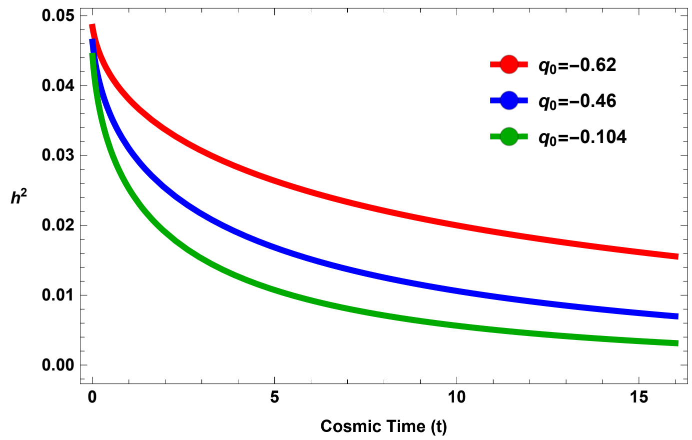

Fig. 5. The evolution of the magnetic field with respect to cosmic time for $m = 0.4$, $c_3 = 1.25$, $\alpha = 0.05$, and $\mu = -6.2734$

In Figure 5, the variation of the magnetic field relative to cosmic time decreases over time. Further, because $h^2 = 0$, for $m = 0$, the universe model turns into a non-magnetic universe model.

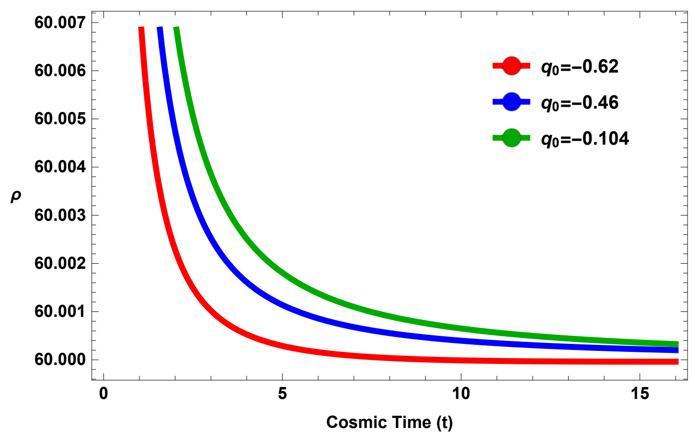

Fig. 6. The evolution of the energy density with respect to cosmic time for $m = 0.4$, $c_3 = 1.25$, $\alpha = 0.05$, $\mu = -6.2734$, and $B_c = 60$

Figure 6 shows $\rho > 0$. As $\rho > 0$, the universe model does not collapse on itself. In addition, it also approaches the bag constant over time.

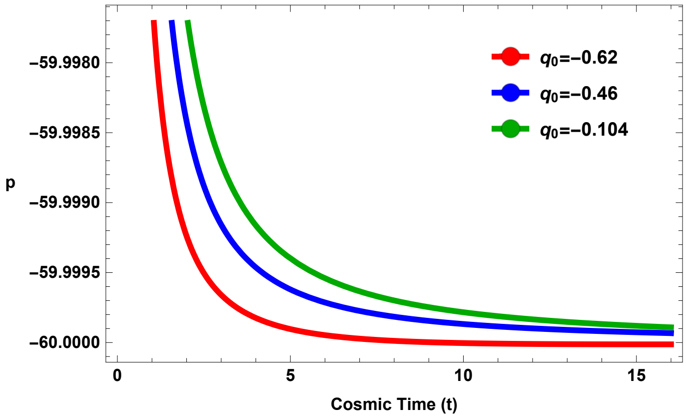

Fig. 7. The evolution of the pressure with respect to cosmic time for $m = 0.4$, $c_3 = 1.25$, $\alpha = 0.05$, $\mu = -6.2734$, and $B_c = 60$

Figure 7 shows that in the universe model, pressure decreases and approaches $-B_c$ over time.

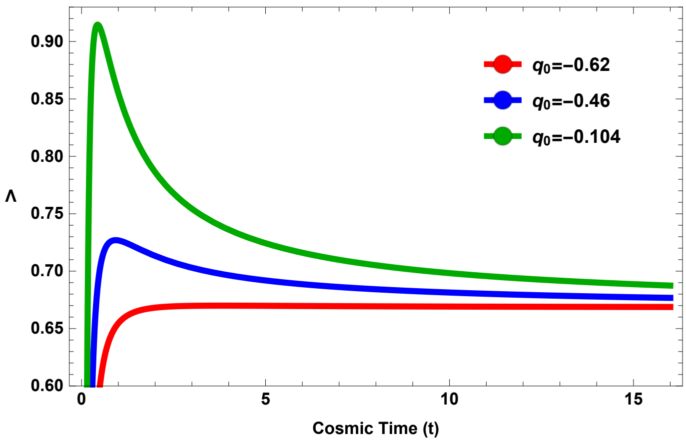

Fig. 8. The evolution of the cosmological term with respect to cosmic time for $m = 0.4$, $c_3 = 1.25$, $\alpha = 0.05$, $\mu = -6.2734$, and $B_c = 60$

Figure 8 shows that the cosmological term is positive. Therefore, it contributes to the accelerating expansion of the universe.

Author Contributions

All the authors contributed equally to this work. They all read and approved the last version of the manuscript.

Conflicts of Interest

The authors declare no conflict of interest.

Acknowledgments

This work was supported by the Office of Scientific Research Projects Coordination at Çanakkale Onsekiz Mart University, Grant Number: FYL-2020-3264.

References

[1] A. G. Riess, A. V. Filippenko, P. Challis, A. Clocchiatti, A. Diercks, P. M. Garnavich, R. L. Gilliland, C. J. Hogan, S. Jha, R. P. Kirshner, B. Leibundgut, M. M. Phillips, D. Reiss, B. P. Schmidt, R. A. Schommer, R. C. Smith, J. Spyromilio, C. Stubbs, N. B. Suntzeff, J. Tonry, *Observational Evidence from Supernovae for an Accelerating Universe and a Cosmological Constant*, The Astronomical Journal 116 (3) (1998) 1009–1038.

[2] S. Perlmutter, G. Aldering, G. Goldhaber, R. A. Knop, P. Nugent, P. G. Castro, S. Deustua, S. Fabbro, A. Goobar, D. E. Groom, I. M. Hook, A. G. Kim, M. Y. Kim, J. C. Lee, N. J. Nunes, R. Pain, C. R. Pennypacker, R. Quimby, C. Lidman, R. S. Ellis, M. Irwin, R. G. McMahon, P. Ruiz-Lapuente, N. Walton, B. Schaefer, B. J. Boyle, A. V. Filippenko, T. Matheson, A. S. Fruchter, N. Panagia, H. J. M. Newberg, W. J. Couch, T. S. C. Project, *Measurements of Ω and Λ from 42 High-Redshift Supernovae*, The Astrophysical Journal 517 (2) (1999) 565–586.

[3] D. N. Spergel, L. Verde, H. V. Peiris, E. Komatsu, M. R. Nolta, C. L. Bennett, M. Halpern, G. Hinshaw, N. Jarosik, A. Kogut, M. Limon, S. S. Meyer, L. Page, G. S. Tucker, J. L. Weiland, E. Wollack, E. L. Wright, *First-Year Wilkinson Microwave Anisotropy Probe (WMAP) Observations: Determination of Cosmological Parameters*, The Astrophysical Journal Supplement Series 148 (1) (2003) 175–194.

[4] T. Harko, F. S. N. Lobo, S. Nojiri, S. D. Odintsov, *f(R,T) Gravity*, Physical Review D 84 (2) (2011) 024020.

[5] B. Li, J. D. Barrow, D. F. Mota, *Cosmology of Modified Gauss-Bonnet Gravity*, Physical Review D 76 (4) (2007) 1–9.

[6] G. Lyra, *Über Eine Modifikation der Riemannschen Geometrie*, Mathematische Zeitschrift 54 (1) (1951) 52–64.

[7] R. K. Tiwari, D. Sofuoğlu, V. K. Dubey, *Phase Transition of LRS Bianchi Type-I Cosmological Model in f(R,T) Gravity*, International Journal of Geometric Methods in Modern Physics 17 (12) (2020) 2050187–1315. doi:10.1142/S021988782050187X.

[8] R. K. Tiwari, D. Sofuoğlu, S. K. Mishra, *Accelerating Universe with Varying Λ in f(R, T) Theory of Gravity*, New Astronomy 83 (2021) 101476. doi:10.1016/j.newast.2020.101476.

[9] M. Zubair, H. Javaid, H. Azmat, E. Gudekli, *Relativistic Stellar Model in f(R , T) Gravity using Karmarkar Condition*, New Astronomy 88 (2021) 101610. doi:10.1016/j.newast.2021.101610.

[10] R. K. Tiwari, D. Sofuoğlu, A. Beesham, *FRW universe in f(R,T) Gravity*, International Journal of Geometric Methods in Modern Physics 18 (7) (2021) 2150104. doi:10.1142/S0219887821501048.

[11] D. Momeni, R. Myrzakulov, E. Güdekli, *Cosmological Viable Mimetic f(R) and f(R, T) Theories via Noether Symmetry*, International Journal of Geometric Methods in Modern Physics 12 (10) (2015) 1550101. arXiv:1502.00977, doi:10.1142/S0219887815501017.

[12] D. Sofuoğlu, *Gödel Universe in f(R,T) Gravity*, International Journal of Modern Physics D 28 (7) (2019) 1950089. doi:10.1142/S0218271819500895.

[13] S. Aygün, *Various Dark Energy Models with Time-Varying G and Λ in f(R, T) Gravitation Theory*, Modern Physics Letters A 34 (34) (2019) 1950280. doi:10.1142/S0217732319502808.

[14] A. Kabak, S. Aygün, *Scalar Field Solutions for Anisotropic Universe Models in Various Gravitation Theories*, International Journal of Geometric Methods in Modern Physics 17 (2) (2020) 2050025–586. doi:10.1142/S0219887820500255.

[15] S. Aygün, C. Aktaş, P. K. Sahoo, B. K. Bishi, *Scalar Field Cosmology in f(R, T) Gravity with* Λ, Gravitation and Cosmology 24 (3) (2018) 302–307. doi:10.1134/S0202289318030039.

[16] P. K. Sahoo, *Kaluza-Klein Universe Filled with Wet Dark Fluid in f(R,T) Theory of Gravity*, Acta Physica Polonica B, Proceedings Supplement 10 (2) (2017) 369.

[17] R. Nagpal, J. K. Singh, S. Aygün, *FLRW Cosmological Models with Quark and Strange Quark Matters in f(R,T) Gravity*, Astrophysics and Space Science 363 (6) (2018) 114.

[18] P. K. Sahoo, P. Sahoo, B. K. Bishi, S. Aygün, *Magnetized Strange Quark Model with Big Rip Singularity in f(R, T) Gravity*, Modern Physics Letters A 32 (21) (2017) 1750105.

[19] J. I. Kapusta, Finite-Temperature Field Theory, 1993.

[20] V. Singh, A. Beesham, *LRS Bianchi I Model with Strange Quark Matter and* $\Lambda(t)$ *in f(R , T) Gravity*, New Astronomy 89 (2021) 101634. doi:10.1016/j.newast.2021.101634.

[21] S. D. Katore, S. P. Hatkar, S. N. Bayaskar, *Some Special Solutions in Bianchi Type* VI_0 *Cosmological Models with Modified Chaplygin Gas in General Relativity*, International Journal of Modern Physics D 24 (2) (2015) 1550017.

[22] C. Aktaş, *Magnetized Strange Quark Matter in Reconstructed f(R,T) Gravity for Bianchi I and V Universes with Cosmological Constant*, Turkish Journal of Physics 41 (5) (2017) 469–476.

[23] A. Pradhan, R. Bali, *Magnetized Bianchi Type* VI_0 *Barotropic Massive String Universe with Decaying Vacuum Energy Density* Λ, arXiv e-prints (2008) arXiv:0805.3469.

[24] C. Aktaş, S. Aygün, P. K. Sahoo, *Relationship between Magnetic Field and Anisotropy Parameter in Gravitation Theories*, Modern Physics Letters A 33 (24) (2018) 1850135. doi: 10.1142/S0217732318501353.

[25] P. K. Sahoo, P. Sahoo, B. K. Bishi, S. Aygün, *Magnetized Strange Quark Matter in f(R, T) Gravity with Bilinear and Special Form of Time Varying Deceleration Parameter*, New Astronomy 60 (2018) 80–87. arXiv:1707.00979, doi:10.1016/j.newast.2017.10.010.

[26] C. Aktaş, I. Yilmaz, *Magnetized Quark and Strange Quark Matter in the Spherical Symmetric Space-Time Admitting Conformal Motion*, General Relativity and Gravitation 39 (6) (2007) 849–862. arXiv:0705.2930, doi:10.1007/s10714-007-0426-2.

[27] O. Özdemir, C. Aktaş, *Anisotropic Universe Models with Magnetized Strange Quark Matter in f(R) Gravity Theory*, Modern Physics Letters A 35 (14) (2020) 2050111–1258. doi:10.1142/S0217732320501114.

[28] C. Aktaş, S. Aygün, *Magnetized Strange Quark Matter Solutions in f(R, T) Gravity with Cosmological Constant*, Chinese Journal of Physics 55 (1) (2017) 71–78. doi:10.1016/j.cjph.2016.12.003.

[29] S. Aygün, H. Cağlar, D. Taşer, C. Aktaş, *Quark and Strange Quark Matter Solutions for Higher Dimensional FRW Universe in Lyra Geometry*, European Physical Journal Plus 130 (2015) 12. doi:10.1140/epjp/i2015-15012-x.

[30] S. Aygün, C. Aktaş, İ. Yılmaz, *Strange Quark Matter Solutions for Marder's Universe in f(R,T) Gravity with* Λ, Astrophysics Space Science 361 (12) (2016) 380. doi:10.1007/s10509-016-2956-0.

[31] C. Kömürcü, C. Aktaş, *Investigation of the Magnetized String Distribution in the Marder Universe with the Cosmological Term in f(R,T) Theory*, Modern Physics Letters A 35 (32) (2020) 2050263.

[32] C. G. Tsagas, J. D. Barrow, *A Gauge-Invariant Analysis of Magnetic Fields in General-Relativistic Cosmology*, Classical and Quantum Gravity 14 (9) (1997) 2539–2562.

[33] J. D. Barrow, R. Maartens, C. G. Tsagas, *Cosmology with Inhomogeneous Magnetic Fields*, Physics Reports 449 (6) (2007) 131–171.

[34] H. Sotani, K. Kohri, T. Harada, *Restricting Quark Matter Models by Gravitational Wave Observation*, Physical Review D (2004) 084008.

[35] S. K. J. Pacif, K. Myrzakulov, R. Myrzakulov, *Cosmological Parametrizations and Their Scalar Field Descendents*, International Journal of Geometric Methods in Modern Physics 14 (7) (2017) 1750111.

Journal of
New Theory
ISSN: 2149-1402

34 (2021) 86-98
Journal of New Theory
https://dergipark.org.tr/en/pub/jnt
Open Access

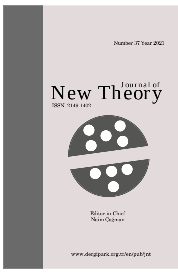

On the Existence of Symmetric Positive Solutions for SSBVPs on Time Scales

Cansel Kuyumcu [1], Erbil Çetin [2]

Article History
Received: 13 Dec 2021
Accepted: 29 Dec 2021
Published: 31 Dec 2021
10.53570/jnt.1036239
Research Article

Abstract − This paper considers symmetric positive solutions for the system of second-order boundary value problems (SSBVPs) on time scales using the Krasnosel'skii fixed point theorem. We then demonstrate two examples. Finally, we discuss the need for further results.

Keywords − *Time scale, symmetric positive solution, boundary value problem, Krasnosel'skii fixed point theorem*

Mathematics Subject Classification (2020) − 34K42, 34A05

1. Introduction

Hilger [1] first proposed the concept of time scales. The time-scale approach, used to model phenomena that manifest partly in discrete-time and continuous-time, unifies difference and differential equations. [2-5] provide heat transfer, stock market, economic, epidemic models and biological by utilising this concept. There has been an appreciable interest and research about boundary value problems on time scales in the past two decades. Moreover, there have been many results recently about the existence and multiplicity of symmetric positive solutions (SPSs) for nonlinear second-order and higher-order differential and dynamics equations with boundary conditions [6-14].

In [6] Qu investigated existence of positive solutions for following second order differential equations

$$\begin{cases} -u''(t) = f(t, v), \\ -v''(t) = g(t, u), \qquad t \in [0,1] \end{cases}$$

with following boundary conditions

$$\begin{aligned} u(t) &= u(1-t), \qquad u'(0) - u'(1) = u(\xi_1) + u(\xi_2) \\ v(t) &= v(1-t), \qquad v'(0) - v'(1) = v(\xi_1) + v(\xi_2) \end{aligned}$$

where $0 < \xi_1 < \xi_2 < 1$.

Inspired by the studies mentioned above, we will study the existence of SPSs for the following system of second-order boundary values problems (SSBVPs),

[1]canselkuyumcuuu@gmail.com; [2]erbil.cetin@ege.edu.tr (Corresponding Author)
[1,2]Department of Mathematics, Faculty of Sciences, Ege University, İzmir, Turkey

$$\begin{cases} -\vartheta^{\Delta\nabla}(t) = f(t,\varphi), & t \in \mathbb{T}_\kappa^\kappa \\ -\varphi^{\Delta\nabla}(t) = g(t,\vartheta), & t \in \mathbb{T}_\kappa^\kappa \end{cases} \tag{1}$$

subject to the boundary conditions

$$\begin{cases} \vartheta(t) = \vartheta(b-t+a), & \alpha\left[\vartheta^\Delta(a) - \vartheta^\Delta(\rho(b))\right] = \vartheta(\tau_1) + \vartheta(\tau_2) \\ \varphi(t) = \omega(b-t+a), & \alpha\left[\varphi^\Delta(a) - \varphi^\Delta(\rho(b))\right] = \varphi(\tau_1) + \varphi(\tau_2) \end{cases} \tag{2}$$

where $\mathbb{T}$ is a bounded symmetric time-scale (with $a = \min \mathbb{T}$ and $b = \max \mathbb{T}$), $\tau_1, \tau_2 \in \mathbb{T}$ such that $\tau_1 = b - \tau_2 + a$, $\alpha \geq b - a$ and $f, g: \mathbb{T} \times \mathbb{R}^+ \to \mathbb{R}^+$ are ld-continuous functions, both $f(.,s)$ and $g(.,s)$ are symmetric on $\mathbb{T}$ time-scale such that $f(t,0) \equiv g(t,0) \equiv 0$.

The second section of the present paper provides some of the basic definitions and lemmas needed for the next sections. Section 3 proves SPSs for the system (1)-(2) using the Krasnosel'skii fixed point theorem and presents two examples to illustrate the main results herein. Finally, we discuss the results and future studies. This study is a part of the first author's master's thesis.

2. Preliminaries

This section presents some basic definitions and results concerning about time scale theory which can be in [15-17]. Let $\mathbb{T}$, a nonempty closed subset of $\mathbb{R}$, be a time scale such that $a = \min \mathbb{T}$ and $b = \max \mathbb{T}$. The jump operators $\sigma, \rho : \mathbb{T} \to \mathbb{T}$ are defined by $\sigma(t) \coloneqq \inf\{s \in \mathbb{T} : s > t\}$, $\rho(t) \coloneqq \sup\{s \in \mathbb{T} : s < t\}$ where $\inf \emptyset = a$ and $\sup \emptyset = b$ so that $\rho(a) = a$ and $\sigma(b) = b$. A point $t \in \mathbb{T}$ is called right scattered, right dense, left scattered, and left dense if $\sigma(t) > t$, $\sigma(t) = t$, $\rho(t) < t$ and $\rho(t) = t$ respectively.

If a function x from $\mathbb{T}$ to $\mathbb{R}$ is continuous at all left dense points and has finite right-sided limits at all right dense points of $\mathbb{T}$, then it is said to be ld-continuous on $\mathbb{T}$. Moreover, $C_{ld}(\mathbb{T})$ denotes the set of ld-continuous functions $x: \mathbb{T} \to \mathbb{R}$. Here, $C_{ld}(\mathbb{T})$ is a Banach space with below norm $\| x \| \coloneqq \max_{t\in\mathbb{T}}|x(t)|$, $x \in C_{ld}(\mathbb{T})$.

Throughout this paper, let define the delta and nabla differentiability sets $\mathbb{T}^\kappa \coloneqq \mathbb{T} - (\rho(b), b]$, $\mathbb{T}_\kappa \coloneqq \mathbb{T} - [a, \sigma(a))$ and $\mathbb{T}_\kappa^\kappa \coloneqq \mathbb{T} - ([a,\sigma(a)) \cup (\rho(b), b])$ which are closed. Therefore they are time scales too, and we are also able to define the above space and norm using $\mathbb{T}_\kappa^\kappa$ instead of $\mathbb{T}$.

Definition 2.1. [16] Let f be a function from $\mathbb{T}$ to $\mathbb{R}$. Then, f is delta differentiable at $t \in \mathbb{T}^\kappa$ if there exists a number $f^\Delta(t)$ with the following property: for any $\varepsilon > 0$ there exists a $\delta > 0$ such that $s \in \mathbb{T}$ and

$$|t - s| < \delta \Rightarrow |f(\sigma(t)) - f(s) - f^\Delta(t)(\sigma(t) - s)| \leq \varepsilon|\sigma(t) - s|$$

Here, f is said to be delta differentiable, if f is delta differentiable, for all $t \in \mathbb{T}^\kappa$.

Definition 2.2. [16] Let f be a function from $\mathbb{T}$ to $\mathbb{R}$. Then, f is nabla differentiable at $t \in \mathbb{T}_\kappa$ if there exists a number $f^\nabla(t)$ with the following property: for any $\varepsilon > 0$ there exists a $\delta > 0$ such that $s \in \mathbb{T}$ and

$$|t - s| < \delta \Rightarrow \left|f(\rho(t)) - f(s) - f^\nabla(t)(\rho(t) - s)\right| \leq \varepsilon|\rho(t) - s|$$

Here, f is said to be nabla differentiable, if f is nabla differentiable, for all $t \in \mathbb{T}_\kappa$.

Definition 2.3. [16] Let F be a function from $\mathbb{T}$ to $\mathbb{R}$. Then, F is called a nabla antiderivative of $f: \mathbb{T} \to \mathbb{R}$ provided $F^\nabla(t) = f(t)$ holds for all $t \in \mathbb{T}_\kappa$. Moreover, the nabla integral of f is defined as follows:

$$\int_a^t f(s)\nabla s = F(t) - F(a), \text{for all } t \in \mathbb{T}$$

Definition 2.4. [12] Let $\mathbb{T}$ be a time scale. Then, $\mathbb{T}$ is called symmetric, if $b - t + a \in \mathbb{T}$, for all $t \in \mathbb{T}$.

Definition 2.5. [12] Let ϑ be a function from $\mathbb{T}$ to $\mathbb{R}$. If, for all $t \in \mathbb{T}$, $\vartheta(t) = \vartheta(b - t + a)$, then ϑ is called symmetric on $\mathbb{T}$.

Definition 2.6. Let ϑ, φ be functions from $\mathbb{T}$ to $\mathbb{R}$. If a pair of (ϑ, φ) is a solution of $SSBVP$ (1)–(2) and ϑ, φ are symmetric on $\mathbb{T}$, then a pair of (ϑ, φ) is called a symmetric solution of $SSBVP$ (1)–(2) on $\mathbb{T}$.

Definition 2.7. [19] Let $\mathbb{X}$ be a real Banach space. A nonempty closed set $P \subset \mathbb{X}$ is called a cone of $\mathbb{X}$ if it satisfies the following two conditions:

i. $y \in P, \gamma > 0$ implies $\gamma y \in P$

ii. $y, -y \in P$ implies $y = 0$

Theorem 2.8. [18,19] Let $\mathbb{B}$ be a Banach space, and $P \subset \mathbb{B}$ is a cone in $\mathbb{B}$. Assume that ω_1 and ω_2 are open subsets of $\mathbb{B}$ with $0 \in \omega_1$ and $\overline{\omega_1} \subset \omega_2$. Let $T: P \cap (\overline{\omega_2} \setminus \omega_1) \to P$ be a completely continuous operator such that either

i. $\forall u \in P \cap \partial\omega_1: \|Tu\| \le \|u\|, \forall u \in P \cap \partial\omega_2: \|Tu\| \ge \|u\|$

or

ii. $\forall u \in P \cap \partial\omega_1: \|Tu\| \ge \|u\|, \forall u \in P \cap \partial\omega_2: \|Tu\| \le \|u\|$

holds. Then, T has a fixed point in $P \cap (\overline{\omega_2} \setminus \omega_1)$.

Hereinafter, $\mathbb{T}$ is a symmetric time scale with $a = \min \mathbb{T}$ and $b = \max \mathbb{T}$, and $\tau_1, \tau_2 \in \mathbb{T}$ such that $\tau_1 = b - \tau_2 + a$.

Lemma 2.9. Let $h \in \mathcal{C}_{ld}(\mathbb{T})$ and $q(t) \not\equiv 0$. When $\tau_1, \tau_2 \in \mathbb{T}$ such that $\tau_1 = b - \tau_2 + a$ and $\alpha \ge b - a$, then the BVP

$$\vartheta^{\Delta\nabla}(t) = -q(t), t \in \mathbb{T}_\kappa^\kappa \tag{3}$$

$$\vartheta(t) = \vartheta(b - t + a), \alpha\left[\vartheta^{\Delta}(a) - \vartheta^{\Delta}\big(\rho(b)\big)\right] = \vartheta(\tau_1) + \vartheta(\tau_2) \tag{4}$$

has a unique solution

$$\vartheta(t) = \int_a^b G(t,s)q(s)\nabla s$$

where

$$G(t,s) = G_1(t,s) + G_2(s), \tag{5}$$

here

$$G_1(t,s) = \frac{1}{b-a}\begin{cases}(b-t)(s-a), s \le t\\ (b-s)(t-a), t \le s\end{cases}$$

and

$$G_2(s) = \frac{1}{2}\begin{cases}\alpha + a - s, a \le s \le \tau_1\\ \alpha + \tau_2 - b,\ \tau_1 \le s \le \tau_2\\ \alpha - b + s, \tau_2 \le s \le b.\end{cases}$$

Proof. Let assume that $\vartheta \in \mathcal{C}_{ld}(\mathbb{T})$ is a solution of (3)–(4). By integration of both sides of (3) from a to t, we get

$$\vartheta^{\Delta}(t) = \vartheta^{\Delta}(a) - \int_a^t q(s)\nabla s \tag{6}$$

Integrating again, we have

$$\vartheta(t) = \vartheta(a) + (t-a)\vartheta^{\Delta}(a) - \int_a^t (t-s)q(s)\nabla s \tag{7}$$

Plug in $t = b$ in (7), we find

$$\vartheta(b) = \vartheta(a) + (b-a)\vartheta^{\Delta}(a) - \int_a^b (b-s)q(s)\nabla s$$

Using boundary conditions (4), we find

$$\vartheta^{\Delta}(a) = \frac{1}{b-a}\int_a^b (b-s)q(s)\nabla s \tag{8}$$

Substituting (8) to (7), we get

$$\vartheta(t) = \vartheta(a) + (t-a)\frac{1}{b-a}\int_a^b (b-s)q(s)\nabla s - \int_a^t (t-s)q(s)\nabla s \tag{9}$$

From (4), we have

$$\alpha\int_a^{\rho(b)} q(s)\nabla s \;=\; 2\vartheta(a) + (\tau_1 - a)\frac{1}{b-a}\int_a^b (b-s)q(s)\nabla s - \int_a^{\tau_1} (\tau_1 - s)q(s)\nabla s$$

$$+(\tau_2 - a)\frac{1}{b-a}\int_a^b (b-s)q(s)\nabla s - \int_a^{\tau_2} (\tau_2 - s)q(s)\nabla s$$

Therefore,

$$\begin{aligned}\vartheta(a) = \frac{1}{2}\Bigg[&\int_a^{\tau_1} \left[\alpha + \frac{(2a-\tau_1-\tau_2)(b-s)}{b-a} + (\tau_1 - s) + (\tau_2 - s)\right] q(s)\nabla s \\ &+ \int_{\tau_1}^{\tau_2} \left[\alpha + \frac{(2a-\tau_1-\tau_2)(b-s)}{b-a} + (\tau_2 - s)\right] q(s)\nabla s \\ &+ \int_{\tau_2}^{\rho(b)} \left[\alpha + \frac{(2a-\tau_1-\tau_2)(b-s)}{b-a}\right] q(s)\nabla s\Bigg]\end{aligned} \tag{10}$$

and from $\tau_1 = b - \tau_2 + a$,

$$\vartheta(a) = \frac{1}{2}\left[\int_a^{\tau_1} (\alpha + a - s)\, q(s)\nabla s + \int_{\tau_1}^{\tau_2} (\alpha + \tau_2 - b)\, q(s)\nabla s + \int_{\tau_2}^{\rho(b)} (\alpha + s - b)\; q(s)\nabla s\right] \tag{11}$$

Substituting (11) to (9), we have

$$\begin{aligned}\vartheta(t) &= \frac{1}{b-a}\int_a^b (t-a)(b-s)q(s)\nabla s - \int_a^t (t-s)q(s)\nabla s + \int_a^b G_2(s)q(s)\nabla s \\ &= \int_a^b G(t,s)q(s)\nabla s\end{aligned}$$

This proof is completed. □

Lemma 2.10. For $t,s \in \mathbb{T}$, we have $G(t,s) \geq 0$ and $\min_{t\in\mathbb{T}} G_2(t) = G_2(\tau_1) = G_2(\tau_2)$.

Proof. It is evident from (5). □

Lemma 2.11. For $t,s \in \mathbb{T}$, let $m_{G_2} = \min_{t\in\mathbb{T}} G_2(t) = G_2(\tau_1) = G_2(\tau_2)$ and $L = \frac{4m_{G_2}}{4m_{G_2}+(b-a)}$, then the function $G(t,s)$ satisfies

$$LG(s,s) \leq G(t,s) \leq G(s,s) \text{ for } t,s \in \mathbb{T} \tag{12}$$

Proof. For $s \leq t$, we get

$$\frac{G_1(t,s)}{G_1(s,s)} = \frac{b-t}{b-s} \leq \frac{b-s}{b-s} = 1$$

For $t \leq s$, we get

$$\frac{G_1(t,s)}{G_1(s,s)} = \frac{t-a}{s-a} \leq \frac{s-a}{s-a} = 1$$

Therefore, we have $G_1(t,s) \leq G_1(s,s)$. Thus,

$$\mathrm{G(t,s)} = G_1(t,s) + G_2(s) \leq G_1(s,s) + G_2(s) = G(s,s)$$

We know $G_2(s) \geq 0$ from Lemma 2.9. Therefore, it is evident that $m_{G_2} \geq 0$. By using $\frac{(b-s)(s-a)}{b-a} \leq \frac{b-a}{4}$, we have

$$\begin{aligned}G(t,s) &= G_1(t,s) + G_2(s) \\ &\geq G_2(s) \\ &= \frac{4m_{G_2}+b-a}{4m_{G_2}+b-a} G_2(s) \\ &= LG_2(s) + \frac{4}{4}\frac{(b-a).m_{G_2}}{4m_{G_2}+b-a} \\ &= LG_2(s) + L\frac{(b-a)}{4} \\ &\geq LG_2(s) + L\frac{(b-s)(s-a)}{b-a} \\ &= LG_2(s) + LG_1(s,s) \\ &= LG(s,s)\end{aligned}$$

It is evident that $LG(s,s) \leq G(t,s) \leq G(s,s)$ for $t,s \in \mathbb{T}$. This proof is completed. □

Lemma 2.12. $G(t,s)$ Green function is symmetric on $\mathbb{T}$. i.e., for $t,s \in \mathbb{T}$,

$$G(b-t+a,b-s+a)=G(t,s)$$

Proof. Using $\tau_1 = b-\tau_2+a$ and Definition 2.5 and (5), we have

$$\begin{aligned} G_1(b-t+a,b-s+a) &= \frac{1}{b-a}\begin{cases}(b-b+t-a)(b-s+a-a), b-s+a\le b-t+a\\(b-b+s-a)(b-t+a-a), b-t+a\le b-s+a\end{cases}\\ &= \frac{1}{b-a}\begin{cases}(t-a)(b-s), t\le s\\(s-a)(b-t), s\le t\end{cases}\\ &= G_1(t,s)\end{aligned}$$

and

$$\begin{aligned} G_2(b-s+a) &= \frac{1}{2}\begin{cases}\alpha+a-b+s-a, a\le b-s+a\le \tau_1\\ \alpha+\tau_2-b, \tau_1\le b-s+a\le\tau_2\\ \alpha-b+b-s+a, \tau_2\le b-s+a\le b\end{cases}\\ &= \frac{1}{2}\begin{cases}\alpha-b+s, a-b-a\le -s\le \tau_1-b-a\\ \alpha+\tau_2-b, \tau_1-b-a\le -s\le\tau_2-b-a\\ \alpha+a-s, \tau_2-b-a\le -s\le b-b-a\end{cases}\\ &= \frac{1}{2}\begin{cases}\alpha+a-s, \tau_2\le s\le b\\ \alpha+\tau_2-b, \tau_1\le s\le\tau_2\\ \alpha-b+s, a\le s\le\tau_1\end{cases}\\ &= G_2(s)\end{aligned}$$

Therefore,

$$G(b-t+a,b-s+a)=G_1(b-t+a,b-s+a)+G_2(b-s+a)=G_1(t,s)+G_2(s)$$

Eventually, for $t,s\in\mathbb{T}, G(b-t+a,b-s+a)=G(t,s)$. The proof is completed. □

3. Main Results

This section studies the existence of the SPSs of the SSBVP (1)-(2). First, we assume the following conditions:

(H_1) $f\colon \mathbb{T}\times\mathbb{R}^+\to\mathbb{R}^+$ is a ld-continuous function such that $f(.,s)$ is symmetric on $\mathbb{T}$ and $f(t,0)\equiv 0$,

(H_2) $g\colon \mathbb{T}\times\mathbb{R}^+\to\mathbb{R}^+$ is a ld-continuous function such that $g(.,s)$ is symmetric on $\mathbb{T}$ and $g(t,0)\equiv 0$.

Second, we give the following assumptions:

$$\overline{f_0}=\overline{\lim_{x\to 0^+}}\max_{t\in\mathbb{T}}\frac{f(t,x)}{x},\qquad \overline{g_0}=\overline{\lim_{x\to 0^+}}\max_{t\in\mathbb{T}}\frac{g(t,x)}{x},$$

$$\underline{f_0}=\underline{\lim_{x\to 0^+}}\min_{t\in\mathbb{T}}\frac{f(t,x)}{x},\qquad \underline{g_0}=\underline{\lim_{x\to 0^+}}\min_{t\in\mathbb{T}}\frac{g(t,x)}{x},$$

$$\overline{f_\infty}=\overline{\lim_{x\to \infty}}\max_{t\in\mathbb{T}}\frac{f(t,x)}{x},\qquad \overline{g_\infty}=\overline{\lim_{x\to \infty}}\max_{t\in\mathbb{T}}\frac{g(t,x)}{x},$$

$$\underline{f_\infty}=\underline{\lim_{x\to \infty}}\min_{t\in\mathbb{T}}\frac{f(t,x)}{x},\qquad \underline{g_\infty}=\underline{\lim_{x\to \infty}}\min_{t\in\mathbb{T}}\frac{g(t,x)}{x}$$

Now, let $\mathbb{B}=C_{ld}(\mathbb{T})$ be a Banach space with $\|\vartheta\|=\max_{t\in\mathbb{T}}|\vartheta(t)|$, and determine cone $P\subset\mathbb{B}$ by

$$P=\left\{\vartheta\in\mathbb{B}\,\middle|\, \vartheta(t)\ge 0 \text{ for } t\in\mathbb{T}, \vartheta(t) \text{ is symmetric on } \mathbb{T}, \min_{t\in\mathbb{T}}\vartheta(t)\ge L\|\vartheta\| \text{ and } \vartheta^{\Delta\nabla}(t)\le 0 \text{ for } t\in\mathbb{T}_\kappa^\kappa\right\}$$

Besides, define the integral operator T from P to $\mathbb{B}$ by

$$T\vartheta(t) = \int_a^b G(t,s)f(s, \int_a^b G(s,\zeta)g(\zeta,\vartheta(\zeta))\nabla\zeta)\nabla s \tag{13}$$

Thus,

$$T\vartheta(t)^{\Delta\nabla} = -f(s, \int_a^b G(s,\zeta)g(\zeta,\vartheta(\zeta))\nabla\zeta)$$

Hence, for $\vartheta \in P$, $T\vartheta \geq 0$ on $\mathbb{T}$ and $T\vartheta^{\Delta\nabla} \leq 0$ on $\mathbb{T}_\kappa^\kappa$.

Since ϑ, f and g are symmetric on $\mathbb{T}$, then

$$\begin{aligned} T\vartheta(b-t+a) &= \int_b^a G(b-t+a,b-s+a)f(b-s+a, \int_a^b G(b-s+a,\zeta)g(\zeta,\vartheta(\zeta))\nabla\zeta)\nabla(b-s+a) \\ &= \int_a^b G(t,s)f(b-s+a, \int_b^a G(b-s+a,b-\zeta+a)g(b-\zeta+a,\vartheta(b-\zeta+a))\nabla(b-\zeta+a))\nabla s \\ &= \int_a^b G(t,s)f(s, \int_a^b G(s,\zeta)g(\zeta,\vartheta(\zeta))\nabla\zeta)\nabla s \\ &= T\vartheta(t) \end{aligned}$$

for all $t \in \mathbb{T}$. This implies that $T\vartheta(t)$ is symmetric on $\mathbb{T}$. It is easy to verify that $\min_{t\in\mathbb{T}} T\vartheta(t) \geq L\|T\vartheta\|$. Consequently $T: P \to P$.

Lemma 3.1. Suppose that (H_1) and (H_2) hold. Then, for $\vartheta, \varphi \in \mathbb{B}$, a pair of (ϑ, φ) is a solution of SSBVP (1)-(2) iff ϑ is a fixed point of the operator T and $\varphi(t)=\int_a^b G(t,\zeta)g(\zeta,\vartheta(\zeta))\nabla\zeta$

Proof. The proof is clear from Lemma 2.9. ◻

Lemma 3.2. Suppose that (H_1) and (H_2) hold. Then, the operator $T: P \to P$ is completely continuous.

Proof. Suppose that $K \subset P$ is a bounded set. Let $N \geq 0$ be such that $\|\vartheta\| \leq N$ for $\vartheta \in K$, we have

$$\begin{aligned} |T\vartheta(t)| &\leq \int_a^b G(s,s)f(s, \int_a^b G(s,\zeta)g(\zeta,\vartheta(\zeta))\nabla\zeta)\,\nabla s \\ &\leq \int_a^b G(s,s) \sup_{a<s<b} \left| f(s, \int_a^b G(s,\zeta)g(\zeta,\vartheta(\zeta))\nabla\zeta) \right| \nabla s \\ &= \sup_{a<s<b} \left| f(s, \int_a^b G(s,\zeta)g(\zeta,\vartheta(\zeta))\nabla\zeta) \right| \int_a^b G(s,s)\nabla s \end{aligned}$$

for every $t \in \mathbb{T}$. This implies that $T(K)$ is bounded. By the Arzela-Ascoli theorem. We can easily see that T is a completely continuous operator. Thus, the proof is completed. ◻

For convenience, we denote

$$m := \int_a^b G(z,z)\nabla z \tag{14}$$

Theorem 3.3. Suppose that (H_1) and (H_2) are satisfied. If $\overline{f_0} = \overline{g_0} = 0$ and $\underline{f_\infty} = \underline{g_\infty} = \infty$ hold, then SSBVP (1)-(2) has a symmetric positive solution (ϑ, φ).

Proof. Because of $\overline{f_0} = \overline{g_0} = 0$ uniformly on $\mathbb{T}$, we may choose a $c_1 > 0$ such that

$$f(t,\vartheta) \le \gamma_1 \vartheta, \qquad g(t,\vartheta) \le \gamma_1 \vartheta, \qquad 0 < \vartheta \le c_1, \qquad t \in \mathbb{T}$$

where $\gamma_1 \le \frac{1}{m}$. Note that

$$\int_a^b G(s,\zeta) g(\zeta, \vartheta(\zeta)) \nabla\zeta \le \int_a^b G(\zeta,\zeta)\gamma_1 \vartheta(\zeta) \nabla\zeta \le \gamma_1 \int_a^b G(\zeta,\zeta) \|\vartheta\| \nabla\zeta \le \|\vartheta\| \le c_1$$

If ω_1 is a ball in $\mathbb{B}$ centred at the origin with a radius c_1 and if $\vartheta \in P \cap \partial\omega_1$, then we have

$$\begin{aligned}
\|T\vartheta(t)\| &= \max_{t\in\mathbb{T}} \int_a^b G(t,s) f(s, \int_a^b G(s,\zeta) g(\zeta,\vartheta(\zeta)) \nabla\zeta) \nabla s \\
&\le \int_a^b G(s,s)\gamma_1 \int_a^b G(s,\zeta) g\big(\zeta,\vartheta(\zeta)\big) \nabla\zeta \, \nabla s \\
&\le \gamma_1 \int_a^b G(s,s)\nabla s \int_a^b G(\zeta,\zeta)\gamma_1 \vartheta(\zeta) \nabla\zeta \\
&\le {\gamma_1}^2 \int_a^b G(s,s)\nabla s \int_a^b G(\zeta,\zeta) \|\vartheta\| \nabla\zeta \\
&= {\gamma_1}^2 m^2 \|\vartheta\| \le \|\vartheta\|
\end{aligned}$$

and so $\|T\vartheta(t)\| \le \|\vartheta\|$ for all $\vartheta \in P \cap \partial\omega_1$.

Next, we use the assumption $\underline{f_\infty} = \underline{g_\infty} = \infty$ uniformly on $\mathbb{T}$. There exists a $c_2 > 0$ large enough such that $f(t,\vartheta) \ge \mu\vartheta, g(t,\vartheta) \ge \mu\vartheta, \vartheta > c_2$, for $t \in \mathbb{T}$ where $\mu \ge \frac{1}{L^{\frac{3}{2}} m}$. If we define $\omega_2 = \left\{\vartheta \in \mathbb{B} \,\middle|\, \|\vartheta\| < \frac{2c_2}{\sqrt{L}}\right\}$, for $t \in \mathbb{T}$, $\vartheta \in P$ and $\|\vartheta\| = \frac{2c_2}{\sqrt{L}}$, we have

$$\int_a^b G(s,\zeta) g\big(\zeta,\vartheta(\zeta)\big) \nabla\zeta \ge L \int_a^b G(\zeta,\zeta)\mu\vartheta(\zeta)\nabla\zeta \ge L\mu \int_a^b G(\zeta,\zeta)\nabla\zeta L \|\vartheta\| = L^2 \mu m \|\vartheta\| \ge \sqrt{L}\|\vartheta\| = 2c_2 > c_2$$

For $\vartheta \in P \cap \partial\omega_2$, we have

$$\begin{aligned}
\|T\vartheta(t)\| &\ge L \int_a^b G(s,s)\mu \int_a^b G(s,\zeta) g\big(\zeta,\vartheta(\zeta)\big) \nabla\zeta \, \nabla s \\
&\ge L^2 \mu \int_a^b G(s,s)\nabla s \int_a^b G(\zeta,\zeta)\mu\vartheta(\zeta)\nabla\zeta \\
&\ge L^2 \mu^2 \int_a^b G(s,s)\nabla s \int_a^b G(\zeta,\zeta) L \|\vartheta\| \nabla\zeta \\
&= \mu^2 L^3 m^2 \|\vartheta\| \ \ge \|\vartheta\|
\end{aligned}$$

and so $\|T\vartheta(t)\| \geq \|\vartheta\|$ for all $\vartheta \in P \cap \partial\omega_2$. As a conclusion, from (i) of Theorem 2.8, T has a fixed point in $P \cap (\overline{\omega_2} \setminus \omega_1)$ and so the SSBVP (1)-(2) has a symmetric positive solution (ϑ, φ). □

Theorem 3.4. Assume (H_1) and (H_2) are satisfied. If $\underline{f_0} = \underline{g_0} = \infty$ and $\overline{f_\infty} = \overline{g_\infty} = 0$ hold, then SSBVP (1)-(2) has a symmetric positive solution (ϑ, φ).

Proof. Firstly, let $\underline{f_0} = \underline{g_0} = \infty$ hold. For $t \in \mathbb{T}$, there exists a $\overline{c_3} > 0$ such that

$$f(t,\vartheta) \geq \mu\vartheta, g(t,\vartheta) \geq \mu\vartheta, 0 < \vartheta < \overline{c_3}$$

such that $\mu \geq \frac{1}{L^{\frac{3}{2}}m}$. Now from $g(t,0) \equiv 0$ and $g(t,s)$ is continuous, we know that there exists a number $c_3 \in (0, \overline{c_3})$ such that $g(t,s) \leq \frac{\overline{c_3}}{m}$ for each $\vartheta \in (0, \overline{c_3}]$ and $t \in \mathbb{T}$. Then, for all $\vartheta \in P$ and $\|\vartheta\| = \overline{c_3}$, note that

$$\int_a^b G(s,\zeta)g(\zeta,\vartheta(\zeta))\nabla\zeta \leq \int_a^b G(\zeta,\zeta)\frac{\overline{c_3}}{m}\nabla\zeta = \overline{c_3}$$

Let $\omega_3 = \{\vartheta \in \mathbb{B} \mid \|\vartheta\| < c_3\}$. For $\vartheta \in P \cap \partial\omega_3$, then we have

$$\begin{aligned} \|T\vartheta(t)\| &\geq L\int_a^b G(s,s)\mu\int_a^b G(s,\zeta)g(\zeta,\vartheta(\zeta))\nabla\zeta\,\nabla s \\ &\geq L^2\mu\int_a^b G(s,s)\nabla s\int_a^b G(\zeta,\zeta)\mu\vartheta(\zeta)\nabla\zeta \\ &\geq L^2\mu^2\int_a^b G(s,s)\nabla s\int_a^b G(\zeta,\zeta)L\|\vartheta\|\nabla\zeta \geq \|\vartheta\| \end{aligned}$$

For $\vartheta \in P \cap \partial\omega_3$, we have $\|T\vartheta(t)\| \geq \|\vartheta\|$. Next, since $\overline{f_\infty} = \overline{g_\infty} = 0$, there exists a $c_4 > 0$ such that

$$f(t,\vartheta) \leq \gamma_4\vartheta, \qquad g(t,\vartheta) \leq \gamma_4\vartheta, \qquad \vartheta > c_4, \qquad t \in \mathbb{T} \tag{15}$$

where $\gamma_4 \leq \frac{1}{m}$. We consider two cases.

Case 1. Assume $f(t,s)$ is bounded on $\mathbb{T} \times [0,\infty)$. Therefore, there is an $M > 0$ such that $f(t,s) \leq M$, for $t \in \mathbb{T}$ and $s \in [0,\infty)$. Let $c_4{}^* \geq \max\{2c_4, Mm\}$. Then, for $\vartheta \in P$ with $\|\vartheta\| = c_4{}^*$,

$$\|T\vartheta(t)\| \leq \int_a^b G(s,s)M\nabla s = Mm \leq \max\{2c_4, Mm\} \leq c_4{}^* = \|\vartheta\|$$

Case 2. Assume $f(t,s)$ is unbounded on $\mathbb{T} \times [0,\infty)$. Then,

$$h(c) \coloneqq \max\{f(t,s) | t \in \mathbb{T}, 0 \leq s \leq c\} \tag{16}$$

such that $\lim_{c\to\infty} h(c) = \infty$. Therefore, we can choose $c_4{}^* \geq \max\{2c, c_4\}$ such that $h(c) \leq h(c_4{}^*)$ for $0 \leq c \leq c_4{}^*$. Since $\overline{c_4} \leq c_4{}^*$, (15) and (16), then we get $f(t,s) \leq h(c_4{}^*) \leq \gamma_4 c_4{}^*$, for $t \in \mathbb{T}$ and $s \in [0, c_4{}^*]$. For $\vartheta \in P$ and $\|\vartheta\| = c_4{}^*$, we have

$$\|T\vartheta(t)\| \leq \int_a^b G(s,s)\gamma_4 c_4{}^*\nabla s = \gamma_4 c_4{}^* m \leq c_4{}^* = \|\vartheta\|$$

So, we obtain $\|T\vartheta(t)\| \leq \|\vartheta\|$ for all $\vartheta \in P \cap \partial\omega_4$, where $\omega_4 = \{\vartheta \in \mathbb{B} | \|\vartheta\| \leq c_4{}^*\}$ in both cases. By (ii) of Theorem 2.8 that T has a fixed point in $P \cap (\overline{\omega_4} \setminus \omega_3)$ and so the SSBVP (1)-(2) has a symmetric positive solution (ϑ, φ). □

We will provide sufficient conditions for two SPSs for SSBVP (1)-(2).

(H_3) There exists a constant $R_1 > 0$ such that $f(t,s) \leq \frac{R_1}{m}$ and $g(t,s) \leq \frac{R_1}{m}$, for $t \in \mathbb{T}, s \in [0, R_1]$.

(H_4) There exists a constant $R_2 > 0$ such that $f(t,s) \geq \frac{R_2}{Lm}$ and $g(t,s) \leq \frac{R_2}{m}$, for $t \in \mathbb{T}, s \in [0, R_2]$.

Theorem 3.5. Assume that (H_1), (H_2) and (H_3) are satisfied. If $\underline{f_\infty} = \underline{g_\infty} = \infty$ and $\underline{f_0} = \underline{g_0} = \infty$ hold, then the SSBVP (1)-(2) has two SPSs (ϑ_1, φ_1) and (ϑ_2, φ_2).

Proof. At first, from Lemma 2.9 and (H_3), we can obtain $\int_a^b G(s,\zeta)g(\zeta,\vartheta(\zeta)\nabla\zeta \in [0, R_1]$. Thus $\|T\vartheta(t)\| \leq \frac{R_1}{m}\int_a^b G(s,s)\nabla s = R_1 = \|\vartheta\|$. Then $\|T\vartheta(t)\| \leq \|\vartheta\|$ for $\forall\vartheta \in P \cap \partial\omega_5$, where $\omega_5 = \{\vartheta \in \mathbb{B} \mid \|\vartheta\| < R_1\}$. For another hand, from Theorem 3.3 and Theorem 3.5, we have $\|T\vartheta(t)\| \geq \|\vartheta\|$ for $\forall\vartheta \in P \cap \partial\omega_2$ where $c_2 > R_1$and $\|T\vartheta(t)\| \geq \|\vartheta\|$ for $\forall\vartheta \in P \cap \partial\omega_3$ where $R_1 > c_3$.

It follows from Theorem 2.8 that T has a fixed point ϑ_1 in $P \cap (\overline{\omega_5} \setminus \omega_3)$ and a fixed point ϑ_2 in $P \cap (\overline{\omega_2} \setminus \omega_5)$. (ϑ_1, φ_1) and (ϑ_2, φ_2) are SPSs of the SSBVP (1)-(2). □

Theorem 3.6. Assume that (H_1), (H_2) and (H_4) are satisfied. If $\overline{f_0} = \overline{g_0} = 0$ and $\overline{f_\infty} = \overline{g_\infty} = 0$ hold, then the SSBVP (1)-(2) has two SPSs.

Proof. It could be proved in a similar way to Theorems 3.5. □

Example 3.6. On a bounded symmetric time scale $\mathbb{T} = \{1,2,3,4,5,6,7,8,9,10\}$ we consider following SSBVP

$$\begin{aligned} \vartheta^{\Delta\nabla}(t) &= -\varphi^2(t)\left(\frac{11}{2} - t\right)^2, \qquad t \in \mathbb{T}_\kappa^\kappa = \{2,3,4,5,6,7,8,9\} \\ \varphi^{\Delta\nabla}(t) &= -\vartheta^4(t)\left(\frac{11}{2} - t\right)^2, \qquad t \in \mathbb{T}_\kappa^\kappa = \{2,3,4,5,6,7,8,9\} \end{aligned} \tag{17}$$

and boundary conditions

$$\begin{aligned} \vartheta(t) = \vartheta(11-t), &\qquad 9(\vartheta^\Delta(1) - \vartheta^\Delta(9)) = \vartheta(3) + \vartheta(8) \\ \varphi(t) = \varphi(11-t), &\qquad 9(\varphi^\Delta(1) - \varphi^\Delta(9)) = \varphi(3) + \varphi(8) \end{aligned} \tag{18}$$

In this problem, $[1,10]_\mathbb{T}$ is symmetric, $a = 1, b = 10, \sigma(a) = 2$, $\rho(b) = 9$, $\tau_1 = 3$ and $\tau_2 = 8$. We see that easily $f(t,\varphi) = \left(\frac{11}{2} - t\right)^2 \varphi^2$ and $g(t,\vartheta) = \left(\frac{11}{2} - t\right)^2 \vartheta^4$ are satisfies the conditions (H_1) and (H_2) and also

$$\overline{f_0} = \overline{\lim_{\varphi\to 0^+}} \max_{t\in\mathbb{T}} \frac{f(t,\varphi)}{\varphi} = \overline{\lim_{\varphi\to 0^+}} \max_{t\in\mathbb{T}} (\frac{11}{2} - t)^2\varphi = 0$$

$$\overline{g_0} = \overline{\lim_{\vartheta\to 0^+}} \max_{t\in\mathbb{T}} \frac{g(t,\vartheta)}{\vartheta} = \overline{\lim_{\vartheta\to 0^+}} \max_{t\in\mathbb{T}} (\frac{11}{2} - t)^2\vartheta^3 = 0$$

$$\underline{f_\infty} = \underline{\lim_{\varphi\to\infty}} \min_{t\in\mathbb{T}} \frac{f(t,\varphi)}{\varphi} = \underline{\lim_{\varphi\to\infty}} \min_{t\in\mathbb{T}} (\frac{11}{2} - t)^2\varphi = \infty$$

$$\underline{g_\infty} = \underline{\lim_{\vartheta\to\infty}} \min_{t\in\mathbb{T}} \frac{g(t,\vartheta)}{\vartheta} = \underline{\lim_{\vartheta\to\infty}} \min_{t\in\mathbb{T}} (\frac{11}{2} - t)^2\vartheta^3 = \infty$$

As a result, all conditions of Theorem 3.3 are satisfied. From Theorem 3.3, SSBVP (17)-(18) has one SPS.

Example 3.7. On a bounded symmetric time scale $\mathbb{T} = \{0\} \cup [1,2] \cup \{3\}$ we consider the following system

$$\begin{cases} \vartheta^{\Delta\nabla}(t) = -f\big(t,\varphi(t)\big), t \in \mathbb{T}_\kappa^\kappa = [1,2] \\ \varphi^{\Delta\nabla}(t) = -g\big(t,\vartheta(t)\big), t \in \mathbb{T}_\kappa^\kappa = [1,2] \end{cases} \tag{19}$$

with boundary conditions

$$\begin{cases} \vartheta(t) = \vartheta(3-t), \qquad 3(\vartheta^\Delta(0) - \vartheta^\Delta(2)) = \vartheta(1) + \vartheta(2) \\ \varphi(t) = \varphi(3-t), \qquad 3(\varphi^\Delta(0) - \varphi^\Delta(2)) = \varphi(1) + \varphi(2) \end{cases} \tag{20}$$

where $f(t,\varphi) = \frac{\left(\left|t-\frac{3}{2}\right|+1\right)(\sqrt{\varphi}+\varphi^2)}{440}$ and $g(t,\vartheta) = \frac{\left(\left|t-\frac{3}{2}\right|+1\right)(2\sqrt{\vartheta}+\vartheta^2)}{880}$. Here $a = 0, b = 3, \sigma(a) = 1$, $\rho(b) = 2$, $\tau_1 = 1$, $\tau_2 = 2$ and $[0,3]_\mathbb{T}$ is symmetric. We see that easily $f(t,\varphi)$ and $g(t,\vartheta)$ are satisfies the conditions (H_1) and (H_2). Furthermore, we find

$$\underline{f_0} = \underline{\lim_{\varphi\to 0^+}} \min_{t\in\mathbb{T}} \frac{f(t,\varphi)}{\varphi} = \underline{\lim_{\varphi\to 0^+}} \min_{t\in\mathbb{T}} \frac{\left(\left|t-\frac{3}{2}\right|+1\right)\left(\sqrt{\varphi}+\varphi^2\right)}{440\varphi} = \infty$$

$$\underline{g_0} = \underline{\lim_{\vartheta\to 0^+}} \min_{t\in\mathbb{T}} \frac{g(t,\vartheta)}{\vartheta} = \underline{\lim_{\vartheta\to 0^+}} \min_{t\in\mathbb{T}} \frac{\left(\left|t-\frac{3}{2}\right|+1\right)\left(2\sqrt{\vartheta}+\vartheta^2\right)}{880\vartheta} = \infty$$

$$\underline{f_\infty} = \underline{\lim_{\varphi\to \infty}} \min_{t\in\mathbb{T}} \frac{f(t,\varphi)}{\varphi} = \underline{\lim_{\varphi\to \infty}} \min_{t\in\mathbb{T}} \frac{\left(\left|t-\frac{3}{2}\right|+1\right)\left(\sqrt{\varphi}+\varphi^2\right)}{440\omega} = \infty$$

$$\underline{g_\infty} = \underline{\lim_{\vartheta\to \infty}} \min_{t\in\mathbb{T}} \frac{g(t,\vartheta)}{\vartheta} = \underline{\lim_{\vartheta\to \infty}} \min_{t\in\mathbb{T}} \frac{\left(\left|t-\frac{3}{2}\right|+1\right)\left(2\sqrt{\vartheta}+\vartheta^2\right)}{880\vartheta} = \infty$$

We calculate

$$m = \int_0^3 G(s,s)\nabla s = \frac{44}{9}$$

If we choose $R_1 = 2$, then we have $\frac{R_1}{m} = 0.409$ and $f(t,s) \leq \frac{R_1}{m}$ and $g(t,s) \leq \frac{R_1}{m}$ for $t \in \mathbb{T}, s \in [0,R_1]$. So, f and g satisfy the condition (H_3). Consequently, all conditions of Theorem 3.5 are satisfied. From Theorem 3.5, SSBVP (19)-(20) has at least two SPSs.

4. Conclusion

In this study, we obtain sufficient conditions that guarantee at least one and two SPSs of the system (1)-(2) on a symmetric time scale. This paper generalizes Qu's study in 2009 [6], which is the existence of SPSs of second-order differential equation systems with four-point boundary conditions to dynamic equation systems on symmetric time scales. To investigate the symmetric solutions of dynamic equations on time scales, researchers use Definition 2.4. A time scale that is symmetric in the sense of Definition 2.4 must satisfy $b - t + a \in \mathbb{T}$, for all $t \in \mathbb{T}$. Because of this $\overline{q^\mathbb{Z}}$ is not symmetric where $q > 1$. Therefore, this definition does not generalize all time scales. If a new symmetric definition can be found, including the q-difference time scales, it will be more general. Also, in the future someone can work on this problem for existence of one, two and three symmetric positive solutions by using Schauder fixed point theorem, Avery–Anderson–Henderson fixed point theorem, Legget–Williams fixed point theorem. Furthermore, this boundary values problem can be considered with impulsive boundary conditions.

Author Contributions

All the authors contributed equally to this work. They all read and approved the last version of the manuscript.

Conflict of Interest

The authors declare no conflict of interest.

References

[1] S. Hilger, *Ein Masskettenkalkül mit Anwendug auf zentrumsmanningfaltigkeiten*, PhD Dissertation, Universitat Würzburg (1988) Germany.

[2] F. M. Atıcı, D. C. Biles, A. Lebedinsky, *An Application of Time Scales to Economics*, Mathematical and Computer Modelling 43 (2006) 718–726.

[3] M. A. Jones, B. Song, D. M. Thomas, Cont*rolling Wound Healing Through Debridement*, Mathematical and Computer Modelling 40 (2004) 1057–1064.

[4] V. Spedding, *Taming Nature's Numbers*, New Scientist (2003) 28–32.

[5] D. M. Thomas, L. Vandemuelebroeke, K. Yamaguchi, *A Mathematical Evolution Model for Phytoremediation of Metals*, Discrete and Continuous Dynamical Systems Series B 5(2) (2005) 411–422.

[6] H. Qu, *The Symmetric Positive Solutions of Four-point Problems for Nonlinear Boundary Value Second-order Differential Equations*, International Journal of Mathematical Analysis, 3(40) (2009) 1969–1979.

[7] J. Henderson and H. B. Thompson, *Multiple Symmetric Positive Solutions for a Second Order Boundary Value Problem*, Proceedings of the American Mathematical Society 128 (2000) 2373–2379.

[8] F. Li, Y. Zhang, *Multiple Symmetric Nonnegative Solutions of Second-order Ordinary Differential Equations*, Applied Mathematics Letters 17 (2004) 261–267.

[9] Q. Yao, *Existence and Iteration of n Symmetric Positive Solutions for a Singular Two-point Boundary Value Problem,* Computers & Mathematics with Applications 47 (2004) 1195–1200.

[10] Y. P. Sun, *Existence and Multiplicity of Symmetric Positive Solutions for Three-point Boundary Value Problem,* Applied Mathematics Letters 329 (2007) 998–1009.

[11] N. A. Hamal, F. Yoruk, *Symmetric Positive Solutions of Fourth Order Integral BVP for an Increasing Homeomorphism and Homomorphism with Sign-changing Nonlinearity on Time Scales*, Computers & Mathematics with Applications 59(11) (2010) 3603–3611.

[12] E. Cetin, F. S. Topal, *Symmetric Positive Solutions of Fourth Order Boundary Value Problems for an Increasing Homeomorphism and Homomorphism on Time Scales*, Computers and Mathematics with Applications, 63(3) (2012) 669–678.

[13] K. R. Prasad, A. K. Rao and B. Bharathi, *Positive Solutions for System of 2n-th Order Sturm–Liouville Boundary Value Problems on Time Scales,* Proceedings of the Indian Academy of Sciences: Mathematical Sciences 124 (2014), 67–79.

[14] A. D. Oğuz, F. S. Topal, *Symmetric Positive Solutions for the Systems of Higher-order Boundary Value Problems on Time Scales*, Advances in Pure and Applied Mathematics 8(4) (2017) 285–292.

[15] M. Bohner, A. Peterson, Dynamic Equations on Time Scales, An Introduction with Applications, Birkhäuser, Boston, 2001.

[16] M. Bohner, A. Peterson, (Eds.), Advances in Dynamic Equations on Time Scales, Birkhäuser, Boston, 2003.

[17] S. Hilger, *Analysis on Measure Chains-A Unified Approach to Continuous and Discrete Calculus*, Results in Mathematics 18 (1990) 18–56.

[18] M. Krasnosel'skii, Positive Solutions of Operator Equations, Noordhoff, Groningen, 1964.

[19] F. Deimling, Nonlinear Functional Analysis, Springer, NewYork, 1985.

Journal of
New Theory
ISSN: 2149-1402

37 (2021) 99-107
Journal of New Theory
https://dergipark.org.tr/en/pub/jnt
Open Access

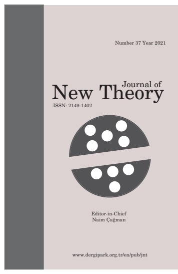

Generating Generalized Cylinder with Geodesic Base Curve According to Darboux Frame

Nabil Mohammed Althibany[1]

Article History
Received: 14 Dec 2021
Accepted: 29 Dec 2021
Published: 31 Dec 2021
10.53570/jnt.1036307
Research Article

Abstract — This paper aims to design a generalized cylinder with a geodesic base curve according to the Darboux frame in Euclidean 3-space. A generalized cylinder is a special ruled surface that is constructed by a continuous fixed motion of a generator line called the ruling along a given curve called the base curve. The necessary and sufficient conditions for the base curve to be geodesic are studied. The main results show that the generalized cylinder with a geodesic base curve is an osculating cylinder whose base curve is a helical geodesic, and the rulings are directed by the unit osculating Darboux vector.

Keywords — *Generalized cylinder, geodesic, Darboux frame, general helix, osculating Darboux vector*

Mathematics Subject Classification (2020) — 53A04, 53A05

1. Introduction

A generalized cylinder is constructed by a constant motion of a straight line called the ruling through a given curve called the base curve. The generalized cylinders are a class of developable ruled surfaces that have no singularities points and can be produced from paper or sheet metal with no distortion. For this construction, the generalized cylinder has been investigated as a basic modeling surface in various fields of science including geometric modeling, computer graphic, architectural designing [1–4].

Geodesic is a characteristic curve that is used to obtain the shortest distance between two points on curved space. Geodesic is a curve that travels through the surface such that its principal normal vector field parallel to the surface normal vector field. The different spaces and surfaces are characterized by their geodesics, the lines and grate circles are geodesics on the plane and the sphere respectively, but the (meridian) circles are not always geodesics on the surface of revolution. The helices are geodesics on the cylinder but the helicoid contains helices that are not geodesics [5–8]. Calculating and visualizing the geodesics on different spaces are important problems in many areas of applications [9–11].

A helical curve (or a helix) is a space curve in Euclidean 3-space whose tangent vector field makes a constant angle with a constant direction. According to the Theorem of Lancret [12], a necessary and sufficient condition that a curve is of constant slope (or general helix) is that the ratio of torsion to curvature is constant. The circular helix is a special helix with both its curvature and torsion are constants, based on this definition, the circle and line are degenerate helices [13]. A circular cylinder contains a helix, a circle, and a line as geodesics. The relation between generalized cylinder, geodesic, and a helix is well known and can be summarized by "a helix is a geodesic on a general cylinder".

A helical geodesic is a curve in which its principal normal vector field parallel to the surface normal vector field and at the same time its tangent vector makes a constant angle with a fixed direction.

[1]althibany1972@yahoo.com
[1]Department of Mathematics, Faculty of Applied Science, Taiz University, Taiz, Yemen

Thus, a helical geodesic is characterized by both two geometric natures, a helix from the Euclidean 3-space viewpoint, and a geodesic from the ambient surface viewpoint, for more details, see [5, 8, 14].

Darboux frame is adapted moving frame defined along a curve that lives on the surface. It is an important tool to study the geometry of surface curves such as geodesic curves. Darboux frame is defined at each point of the surface curve and can be obtained by rotating the Frenet frame around the tangent vector. The Darboux and Frenet frames agree modulo signs along the geodesic curves [15].

An osculating Darboux vector is defined by Izumiya and Otani [16] as the special direction of the Darboux frame that lies in the tangent plane of the surface. They showed that an osculating Darboux vector field has a constant direction if and only if the osculating developable surface is a generalized cylinder. An osculating developable surface is a ruled surface whose rulings are directed by the osculating Darboux vector field along the curve, it is tangent to the surface along the curve and it gives a flat approximation of the surface along the curve [17]. An osculating Darboux vector was studied in [18, 19], it characterizes the helical geodesic on the osculating cylinder as shown in this paper.

Designing the surface or the surfaces family that possess the given curve as a geodesic curve has been studied by Wang et al. [20], where they derived a sufficient condition for the curve to be geodesic on a given surface. After that, Kasap et al. [21] generalized the work of Wang. A developable surface that possesses a base curve as a geodesic has been studied in [22]. Recently in [23], the author studied and classified the ruled surfaces whose base curve is characteristic. After that in [24], we concluded that among all developable surfaces, the generalized cylinder can be equipped with geodesic coordinates if and only if the base curve is a helix and the director vector is a unit Darboux vector.

The main goal of this paper is to design a generalized cylinder whose base curve is geodesic in Euclidean 3- space. The generalized cylinders are a class of ruled surfaces, therefore, we start from a ruled parametrization, then with additional conditions called the cylindrical conditions, we define the generalized cylinder parametrization according to the Darboux frame. After that, and under some geometric constraints, we obtain the base curve as a geodesic curve. The main results show that the generalized cylinder with the geodesic base curve is an osculating cylinder in which the base curve is a helical geodesic and the rulings are directed by a constant unit osculating Darboux vector.

The rest of this paper is organized as follows: In Section 2, some basic notations, facts, and definitions of space curve in Euclidean 3-space and on a surface are reviewed. The main results are studied in Section 3, where the generalized cylinder with a geodesic base curve is generated. Finally, the conclusion is given in Section 4.

2. Preliminary

This section introduces some basic concepts on the classical differential geometry of the curve lying on the surface and in Euclidean 3-space, as well as some basic definitions and notions that are required subsequently. More details can be found in such standard references as [12, 25, 26].

2.1. Curves in Euclidean 3-space

A smooth space curve in 3-dimensional Euclidean space is parameterized by a map $\gamma : I \subseteq \mathbb{R} \to E^3$, γ is called a regular curve if $\gamma' \neq 0$ for every point of an interval $I \subseteq \mathbb{R}$, and if $|\gamma'(s)| = 1$ where $|\gamma'(s)| = \sqrt{\langle \gamma'(s), \gamma'(s) \rangle}$, then γ is said to be of unit speed (or parameterized by arc-length s). For a unit speed regular curve $\gamma(s)$ in E^3, the unit tangent vector $t(s)$ of γ at $\gamma(s)$ is given by $t(s) = \gamma'(s)$. If $\gamma''(s) \neq 0$, the unit principal normal vector n(s) of the curve at $\gamma(s)$ is given by $n(s) = \frac{\gamma''(s)}{\|\gamma''\|}$. The unit vector $b(s) = t(s) \times n(s)$ is called the unit binormal vector of γ at $\gamma(s)$. For each point of $\gamma(s)$ where $\gamma''(s) \neq 0$, we associate the Serret-Frenet frame $\{t, n, b\}$ along the curve γ. As the parameter s traces out the curve, the Serret-Frenet frame moves and satisfies the following Frenet-Serret formula.

$$\begin{cases} t'(s) & = \kappa(s)n(s), \\ n'(s) & = -\kappa(s)t(s) + \tau b(s), \\ b'(s) & = -\tau(s)n(s), \end{cases} \tag{1}$$

where $\kappa = \kappa(s)$ and $\tau = \tau(s)$ are the curvature and torsion functions. When the point moves along the unit speed curve with non vanishing curvature and torision, the Serret-Frenet frame $\{t, n, b\}$ is drawn to the curve at each position of the moving point, this motion consists of translation with rotation and described by the following Darboux vector whose direction is the direction of rotational axis and its magnitude gives the angular velocity of rotation.

$$\omega = \tau t + \kappa b \tag{2}$$

The general helix ($(\frac{\tau}{\kappa} = c)$) lies on a general cylinder and also known as a cylindrical helix. The circular helix (a helix on a circular cylinder) is a special helix with both of $\kappa(s) \neq 0$ and $\tau(s)$ are constants. The Darboux vector is constant for circular helix. For the cylindrical helix, the unit Darboux vector is constant as following

$$\hat{\omega} = \frac{\tau}{\sqrt{\tau^2+\kappa^2}}t + \frac{\kappa}{\sqrt{\tau^2+\kappa^2}}b = \frac{\tau/\kappa}{\sqrt{(\tau/\kappa)^2+1}}t + \frac{1}{\sqrt{(\tau/\kappa)^2+1}}b = \frac{c}{\sqrt{c^2+1}}t + \frac{1}{\sqrt{c^2+1}}b \tag{3}$$

For a regular curve on a surface, there exists another frame called Darboux frame and denoted by $\{t(s), g(s), N(s)\}$, where $t(s)$ is the unit tangent of the curve, $N(s)$ is the unit normal of the surface and g is a unit vector given by $g = N \times t$. Derivative of the Darboux frame is given by the following

$$\begin{cases} t'(s) &= \kappa_g g(s) + \kappa_n N(s), \\ g'(s) &= -\kappa_g t(s) + \tau_g N(s), \\ N'(s) &= -\kappa_n t(s) - \tau_g g(s), \end{cases} \tag{4}$$

where κ_g is the geodesic curvature, κ_n is the normal curvature and τ_g is the geodesic torsion at each point of the curve $\gamma(s)$ which are given by

$$\kappa_g =< \gamma''(s), g >, \qquad \kappa_n =< \gamma''(s), N >, \text{and} \qquad \tau_g =< N', g > \tag{5}$$

The relations between Frenet and Darboux frames can be given by the following matrix form

$$\begin{pmatrix} t \\ g \\ N \end{pmatrix} = \begin{pmatrix} 1 & 0 & 0 \\ 0 & \cos\phi & \sin\phi \\ 0 & -\sin\phi & \cos\phi \end{pmatrix} \begin{pmatrix} t \\ n \\ b \end{pmatrix} \tag{6}$$

where

$$\begin{cases} g(s) &= \cos\phi(s)n(s) + \sin\phi(s)b(s), \\ N(s) &= -\sin\phi(s)n(s) + \cos\phi(s)b(s) \end{cases} \tag{7}$$

Differentiating (7) using (4) and (1), we get the relation between geodesic curvature, normal curvature, and geodesic torsion with curvature and torsion as follows:

$$\kappa_g = \kappa\cos\phi, \qquad \kappa_n = \kappa\sin\phi, \qquad \tau_g = \tau + \frac{d\phi}{ds}, \qquad \text{where } \kappa^2(s) = \kappa_n^2(s) + \kappa_g^2(s) \tag{8}$$

Definition 2.1. A unit-speed curve on a surface is called a geodesic if and only if its geodesic curvature is zero ($\kappa_g = 0$).

Remark 2.2. For a geodesic curve ($\kappa_g = 0$), some geometric quantities along the geodesic curve are congruent up to orientation, the principal normal of the curve and the surface normal are parallel to each other at any point on the curve, the rectifying plane coincides with the tangent plane of the surface, the Frenet and Darboux frames agree modulo signs, the absolute value of the normal curvature and geodesic torsion equal to the ordinary curvature and torsion respectively. By using (7) and (8), the following equations can be calculated easily

$$N = \pm n, \qquad g = \pm b, \qquad \kappa_n = \pm\kappa, \text{and} \qquad \tau_g = \pm\tau \tag{9}$$

3. Generalized Cylinder with Geodesic Base Curve

This section is the main part of the present paper and it consists of three subsections. In the first subsection we give the necessary and sufficient conditions for the ruled parametrization to be generalized cylinder parametrization. The second subsection is devoted to making the base curve of the generalized cylinder is a geodesic. In the third subsection, we prove that the geodesic base curve is a helix, or equivalently a helical geodesic. Th conditions which are assumed are given by Darboux frame and its related geometric quantities. The main result is obtained subsequently and shows that the generalized cylinder with the geodesic base curve is an osculating cylinder whose base curve is a helical geodesic and the rulings are directed by a constant unit osculating Darboux vector.

3.1. Generalized Cylinder

A generalized cylinder is generated by a constant moving of a straight line on a given curve and defined by the following ruled parametrization

$$X(s,v) = \gamma(s) + vD(s), 0 \leq s \leq \ell,\ v \in \mathbb{R}, \text{ where } D'(s) = 0 \tag{10}$$

A unit regular curve $\gamma(s)$ is called the base curve, the line passing through $\gamma(s)$ that is parallel to $D(s)$ is called the ruling. $D(s)$ is a unit director vector field that gives the direction of the ruling, $D'(s) = 0$ is the cylindrical condition which means that the ruling moves in a constant direction. $D(s)$ lies in the tangent plane of the generalized cylinder and can be written using (6) as following

$$D(s) = \cos\theta(s)t(s) + \sin\theta(s)g(s) \tag{11}$$

The derivative of $D(s)$ in terms of the Darboux frame and its derivatives is given by

$$D'(s) = -\sin\theta(s)[\kappa_g(s) + \frac{d\theta}{ds}]t(s) + \cos\theta(s)[\kappa_g(s) + \frac{d\theta}{ds}]g(s) + [\kappa_n(s)\cos\theta(s) + \tau_g(s)\sin\theta(s)]N(s) \tag{12}$$

Definition 3.1. The ruled parametrization with base curve $\gamma(s)$ and a unit director vector D(s) is defined by

$$\begin{cases} X(s,v) &= \gamma(s) + vD(s), 0 \leq s \leq L,\ v \in \mathbb{R}, \text{ where} \\ D(s) &= \cos\theta(s)t(s) + \sin\theta(s)g(s). \end{cases} \tag{13}$$

The following Theorem gives the cylindrical conditions that make the ruled parametrization (13) to be generalized cylinder parametrization

Theorem 3.2. The ruled parametrization (13) is a generalized cylinder if and only if the following conditions are satisfied

$$\begin{aligned} \kappa_g(s) + \frac{d\theta}{ds} &= 0, \\ \kappa_n(s)\cos\theta(s) + \tau_g(s)\sin\theta(s) &= 0 \end{aligned} \tag{14}$$

Proof. By definition, the ruled parametrization (13) is a cylinder if and only if $D'(s)$ vanishes, by using (12) this condition is satisfied provided that (14) are satisfied. □

Definition 3.3. The generalized cylinder with base curve $\gamma(s)$ and a unit director vector D(s) (11) is parameterized by

$$\begin{cases} X(s,v) = \gamma(s) + v[\cos\theta(s)t(s) + \sin\theta(s)g(s))],\ 0 \leq s \leq L,\ v \in \mathbb{R}, \quad \text{where,} \\ \kappa_g(s) + \frac{d\theta}{ds} = 0 \quad \text{and} \quad \kappa_n(s)\cos\theta(s) + \tau_g(s)\sin\theta(s) = 0. \end{cases} \tag{15}$$

The main result of this paper is the following main theorem which is proved in the next section.

Theorem 3.4. Let $X(s,v) = \gamma(s) + vD(s), 0 \leq s \leq L, v \in \mathbb{R}$ be a generalized cylinder, $\gamma(s)$ is a unit speed regular curve with non vanishing curvature and torsion, $D(s)$ is a unit director vector defined by (11) satisfying $D'(s) = 0$. Then the generalized cylinder with geodesic base curve is an osculating cylinder whose base curve is a helical geodesic and $D(s)$ is a constant unit osculating Darboux vector.

3.2. Generalized Cylinder with Geodesic Base Curve

This subsection is devoted to constructing a generalized cylinder parameterized by (15) with the geodesic base curve. For this purpose, three conditions must be satisfied as given in the following

Theorem 3.5. A base curve $\gamma(s)$ of the generalized cylinder parameterized by (15) is a geodesic if and only if the following conditions are satisfied

$$\begin{aligned} \kappa_g(s) &= 0, \\ \frac{d\theta}{ds} &= 0, \\ \kappa_n(s)\cos\theta(s) + \tau_g(s)\sin\theta(s) &= 0 \end{aligned} \tag{16}$$

Proof. By definition (2.1), a base curve $\gamma(s)$ of the generalized cylinder parameterized by (15) is a geodesic if and only if $\kappa_g = 0$ which is the first condition of (16). By substitution it in the cylindrical conditions (14), we get the other conditions of (16). □

Definition 3.6. A generalized cylinder with geodesic base curve is defined by

$$\begin{cases} X(s,v) = \gamma(s) + v[\cos\theta(s)t(s) + \sin\theta(s)g(s)],\ 0 \le s \le L,\ v \in \mathbb{R}, \quad \text{where,} \\ \kappa_g(s) = 0,\ \frac{d\theta}{ds} = 0, \text{ and } \quad \kappa_n(s)\cos\theta(s) + \tau_g(s)\sin\theta(s) = 0 \end{cases} \tag{17}$$

Izumiya and Otani [16] defined the osculating Darboux vector field D_0 and its normalized $\hat{D}_0$ provided $(\kappa_n(s), \kappa_g(s)) \neq (0,0)$ as the following

$$D_0 = \tau_g(s)t(s) - \kappa_n(s)g(s), \quad \hat{D}_0 = \frac{\tau_g(s)}{\sqrt{\tau_g^2(s) + \kappa_n^2(s)}}t - \frac{\kappa_n(s)}{\sqrt{\tau_g^2(s) + \kappa_n^2(s)}}g \tag{18}$$

Proposition 3.7. Suppose that $D(s) = \cos\theta(s)t(s) + \sin\theta(s)g(s)$ is a unit vector field defined along a unit speed surface curve $\gamma(s)$ with $(\tau_g(s), \kappa_n(s)) \neq (0,0)$, then $D(s)$ is a unit osculating Darboux vector field if and only if $\kappa_n(s)\cos\theta(s) + \tau_g(s)\sin\theta(s) = 0$.

Proof. Let $D(s) = \cos\theta(s)t(s) + \sin\theta(s)g(s)$ be unit osculating Darboux vector field. From (18)

$$\cos\theta = \frac{\tau_g(s)}{\sqrt{\tau_g^2(s) + \kappa_n^2(s)}}, \quad \sin\theta(s) = \frac{-\kappa_n(s)}{\sqrt{\tau_g^2(s) + \kappa_n^2(s)}}, \quad \textit{and} \quad \cot\theta = -\frac{\tau_g(s)}{\kappa_n(s)}$$

This implies that $\kappa_n(s)\cos\theta(s) + \tau_g(s)\sin\theta(s) = 0$, and vice versa. □

The condition $\frac{d\theta}{ds} = 0$ implies that the angle function $\theta(s)$ is constant, hence the rulings keep constant angle to a fixed direction $D(s)$, or equivalently $D'(s) = 0$ as a cylindrical condition. This condition with proposition (3.7) insure that the unit osculating Darboux vector field is constant.

Theorem 3.8. A base curve $\gamma(s)$ of the generalized cylinder parameterized by (15) is a geodesic if and only if $D(s)$ is a constant unit osculating Darboux vector.

Definition 3.9. A generalized cylinder with geodesic base curve is defined by

$$\begin{cases} X(s,v) &= \gamma(s) + vD(s), 0 \le s \le L, v \in \mathbb{R} \quad \text{where} \\ D(s) &= \frac{\tau_g(s)}{\sqrt{\tau_g^2(s)+\kappa_n^2(s)}}t(s) - \frac{\kappa_n(s)}{\sqrt{\tau_g^2(s)+\kappa_n^2(s)}}g(s), \quad D'(s) = 0 \end{cases} \tag{19}$$

3.3. Generalized Cylinder with Helical Geodesic Base Curve

In the last subsection, Theorem (3.8) and definition (3.9) presented the conditions that can be applied on the director vector field $D(s)$ to make the base curve of the generalized cylinder to be geodesic. Therefore, this subsection investigates the equivalent conditions that can be applied on the base curve to be geodesic. For this purpose, we start by the following theorem, for proof see [27].

Theorem 3.10. [27] A unit speed curve on a surface with $(\kappa_n(s), \kappa_g(s)) \neq (0,0)$ is a general helix if and only if

$$\frac{1}{(\kappa_n^2(s) + \kappa_g^2(s))^{3/2}}(\kappa_g' \kappa_n - \kappa_n' \kappa_g - \tau_g(\kappa_n^2 + \kappa_g^2)) = constant \tag{20}$$

For a geodesic curve, $\kappa_g(s) = 0$, the condition (20) is rewritten as the following

Corollary 3.11. Let $\gamma(s)$ be a geodesic curve with $\kappa_n(s) \neq 0$. Then, $\gamma(s)$ is a helix if and only if

$$\frac{\tau_g(s)}{\kappa_n(s)} = constant \tag{21}$$

Under the assumption that $\kappa_n(s) \neq 0$, and by substitution (21) in (18), the following corollary determines the relationship between a helix, geodesic curve, and the unit osculating Darboux vector.

Corollary 3.12. Let $\gamma(s)$ be a geodesic curve on a surface with $\kappa_n(s) \neq 0$. Then, $\gamma(s)$ is a helix if and only if the unit osculating Darboux vector field $\hat{D}_0$ is a constant.

The unit osculating Darboux is a vector on the surface that plays a role analogous to the unit Darboux vector (3) in E^3, they characterize the helix on the surface and E^3 respectively, compare proposition (3.7) and corollary (3.12) with their counterparts in [23, 24]. The following theorem gives the satisfying conditions on the base curve and director vector to make a base curve is a geodesic.

Theorem 3.13. A base curve $\gamma(s)$ of the generalized cylinder parameterized by (15) is a geodesic if and only if $\gamma(s)$ is a helix and $D(s)$ is a unit osculating Darboux vector.

Definition 3.14. A generalized cylinder with geodesic base curve is defined by

$$\begin{cases} X(s,v) & = \gamma(s) + vD(s), 0 \leq s \leq L, v \in \mathbb{R}, \quad \text{where,} \\ D(s) & = \frac{\tau_g(s)}{\sqrt{\tau_g^2(s)+\kappa_n^2(s)}} t(s) - \frac{\kappa_n(s)}{\sqrt{\tau_g^2(s)+\kappa_n^2(s)}} g(s), \quad \text{and } \gamma(s) \text{ is a helix.} \end{cases} \tag{22}$$

Theorem 3.15. Let $X(s,v) = \gamma(s) + vD(s), 0 \leq s \leq L, v \in \mathbb{R}$ be a ruled surface, where $\gamma(s)$ is a unit speed regular surface curve with $(\tau_g(s), \kappa_n(s)) \neq (0,0)$, $D(s)$ is a unit direction vector defined by $D(s) = \cos\theta(s)t(s) + \sin\theta(s)g(s)$. Then X(s,v) is a generalized cylinder whose base curve is a geodesic if and only if $\gamma(s)$ is a helix and $D(s)$ is a unit osculating Darboux vector.

A ruled surface whose rulings are directed by the osculating Darboux vector along the curve is called an osculating developable surface [16]. The generalized cylinder defined by (22) is a special case where the unit osculating Darboux vector is a constant and we call it the osculating cylinder.

Theorem 3.16. Let $X(s,v) = \gamma(s) + vD(s), 0 \leq s \leq L, v \in \mathbb{R}$ be a generalized cylinder, where $\gamma(s)$ is a unit speed regular surface curve with $(\tau_g(s), \kappa_n(s)) \neq (0,0)$, and $D(s) = \cos\theta(s)t(s) + \sin\theta(s)g(s)$ satisfies $D'(s) = 0$. Then the following properties are equivalent:

i. X(s,v) is an osculating cylinder,

ii. $D(s)$ is a constant unit osculating Darboux vector,

iii. $\gamma(s)$ is a geodesic,

iv. $\gamma(s)$ is a helix.

Theorem 3.17. Among all generalized cylinders parameterized by (15), only the osculating cylinder (22) has a geodesic base curve.

The approximation of a given surface by a flat surface (developable) along the arbitrary curve is called flat or developable approximation. An osculating developable is tangent to the surface along a curve and it gives a flat approximation of the surface along the curve [17]. The osculating cylinder (22) inherits this property and gives flat approximation of the surface along a helical geodesic. Approximating by an osculating cylinder (22) has nice geometrical properties: globally free of singularities, achieved along a geodesic path, some geometric quantities on both cylinder and the surface along the geodesic curve are congruent up to orientation (2.2), locally like approximating by the ribbon [28], and the cylinder is easy to modeling and reasoning from a mathematical or manufacturing viewpoint. For more details about the flat approximations of surfaces and hypersurfaces see [16, 17, 29].

4. Conclusion

The work in this paper can be separated into two parts as given subsequently in the third section. Firstly, we presented how the generalized cylinder (15) can be parameterized from a ruled parametrization (13) under the cylindrical conditions, see Theorem (3.2) and definition (3.3). Secondly, we showed how the generalized cylinder with geodesic base curve is generated, see Theorem (3.13) and definition (3.14). The generated cylinder is an osculating (22) whose base curve is a helical geodesic and the director vector is a unit osculating Darboux vector. Among all generalized cylinders (15), only the osculating cylinder (22) has geodesic base curve. The unit osculating Darboux vector can be used as a tool not only to generate the osculating cylinder (22), but to characterize the helical geodesic, corollary (3.12). The osculating cylinder (22) has nice geometrical properties, one of them it gives a flat approximation of the surface along a helical geodesic.

Author Contributions

The author read and approved the last version of the manuscript.

Conflicts of Interest

The author declares no conflict of interest.

References

[1] K. H. Chang, Product Design Modeling Using CAD/CAE, The Computer Aided Engineering Design Series, Academic Press, 2014.

[2] R. Goldman, An Integrated Introduction to Computer Graphics and Geometric Modeling, CRC Press, 2009.

[3] S. Guha, Computer Graphics through OpenGL: From Theory to Experiments, Chapman and Hall/CRC, 2018.

[4] H. Pottmann, A. Asperl, M. Hofer, A. Kilian, Architectural Geometry, Bentley Institute Press, Exton, 2007.

[5] M. Tamura, *Surfaces Which Contain Helical Geodesics*, Geometriae Dedicata 42(3) (1992) 311–315.

[6] A. Görgülü, *Surfaces Which Contain Inclined Curves as Geodesics*, Communications Faculty of Sciences University of Ankara Series A1 Mathematics and Statistics 42 (1993) 39–44.

[7] M. Tamura, *Surfaces Which Contain Helical Geodesics in the 3-Sphere*, Memoirs of the Faculty of Science and Engineering Shimane University. Series B. Mathematical Science 37 (2004) 59–65.

[8] D. W. Yoon, *On Constructions of Minimal Surfaces*, Journal of the Chungcheong Mathematical Society 34(1) (2021) 1–15.

[9] I. Hotz, H. Hagen, *Visualizing Geodesics*, In Proceedings Visualization VIS 2000 (Cat. No. 00CH37145) IEEE (2000) 311–318.

[10] G. R. Kumar, P. Srinivasan, V. D. Holla, K. G. Shastry, B. G. Prakash, *Geodesic Curve Computations on Surfaces*, Computer Aided Geometric Design 20(2) (2003) 119–133.

[11] E. Kasap, M. Yapici, F. T. Akyildiz, *A Numerical Study for Computation of Geodesic Curves*, Applied Mathematics and Computation 171(2) (2005) 1206–1213.

[12] D. J. Struik, Lectures on Classical Differential Geometry, 2nd Edition, Dover Publications Inc., New York, 1988.

[13] A. T. Ali, *New Special Curves and Their Spherical Indicatrix*, Global Journal of Advanced Research On Classical and Modern Geometries 1(2) (2012) 28–38.

[14] R. Lopez, G. Ruiz-Hernández, *A Characterization of Isoparametric Surfaces in $\mathbb{R}^3$ Via Normal Surfaces*, Results in Mathematics 67(1) (2015) 87–94.

[15] M. Huard, N. Sprynski, N. Szafran, L. Biard, *Reconstruction of Quasi Developable Surfaces from Ribbon Curves*, Numerical Algorithms 63(3) (2013) 483–506.

[16] S. Izumiya, S. Otani, *Flat Approximations of Surfaces Along Curves*, Demonstratio Mathematica 48(2) (2015) 217–241.

[17] S. I. Honda, S. Izumiya M. Takahashi, *Developable Surfaces Along Frontal Curves on Embedded Surfaces*, Journal of Geometry 110(2) (2019) 1–20.

[18] S. Hananoi, N. Ito, S. Izumiya, *Spherical Darboux Images of Curves on Surfaces*, Beiträge zur Algebra und Geometrie 56(2) (2015) 575–585.

[19] S. Izumiya, K. Saji, N. Takeuchi, *Flat Surfaces Along Cuspidal Edges*, Journal of Singularities 16 (2017) 73–100.

[20] G. J. Wang, K. Tang, C.L. Tai, *Parametric Representation of a Surface Pencil with a Common Spatial Geodesic*, Computer-Aided Design 36(5) (2004) 447–459.

[21] E. Kasap, F.T. Akyildiz, K. Orbay, *A generalization of surfaces family with common spatial geodesic*, Applied Mathematics and Computation 201(1-2) (2008) 781–789.

[22] R. A. Al-Ghefaria, A. B. Rashad, *An Approach for Designing a Developable Surface with a Common Geodesic Curve*, International Journal of Contemporary Mathematical Sciences 8(18) (2013) 875–891.

[23] N. M. Althibany, *Classification of Ruled Surfaces Family with Common Characteristic Curve in Euclidean 3-space*, Turkish Journal of Science 6(2) (2021) 61–70.

[24] N. M. Althibany, *Construction of Developable Surface with Geodesic or Line of Curvature Coordinates*, Journal of New Theory (36) (2021) 75–87.

[25] M. D. Carmo, Differential Geometry of Curves and Surfaces, Prentice-Hall, New Jersey, 1976.

[26] A. N. Pressley, Elementary Differential Geometry, Springer Science & Business Media, 2010.

[27] M. Düldül, B. U. Düldül, *Characterizations of helices by using their Darboux Vectors*, Sigma: Journal of Engineering & Natural Sciences 38(3) (2020) 1299–1306.

[28] M. Raffaelli, J. Bohr, S. Markvorsen, *Cartan Ribbonization and a Topological Inspection*, Proceedings of the Royal Society A 474(2220) (2018) p.20170389.

[29] I. Markina, M. Raffaelli, *Flat Approximations of Hypersurfaces Along Curves*, Manuscripta Mathematica 160(3) (2019) 315–325.